USING DRILLING DATA TO CALCULATE POROSITY & PERMEABILITY

By

ALEXANDRA ELIZABETH CEDOLA

Bachelor of Science in Petroleum & Natural Gas Engineering

New Mexico Institute of Mining & Technology

Socorro, New Mexico

2015

Submitted to the Faculty of the
Graduate College of the
Oklahoma State University
in partial fulfillment of
the requirements for
the Degree of
MASTER OF SCIENCE
May, 2017

USING TYPICAL DRILLING DATA TO

CALCULATE POROSITY & PERMEABILITY

Thesis Approved:

Dr. Geir Hareland

Thesis Adviser

Dr. Runar Nygaard

Dr. Prem Bikkina

ACKNOWLEDGEMENTS

I would like to begin by thanking my advisor, Dr. Geir Hareland, for all of his help, support, and encouragement. He has allowed me to discover what I am truly interested in and his expansive knowledge, specifically in the area of drilling, has enabled me to grow as an engineer. He has also helped me to work on my golf game.

I would like to say thank you to my committee members, Dr. Runar Nygaard and Dr. Prem Bikkina for their help and encouragement. Not only have they helped further my education, they have helped me to better myself as a person.

Thank you to all of my office mates for both their help and their humor. My "Master's Experience" wouldn't have been the same without the random conversations, white board drawings, or discussing what went wrong with the daily lab experiments. I couldn't have done it without y'all.

I would like to thank my family, who has been such an amazing support system for me. I would like to give a special thank you to my cousin Austin, who first got me interested in petroleum engineering. Also, a big thanks to Lakota Sioux for her love, attention, and motivation. Finally, I want to thank my parents, Steve and Kathy, as well as my sister, Lizzy, for always believing in me. They have been my backbone throughout this journey and I can't express how thankful I am for them!

Name: ALEXANDRA ELIZABETH CEDOLA

Date of Degree: MAY, 2017

Title of Study: USING TYPICAL DRILLING DATA TO CALCULATE POROSITY & PERMEABILITY

Major Field: Petroleum & Natural Gas Engineering

Abstract:

Porosity and permeability are two important parameters for reservoir characterization, formation evaluation, and stimulation design. Typically, the methods for obtaining these two parameters are not only costly and time consuming, but can have a high degree of uncertainty. Drilling data can provide great insight into downhole occurrences, but it is commonly overlooked as a source of information. In this work, drilling data and an inverted rate of penetration (ROP) model are utilized to determine unconfined compressive strength (UCS) values at any point where drilling data has been collected. Using UCS and porosity values collected from laboratory measurements, a porosity representative correlation for sandstone and shale formations is established. Additionally, taking gamma ray measurements into consideration, a porosity correlation for mixed lithology zones is developed based on field data from three previously drilled wells in Alberta, Canada. Porosity and permeability data found through laboratory testing for various sandstone and shale formations has been collected and used to establish a correlation between the two parameters for the individual formations. Using the sandstone and shale porosity-UCS correlations, the collected laboratory porosity data is used to determine UCS for the individual sandstone and shale formations. The permeability is plotted with the corresponding UCS values for the various formations and a correlation between the two parameters is developed. Determining UCS from drilling data allows for both porosity and permeability data to be found and could potentially have real-time application potential.

Knowledge of porosity and permeability in unconventional horizontal wells could be beneficial to stimulation design. Having the ability to find the porosity and permeability from drilling data would mean that these two parameters are known throughout a lateral and ultimately allow for optimization of selective stimulation. This could potentially reduce the need for logging, laboratory testing, and overall cost.

TABLE OF CONTENTS

Chapter Page

LIST OF EQUATIONS

Equation Page

LIST OF FIGURES

Figure Page

Figure Page

NOMENCLATURE

a1	Power Gamma Ray Constant	-
a, b, c	Bit Design Constants	-
a_1,b_1,c_1	Empirical Constants	-
API	American Petroleum Institute	-
as	Fitting Constant for Failure Criteria	-
BR	Back Rake	degrees
b_s	Fitting Constant for Failure Criteria	-
b(x)	Function for the Effect of Number of Blades	Dimensionless
CCS	Confined Compressive Strength	psi
D, D_b	Bit Diameter	Inches
d_s	Natural Diamond Cutter Diameter	Inches
fc	Chip Hold Down Function	Dimensionless
GR	Gamma Ray	API
h(x)	Hydraulic Efficiency Function	-
I_m	Modified Jet Impact Force	lb.
K_8	Regression Constant	5.15E-?
K_9	Regression Constant	23.8700
N	Rotary Speed	rev/min
NMR	Nuclear Magnetic Resonance	-
P_e	Effective Differential or Coning Pressure	psi
PDC	Polycrystalline Diamond Compact Bit	-
R	Penetration Rate	ft/m
ROP	Rate of Penetration	m/hr
S	Rock Strength	psi
SR	PDC Cutter Side Rake	degrees
UCS	Unconfined Compressive Strength	MPa
W_f	Wear Function	Dimensionless
WOB, W	Weight on Bit	kN
Δt_c	Compressional Travel Time	µsec/ft
δult	Ultimate Compressive Strength	psi
ε	Rock Ductility	Dimensionless
µ	Mud Viscosity	cP
ρ_m	Mud Density	lb/gal
σ_{UCS}, σ_c	Unconfined Compressive Strength	MPa, psi
σ_{ult}	Ultimate Compressive Strength	kg/cm²
ϕ	Porosity	%

CHAPTER I

INTRODUCTION

Porosity and permeability are two essential parameters for reservoir characterization. Porosity allows for reserve estimations where permeability is indicative of the reservoir deliverability (Denney, 2008, Lenormand & Fonta, 2007). With an increase in the number of horizontal wells, knowledge of porosity and permeability throughout the lateral can help optimize completion strategies and overall hydrocarbon recovery. The methods for porosity and permeability determination can differ depending upon lithology. While there are numerous techniques for determining porosity and permeability in conventional reservoirs, finding these parameters in unconventional reservoirs proves to be much more challenging. In unconventional shale reservoirs, variations in rock composition and rock alterations after deposition can lead to a high degree of uncertainty in the accuracy of data measurements (Zhang et al., 2016). In unconventional tight sandstone reservoirs, conventional logging tools will yield inaccurate porosity measurements because of the complexity of the pore structure (Liang et al., 2013). Having the ability to determine porosity and permeability accurately, quickly, and in a cost effective manner in unconventional horizontal wells could prove to be highly impactful for the drilling, completion, and production decision making process.

1.1 Motivation

Unconventional reservoirs have become an increasingly popular target within the petroleum industry. The reason for this rise in the popularity of unconventional reservoirs, which can be defined as reservoirs with low permeabilities that require improved technology in order to produce hydrocarbons at economical rates (Holditch et al., 2007), is due to depletion in many conventional reservoirs (Bybee, 2011, Snyder & Seale, 2011). In horizontal wells, porosity and permeability determination has proven to be a difficult task. Oftentimes drill cuttings are used to determine porosity and permeability due to the fact that they can be collected throughout the lateral. One of the largest drawbacks of using cuttings for porosity and permeability determination is that to obtain accurate measurements for a specific point within the lateral, a proper understanding of the cuttings transport mechanism must be achieved (Garcia-Hernandez et al., 2007).

1.2 Selective Stimulation

Porosity and permeability are critical parameters for stimulation design and optimization. Having a better understanding of optimal stimulation placement, spacing, and number of fractures is highly influential for successful production (Saldungaray & Palisch, 2013). Utilizing reservoir characteristics can also aid in the planning of perforation placement (Hashmy et al., 2012) which can allow for better reservoir contact.

1.3 Thesis Objective

There have been many correlations that have been developed in order to determine porosity and/or permeability from well logs. A majority of these correlations can only be used to determine these parameters in a specific type of lithology. One drawback associated with many of these correlations is that they may require parameters that are difficult to obtain. Drilling data is a commonly overlooked source for downhole information, but it can provide insight into lithological parameters, pressure data, rock mechanical properties, and many other components.

In this study, correlations for determining porosity and permeability in sandstone and shale formations have been established. The porosity and permeability correlations can be applicable by using unconfined compressive rock strength obtained through the use of conventional drilling data. The correlations are verified with drilling and log data taken from three previously drilled wells in British Columbia, Canada and the feasibility and accuracy of a potential real-time porosity and permeability application is evaluated.

Portions of this thesis have been previously published in conference proceedings (Cedola et al., 2017A, Cedola et al., 2017B, Cedola et al, 2017C) and are presented in Appendix D.

CHAPTER II

REVIEW OF LITERATURE

Porosity and permeability calculations have been predominantly developed for conventional reservoirs. Unconventional reservoirs, which include tight gas, tight oil, shale gas, coal-seam gas, and fractured basement plays (Knackstedt et al., 2013) have become increasingly important within the petroleum industry yet require alternate techniques for reservoir description, completions, and drilling methods. Many of the techniques that have been developed for use in unconventional reservoirs lack consistency/accuracy which can lead to poor understanding of the reservoir.

2.1 Porosity Determination Techniques

Porosity determination has been done in numerous ways, but many of these methods have drawbacks. Knowing the porosity can impact the overall success of a well, provide a basis for reserves estimation (Desport et al., 2011), and allow for more accurate formation evaluation. The Wyllie equation is one of many empirical correlations that can be used to estimate porosity, but this method is susceptible to error in gas formations (Lan et al., 2010). Many of the available correlations are also meant for predominantly sandstone reservoirs and use data that may not accurately represent the actual formation (Horsrud, 2001). While core analysis is considered the most accurate method to determine porosity, laboratory discrepancies can yield different data for identical cores (Luffel & Howard, 1987). There are also numerous logging tools that have been

used for porosity prediction, including the nuclear magnetic resonance (NMR), gamma ray, sonic, density-neutron, and wireline logs. NMR logs have four main features: NMR measurements are emitted by formation fluids rather than by formation rock, direction is not considered, this type of log is only applicable to open holes, and the tool need to be properly calibrated to the wave strength (Hursan et al., 2015). Neutron and density logs can be used in conjunction to estimate porosity in openhole or gas-bearing zones, but these log measurements may need to be verified with cores taken from nearby wells (Ellis et al., 2003). Sonic logs can also be used to predict porosity, but the accuracy of such predictions suffers in areas containing shale (Goldberg & Gurevich, 1998). Gamma ray logs are typically used to determine porosity in shaly formations because this type of log can provide alternate responses in contrasting grain compositions (Katahara, 1995). Wireline logging is another source for porosity determinations, but proper calibration is critical to ensure accuracy.

In horizontal wells, there are a variety of issues in porosity determination. Similar to vertical wells, horizontal well porosity determination is done through logging, wireline tools, and core or cuttings testing. The problems associated in horizontal well porosity determination could be due to micro fractures, tool placement, permeability anisotropy which causes variations in fluid invasion and water saturation at different spots within the wellbore, and that horizontal well porosity measurements are applied throughout a field rather than being specifically for individual wells (Calvert et al., 1998).

2.1.1 Unconfined Compressive Strength Correlations

There have been several methods that have utilized unconfined compressive strength (UCS) to determine porosity. UCS, which can be defined as “The strength of a rock or soil sample when crushed in one direction (uniaxial) without lateral restraint” (Allaby 2013), is important for drill bit selection, wellbore stability determination, and enhanced oil recovery analysis (Nabaei &

Shahbazi, 2012). UCS determination can be done through electrical log-based correlations (Borba et al., 2014, Sayers et al., 2009), uniaxial compression test, scratch tests (Borba et al., 2014), and penetration models (Nabaei & Shahbazi, 2012). For the purpose of this study, three UCS-porosity correlations will be examined in detail: the Onyia method, Sarda method, and Erfourth method.

2.1.2 Onyia Method

Onyia (1988) developed correlations in which UCS data is determined from sonic and density logs. Using these UCS values, correlations between sonic log UCS and porosity as well as density log UCS and porosity was found. For both density and sonic logs, the log-derived UCS was found using the Warren (1987) roller cone penetration rate model (Eq. 1).

$$\sigma_{ult} = \left[\frac{w}{aD^2\varepsilon}\left[\frac{\frac{N}{R}-\frac{b}{D}-\frac{cN\rho_m\mu D}{I_m}}{D}+\frac{\emptyset^2}{4a\varepsilon}\right]\right]^{.5} - \frac{\emptyset w}{2aD\varepsilon^2} \quad (1)$$

Upon comparison, UCS determined from the sonic log was considerably more accurate than that of the density log when compared to the log-derived rock strength values. Sonic log data was chosen to calculate UCS values (Eq. 2) and the UCS values were then further correlated to permeability.

$$\delta_{ult} = \frac{1.00}{K_8(\Delta t_c - K_9)^2} + 2.0 \quad (2)$$

A plot of the sonic log UCS values and the porosity that had been calculated from the Warren ROP model were graphed and the Onyia UCS-porosity correlation was established (Eq. 3).

$$\delta_{ult} = 3.2205 + \frac{102.51}{\emptyset_a} \quad (3)$$

2.1.3 Sarda Method

The purpose of the Sarda UCS-porosity method is to determine UCS values solely from log data (Sarda et al., 1993). Taking a UCS correlation originally developed for ceramic materials, Sarda et al. (1993) was able to relate this to sands and ultimately establish three UCS-porosity correlations for various porosities. The first Sarda UCS-porosity correlation is applicable to sands with a porosity ranging from 0-7% (Eq. 4).

$$\sigma_{UCS} = 357e^{-10.8\emptyset} \tag{4}$$

The second Sarda UCS-porosity correlation is applicable to sand formations with porosity ranging from 0-30% (Eq. 5).

$$\sigma_{UCS} = 258e^{-9\emptyset} \tag{5}$$

The third Sarda UCS-porosity correlation is less accurate than the previous two because very few of the sandstone samples tested had porosity over 30%. The Sarda correlation for sands with porosity above 30% is presented in Eq. 6.

$$\sigma_{UCS} = 111.5e^{-11.6\emptyset} \tag{6}$$

2.1.4 Erfourth Method

The Erfourth method uses cored and cast plaster cylinders that contain Styrofoam inclusions to "mimic" rock (Erfourth et al., 2005). These plaster samples underwent porosity and UCS testing to observe how the Styrofoam inclusions affected these two properties. To create a correlation between UCS and porosity, data were collected for Topopah Spring tuff and the plaster data collected from laboratory and plotted to obtain the Erfourth correlation (Eq. 7).

$$UCS = 194.39e^{\left(-\frac{\emptyset}{12.55}\right)} \quad (7)$$

2.2 Permeability Determination Techniques

Permeability is an important parameter for many reasons, including but not limited to reservoir characterization, stimulation design, reservoir simulation, ultimate hydrocarbon recovery, well planning and placement, pressure analysis, and an understanding of fluid contact (Lacentre & Carrica, 2003). Permeability determination is commonly found from laboratory core analysis, well testing, empirically derived models, multiple regression, and virtual measurement (El-M Shokir et al., 2006, Mohaghegh et al., 1997). Permeability derived from well logs can be greatly influenced by the presence of clay (Li et al., 2015). Many of the correlations used to find permeability, including but not limited to the Timur (1968), Kozeny-Carman (1938), Coates(1974, 1981) and Berg (1970) correlations (Yao & Holditch, 1993), require the knowledge of irreducible water saturation which is a parameter that is neither easily nor reliably obtained (Bazara & Salman, 2009). While core permeability measurements are considered to be the most accurate approach for porosity and permeability determination (Smith & Ziane, 2015), it proves to be extremely costly.

Shale permeability in particular has been difficult to estimate with certainty. Common methods that have produced fairly accurate permeability results in sandstone can have very different results when applied to shales. It was determined that obtaining permeability measurements using the pulse testing method cannot measure the permeabilities exhibited in tight shales. Shale core analysis can prove challenging due to the natural fractures that many shales contain (Luffel et al., 1993).

2.3 Selective Stimulation Optimization

Having an understanding of porosity and permeability within a zone of interest can prove valuable for stimulation design and optimization. Finding reservoir characteristics such as porosity and permeability is commonly done by laboratory analysis on core or cuttings from the point of interest within a well. It has been previously stated that the most accurate way to measure key reservoir parameters is a combination of gamma ray log measurements, sonic log measurements, and core analysis for the well in question (Ortega & Aguilera, 2012). Selective stimulation in horizontal wells can greatly benefit production and hydrocarbon recovery, and having an understanding of porosity and permeability values throughout the lateral can allow for better fracturing placement, direction, and number of stages.

CHAPTER III

METHODOLOGY

The use of drilling data for use in geomechanical predictions has often been overlooked. Using drilling data for porosity and permeability determination could prove beneficial to time, cost, and stimulation design. In this chapter, an investigation as to how drilling data can be used to determine porosity in three different lithologies will be performed. An analysis as to how gamma ray measurements taken at the bit will also be looked at to determine the effect on porosity in zones of varying sandstone and shale content. The development of permeability correlations for multiple sandstone and shale reservoirs is also explained. Establishing porosity and permeability correlations that allow such estimations to be found accurately and for mixed lithologies could have great potential.

3.1 Porosity Determination

Understanding the porosity within a wellbore can be important for a variety of reasons. In unconventional reservoirs, porosity can be estimated by drying, mercury intrusion techniques, gas pycnometers, but because these measurements are commonly performed on small cuttings at surface conditions can provide inaccurate values (Cui et al., 2010). Empirical models to determine porosity have been established by numerous sources, but many rely on the knowledge of residual water saturation which is a parameter that is nearly impossible to estimate. Correlations that utilize UCS for porosity determination are also available. Three of these

porosity-UCS correlations include the Onyia method, the Sarda method, and the Erfourth method. While these methods have been known to predict reasonable porosity values in sandstones, they have not been suggested as a useful porosity predictor in zones of mixed lithology (Onyia, 1988, Sarda et al., 1993, Erfourth et al., 2005).

3.1.1 Porosity-UCS Correlation Model

Drilling data can be inserted into an inverted ROP model and UCS values can be obtained. The inverted ROP model is based on the ROP model originally established by Warren (1987) for roller cone bits (Eq. 8).

$$\frac{1}{ROP} = \left(\frac{aS^2D^3}{NW^2} + \frac{b}{ND} + \frac{cD\rho\mu}{I_m}\right) \tag{8}$$

The ROP model was further modified by Hareland and Hoberock (1993) and integrated bit wear and chip hold-down effects.

$$\frac{1}{ROP} = W_f(f_c(P_e)\left[\frac{a\sigma^2D^3}{W^2N} + \frac{b}{ND}\right] + \frac{cD\rho\mu}{I_m}) \tag{9}$$

A PDC bit model was developed in 1994 (Hareland & Rampersad, 1994) and later modified to solve for confined rock strength (Hareland & Nygaard, 2007) as in Eq. 10.

$$S = \left(\frac{\frac{ROP}{W_f}[RPM*WOB^{(2-b_s)}]}{a*d_b^2}\right)^{\frac{1}{(2-b_s)}} \tag{10}$$

Kerkar et al. (2014) further revised the ROP model for PDC bits, which includes bit wear and bit hydraulics and the equation solved for rock strength is shown in Eq. 11.

$$CCS = \left[\frac{\left(\frac{ROP}{K_1*WOB*RPM^{b_1}*\cos(SR)*W_f*h(x)*b(x)}\right)}{D_B*\tan(BR)}\right]^{\left(\frac{1}{c_1}\right)} \tag{11}$$

Eq.'s (8), (9), (10), and (11) relate ROP to confined compressive strength (CCS), so to determine UCS values, a correlation relating UCS and CCS is used and shown in Eq. (12) (Kerkar et al., 2014).

$$UCS = \frac{CCS}{1+a_s Pc^{b_s}} \quad (12)$$

To determine a correlation between UCS and porosity, laboratory data for various sandstone and shale formations were collected and plotted. A correlation to fit the sandstone data as well as the shale data was developed and will be presented in Chapter IV.

The data used to develop the Cedola sandstone and Cedola shale equations as well as the references from where the data was obtained is listed in Appendix A. To verify the accuracy of both the Cedola sandstone and Cedola shale porosity correlations, a comparison between the two Cedola porosity correlations and the Onyia, Sarda, and Erfourth methods is done. Drilling and log data from three previously drilled wells located in Alberta, Canada were used to determine the accuracy of all of these correlations.

3.1.2 Gamma Ray Porosity

To establish a correlation that can be used to determine porosity in zones with varying sandstone and shale content, gamma ray measurements taken at the bit are considered. Gamma ray logging tools work by measuring radiation levels that are emitted by formation rocks (Crawford & Gaillot, 2010). Because rocks with different types of lithological composition can emit various levels of radiation, the gamma ray log is able to distinctly identify transitions between sandstones and shales (Crawford & Gaillot, 2010). Using gamma ray measurements and the Cedola sandstone and Cedola shale correlations, a correlation for determining porosity in mixed lithology zones is established (Eq. 13).

$$\emptyset_{power\ Gamma\ Ray} = \emptyset_{Cedola\ Shale} + (\emptyset_{Cedola\ Sandstone} - \emptyset_{Cedola\ Shale}) * (\frac{140-GR\ API}{140-40})^{a_1} \quad (13)$$

The power Gamma Ray correlation is compared to neutron log porosity for a mixed lithology reservoir to verify for accuracy.

3.2 Permeability Determination

Permeability prediction has been done by core analysis and correlations using the following log data: Gamma Ray log, Density log, Medium Induction Resistivity log, and Photoelectric logs (Manseur et al., 2002). In horizontal wells, drill cuttings analysis is a common method for permeability determination because they can be indicative of lithologic parameters for specific zones of investigation. While drill cuttings analysis can provide reasonably accurate permeability measurements, the depth at which the cuttings are collected must be established for optimal stimulation design (Ortega & Aguilera, 2014). Using conventional drilling data (i.e. weight on bit (WOB), rate of penetration (ROP), bit rotational speed, bit diameter, formation overbalance, bit wear function, bit hydraulics function, and bit design parameters) to establish a correlation for permeability determination in sandstone and shale reservoirs would reduce the need for logging and coring as well as the uncertainty of measurements found from drill cuttings. While the combination of UCS and permeability data is scarce for both sandstone and shale lithologies, permeability and porosity data is readily available. For this reason, permeability and porosity data from multiple sandstone and shale reservoirs has been collected and plotted. A porosity-permeability correlation for each individual reservoir is developed. Using the collected porosity data, the Cedola sandstone and Cedola shale correlations are rearranged and used to provide UCS values for the respective sandstone and shale reservoirs. Knowing that the porosity and permeability data has been collected concurrently, the correlated UCS values can be plotted against permeability for the individual reservoirs. Using the sandstone and shale UCS versus permeability plots, a correlation between UCS and permeability is established for any particular reservoir.

To demonstrate the accuracy of the permeability correlations, previously published UCS and permeability data for the Montney shale, Bakken shale, and Cardium sandstone formations were gathered (Ghanizadeh et al., 2014). Using the provided range of UCS values, the Cedola sandstone and shale correlations were used to determine porosity values. Utilizing the porosity-permeability correlation for the provided formations, permeability values have been found. The collected UCS and permeability data as well as the correlated UCS and permeability data are plotted to observe whether the two are similar.

To show real-well potential for the permeability correlations, porosity and permeability data found through laboratory analysis for the Nikanassin sandstone and Montney shale are collected. The collected porosity date are used in the respective Nikanassin or Montney permeability correlation and a correlated permeability is determined. Collected permeability and correlated permeability are compared in order to provide insight as to whether the permeability correlations are applicable to actual field data. The UCS as determined from the Cedola sandstone and Cedola shale correlations are also plotted to visualize UCS behavior with permeability variations.

CHAPTER IV

RESULTS & DISCUSSION

4.1 Porosity Correlations

The development of porosity and permeability correlations for different lithologies requires porosity, permeability, and UCS data for various formations or reservoirs. The Cedola sandstone correlations have been developed utilizing UCS and porosity laboratory data for various sandstone reservoirs. The correlation was established by finding the best fit amongst the collected data and is considered applicable for porosity determination for any sandstone lithology zones. The Cedola shale correlation has been established in the same manner as the Cedola sandstone correlation but with various shale reservoir UCS and porosity laboratory values. The power Gamma Ray porosity correlation requires gamma ray log measurements for porosity prediction in zones containing mixed lithology. The permeability correlations presented in this chapter are made for individual sandstone or shale reservoirs rather than a universal correlation.

4.1.1 Cedola Sandstone Correlation

To develop a correlation between UCS and porosity for sandstone lithologies, data for various sandstone reservoirs are collected and plotted in Fig. 1 (Farquhar et al., 1993, Khaksar et al., 2009, Hawkins & McConnell, 1991, Chang, 2004, Kim et al., 2015, Valdes, 2013, Bowen, 2015).

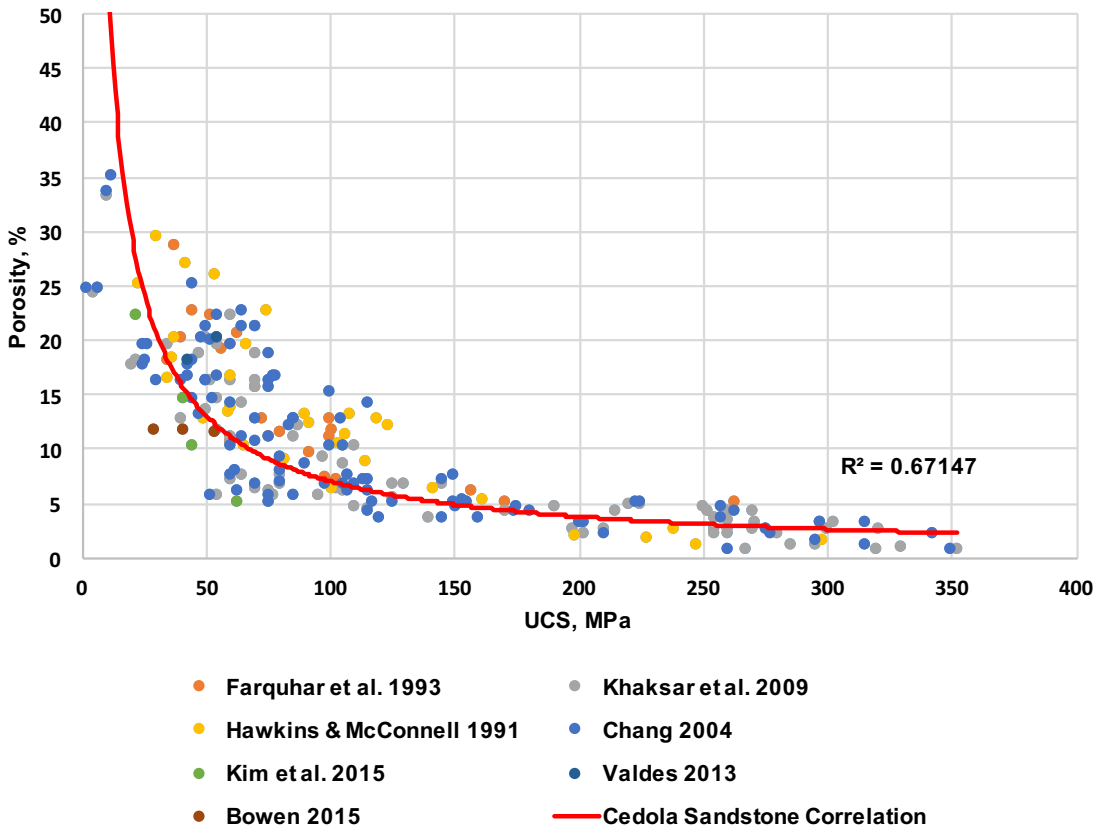

Figure 1. Cedola Sandstone Correlation

The UCS values for the collected data were found from laboratory testing, but the Cedola sandstone correlation is able to use UCS values obtained from drilling data measurements (Eq. 14).

$$\emptyset_{Cedola\ Sandstone} = 424.8 * UCS^{-0.89} \tag{14}$$

To evaluate the Cedola sandstone correlation, a comparison between the Cedola sandstone correlation, Onyia method, Sarda method, and Erfourth method is done (Fig. 2).

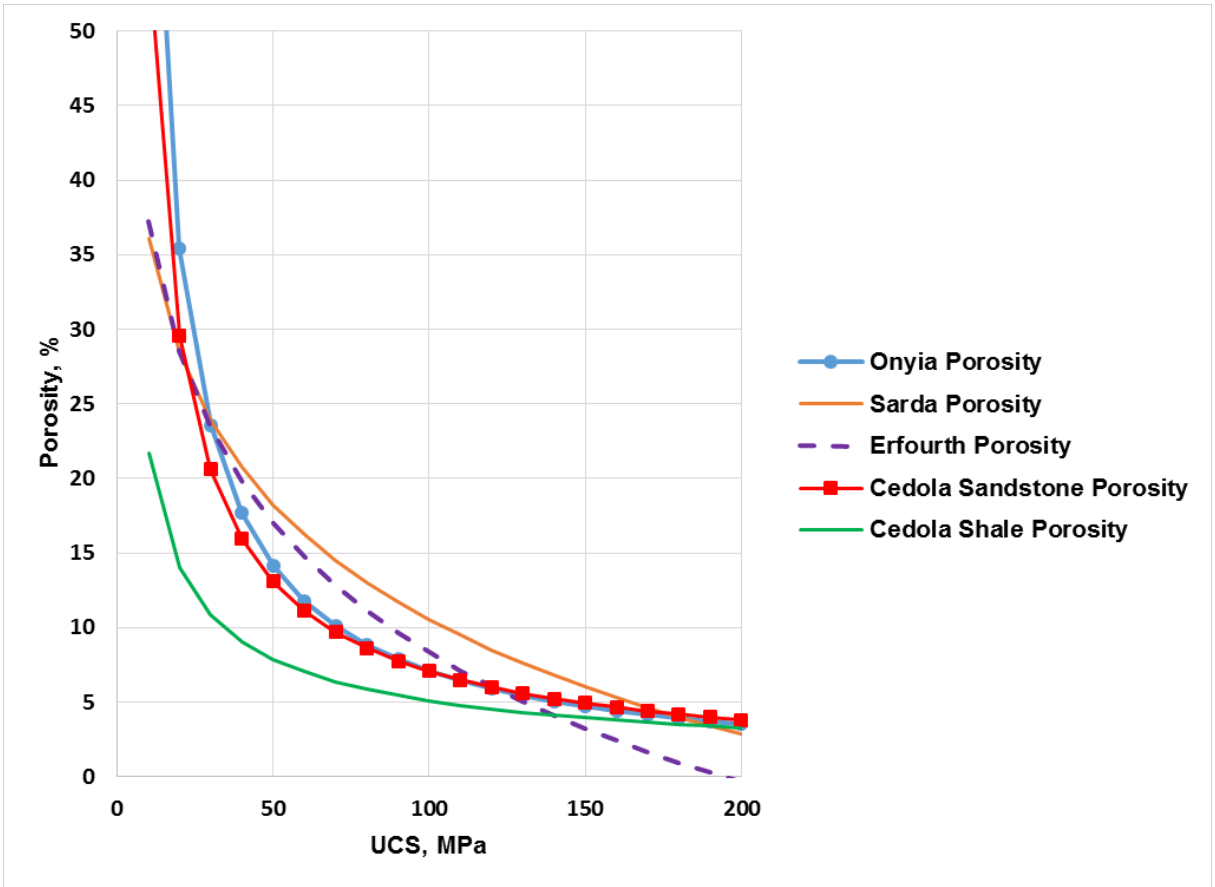

Figure 2. Comparison between the Cedola sandstone correlation and the Onyia, Sarda, and Erfourth porosity methods.

Drilling and log data for three previously drilled wells located in Alberta, Canada are collected and sandstone formation depth intervals identified. For these sandstone depth intervals, neutron porosity data are plotted and the drilling data and inverted ROP model were utilized to obtain UCS values. The UCS values were used to determine porosity from the Cedola sandstone correlation, Onyia method, Sarda method, and Erfourth method. To observe how the previously published correlations compare to the neutron porosity, a plot containing the Onyia porosity, Sarda porosity, Erfourth porosity, and neutron porosity for the Falher sandstone formation has been created (Fig. 3). The Cedola sandstone porosity data for the same Falher sandstone interval are also compared to the neutron porosity in Fig. 4.

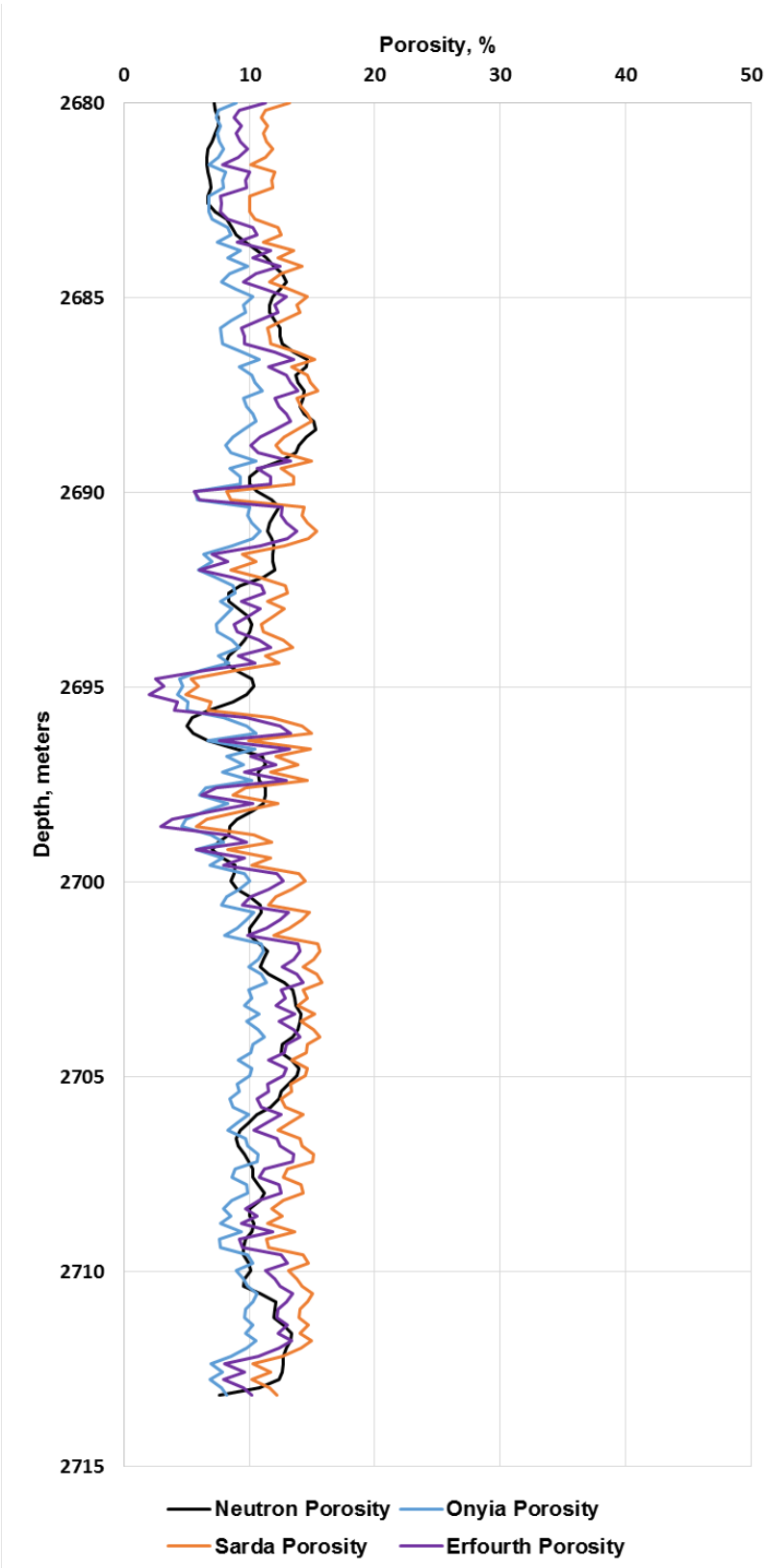

Figure 3. Neutron log porosity comparison to the Onyia, Sarda, and Erfourth correlations for the Falher sandstone.

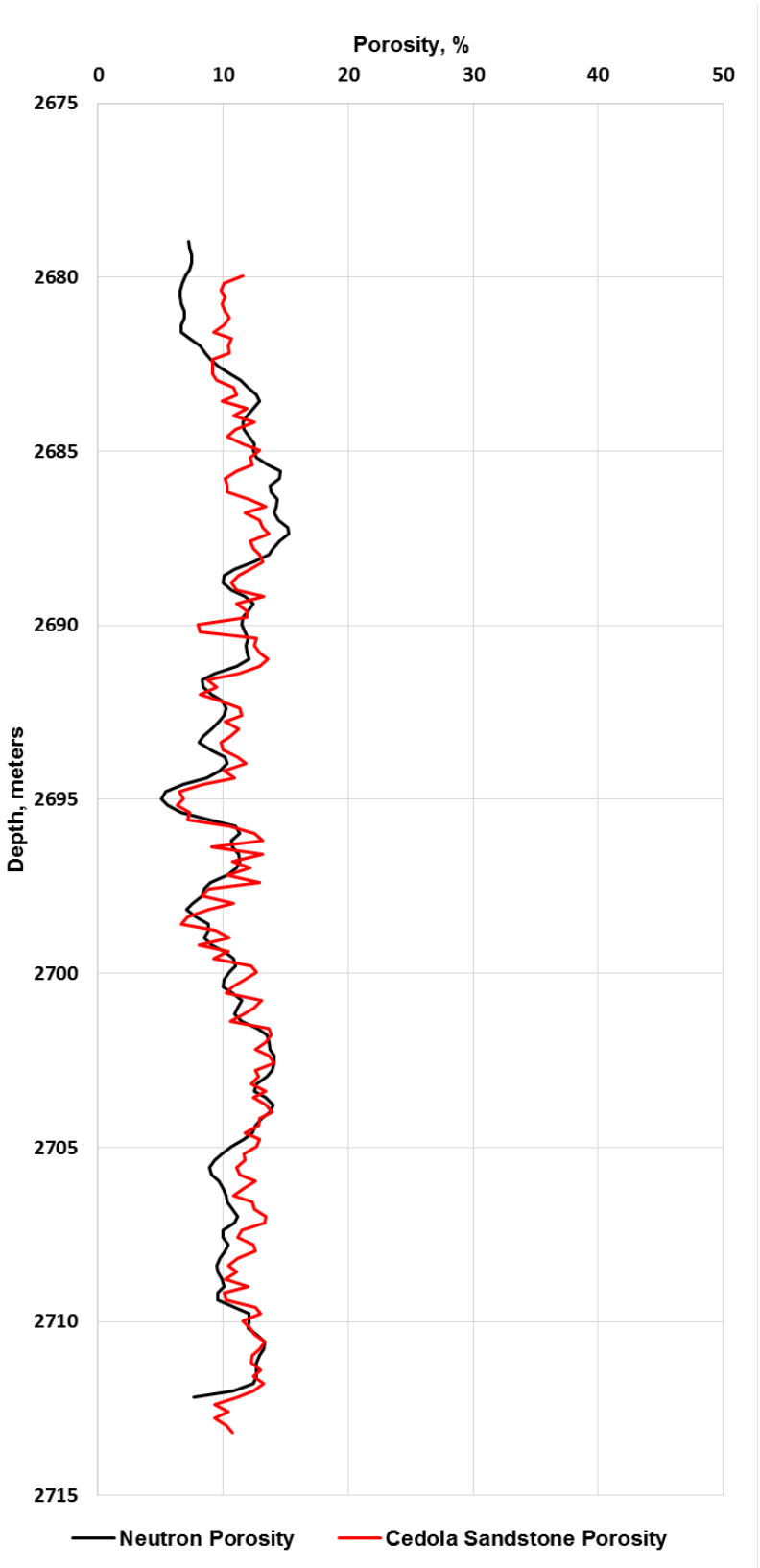

Figure 4. Neutron log porosity comparison to the Cedola sandstone correlation for the Falher sandstone.

4.1.2 Cedola Shale Correlation

Knowing UCS measurements are distinctly different in sandstones and shales, UCS and porosity data are collected from numerous sources (Horsrud, 2001, Chang, 2004, Lashkaripour et al., 2002) to develop a Cedola shale UCS-porosity correlation for shale (Eq. 15) (Fig. 5).

$$\emptyset_{Cedola\ Shale} = 92.429 * UCS^{-0.63} \tag{15}$$

To observe how the Cedola shale correlation compares to the Onyia, Sarda, and Erfourth porosities for a range of normalized UCS values, a plot with all four methods has been made (Fig. 6).

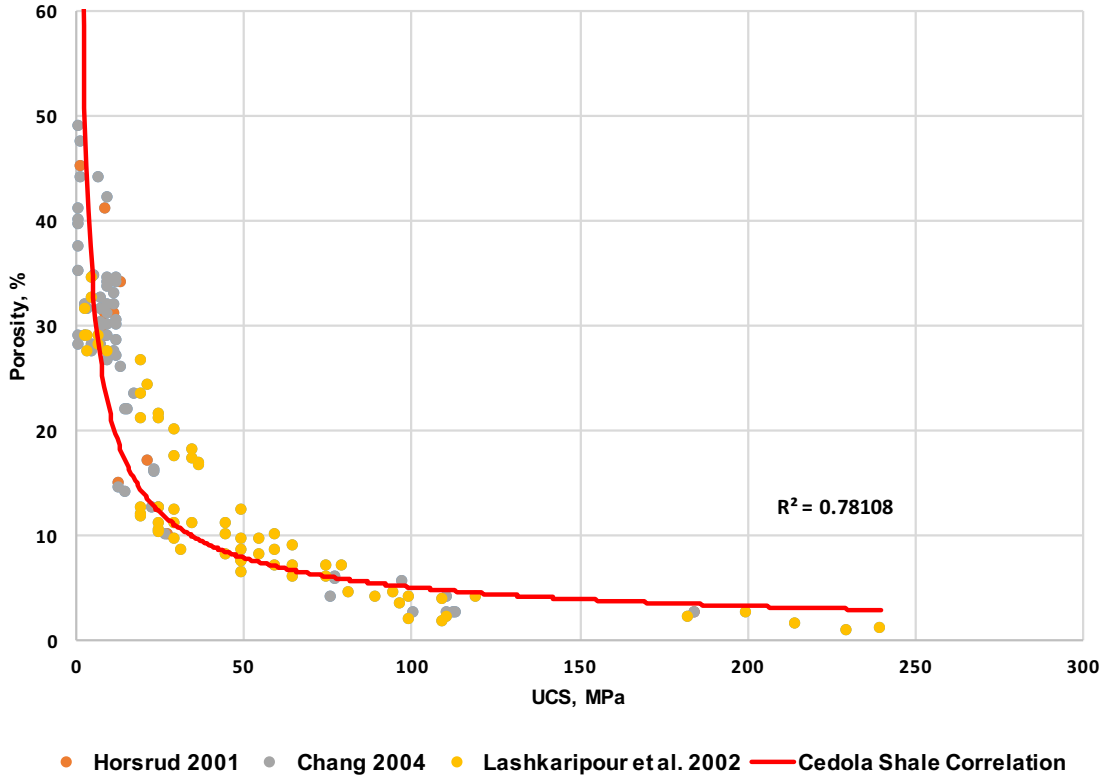

Figure 5. Cedola shale correlation.

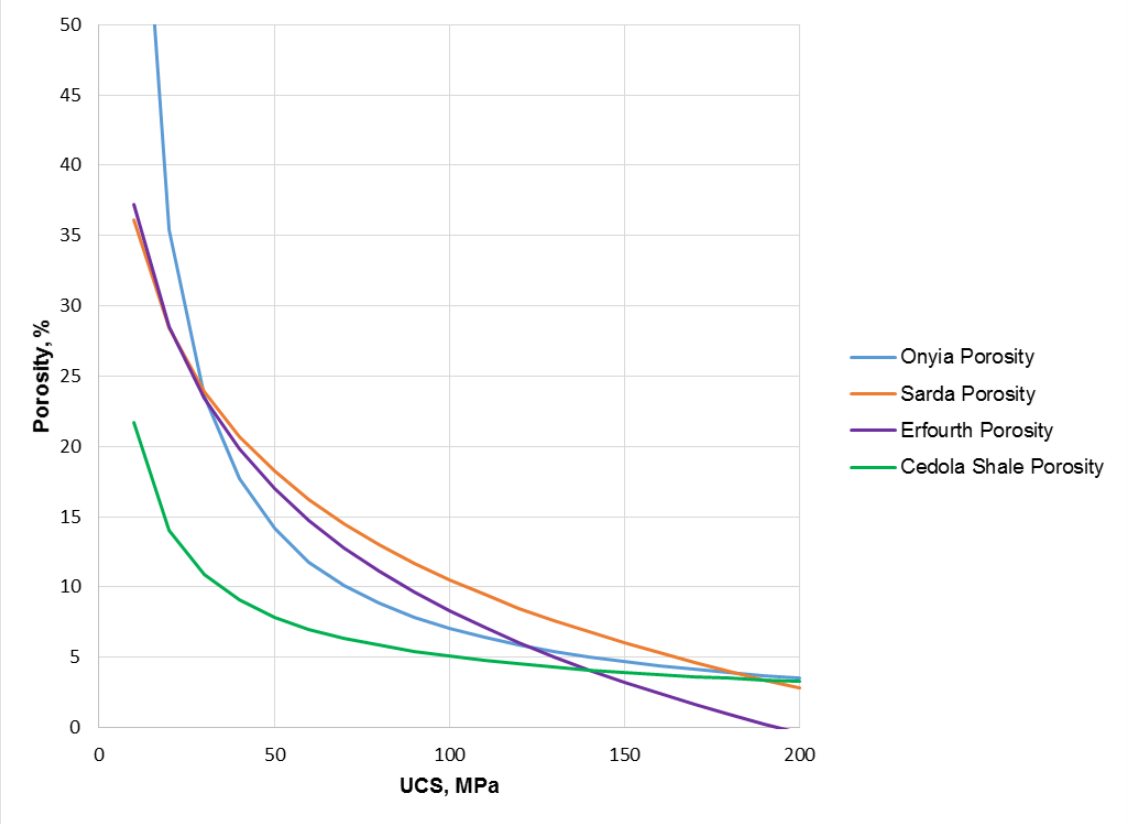

Figure 6. Comparison between the Cedola shale correlation and the Onyia, Sarda, and Erfourth porosity methods.

Again using the drilling data from the three previously drilled wells, shale lithology intervals were identified and the log and drilling data were extracted. Using the drilling data and inverted ROP model, UCS for the shale intervals were obtained and the Cedola shale correlation, Onyia method, Sarda method, and Erfourth method are used to find porosity. A porosity versus depth plot showing the neutron porosity, Onyia porosity, Sarda porosity, and Erfourth porosity allows a comparison between the data sets to be performed (Fig. 7) for the Muskiki shale formation. A second porosity versus depth plot was created to better understand how the Cedola shale correlation compared to the neutron porosity in the same Muskiki shale interval (Fig. 8).

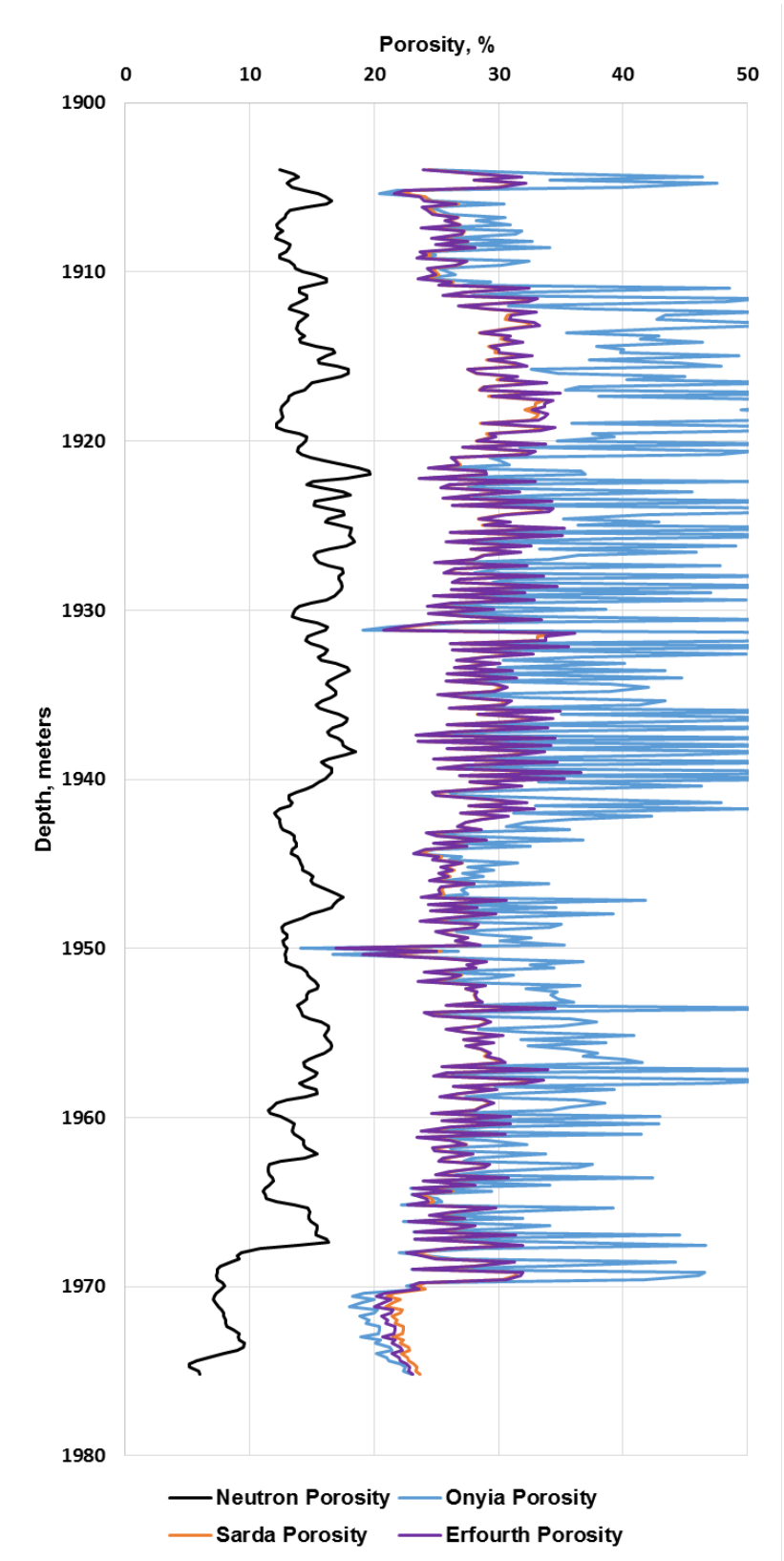

Figure 7. Neutron log porosity comparison to the Onyia, Sarda, and Erfourth correlations for the Muskiki shale.

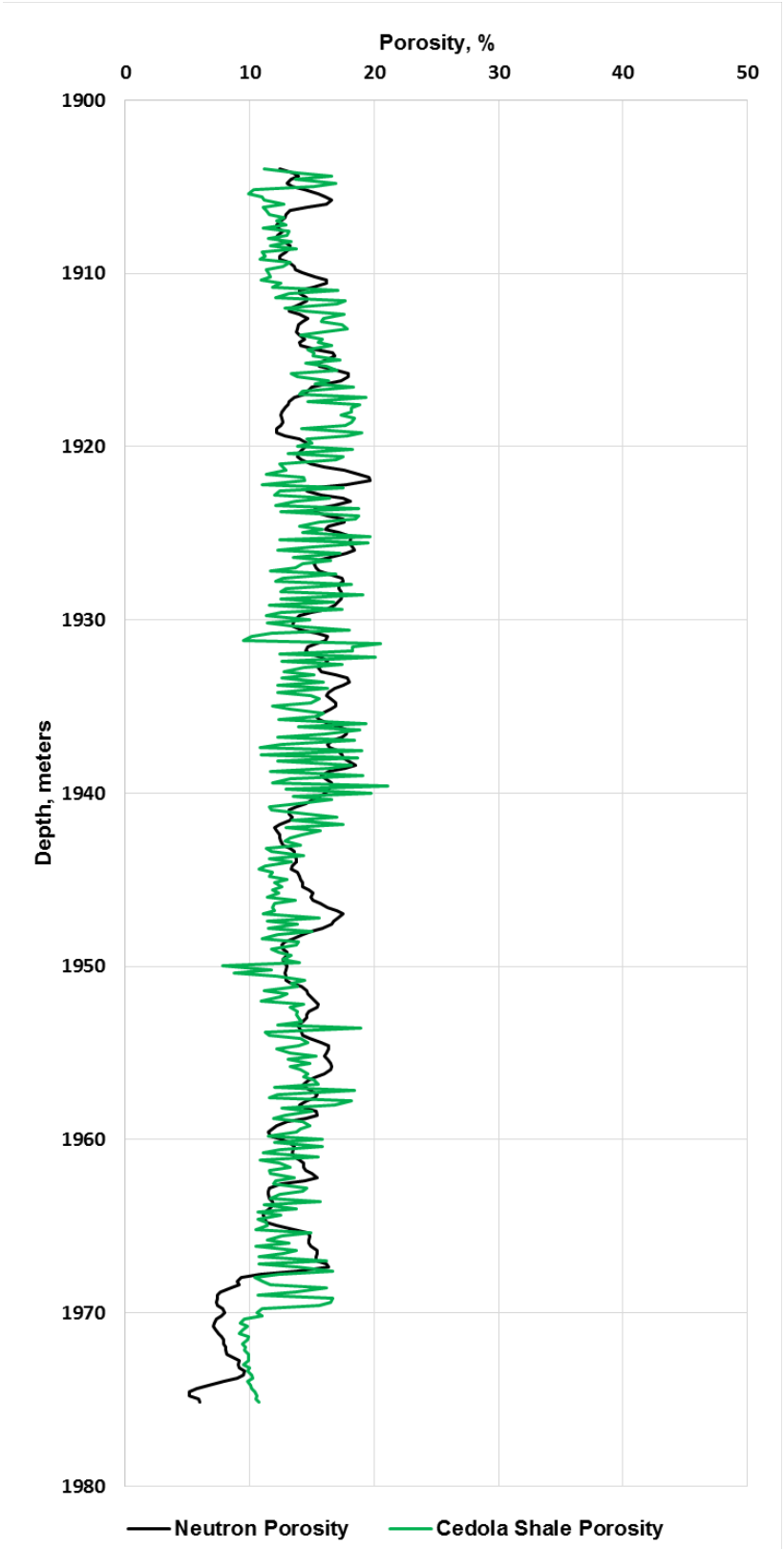

Figure 8. Neutron log porosity comparison to the Cedola shale correlation for the Muskiki shale.

4.1.3 Collected and Correlated Porosity Comparison Discussion

The focus of this section is to analyze whether the porosity correlations established within this work are accurate and feasible for real-time/real-well application. In comparison to the previously published Onyia, Sarda, and Erfourth porosities, the Cedola sandstone and Onyia porosity trends and values appear to be highly similar (Fig. 2). The Erfourth and Sarda porosities appeared similar in Trend to each other but deviated with increasing UCS. For many tight gas sandstone reservoirs, the average porosity ranges from 7-10% (Zee Ma et al. 2016). This would imply that the accuracy of the Sarda and Erfourth methods may have a higher level of uncertainty in unconventional reservoirs. The Cedola sandstone porosity and the Onyia porosity are able to predict porosity values to approximately 3% and are in agreement with one another, which could lead to less uncertainty and better potential for unconventional sandstone reservoir porosity determination.

Comparing neutron log porosity data for the Falher sandstone formation to the Onyia, Sarda, and Erfourth porosities shows that all three methods are similar in trend to the neutron porosity (Fig. 3). When the neutron porosity is above approximately 10%, the Sarda and Erfourth porosities appear to be significantly closer to the neutron porosity. The Onyia method appears to underpredict porosity and never exceeds 10%. The Cedola sandstone correlation is in good agreement with the neutron porosity. The Cedola sandstone correlation is also in agreement with average porosity values for the Falher sandstone, which has been reported to rarely exceed 15% (Harris 2014).

Comparing the Cedola shale correlation to the Onyia, Sarda, and Erfourth methods for given UCS values shows that while the Onyia and Cedola shale correlations are similar in trend, none of the previously published correlations are especially near the Cedola shale porosity data (Fig. 6). One potential reason for the gap in porosity prediction is that Sarda correlation was meant to be used

for sands and that the Erfourth method isn't specific for any lithology. The Onyia method for porosity prediction is said to be applicable to both sandstone and shale formations and does appear to predict similar values to the Cedola shale correlation at higher UCS.

Neutron log data from one of the three previously drilled Alberta wells have been used to determine the accuracy of the Onyia, Sarda, and Erfourth methods in the Muskiki shale formation. All three of the published methods overpredicted porosity (Fig. 7). A comparison between the Muskiki shale and the Cedola shale porosity shows a much better porosity match (Fig. 8). The Cedola Shale correlation appears to be closer to the average porosity range of Muskiki shale, which is reportedly between 1.7-13.4% (Bachu & Underschultz 1992).

4.1.4 Gamma Ray Porosity Correlation

While the Cedola sandstone and Cedola shale correlations are accurate in the respective formation, a correlation that incorporates both Cedola correlations as well as lithology fractions is needed for porosity determination in zones containing both lithology types. Because gamma ray logging tools work to identify the type of lithology at points within a well, these log measurements will be used to aid in establishing such a correlation. Using normalized UCS values, a linear gamma ray porosity correlation (Eq. 15), which solely utilizes the Cedola sandstone and shale correlations, set gamma ray API value, maximum gamma ray API cutoff, and minimum gamma ray API cutoff is plotted in Fig. 9.

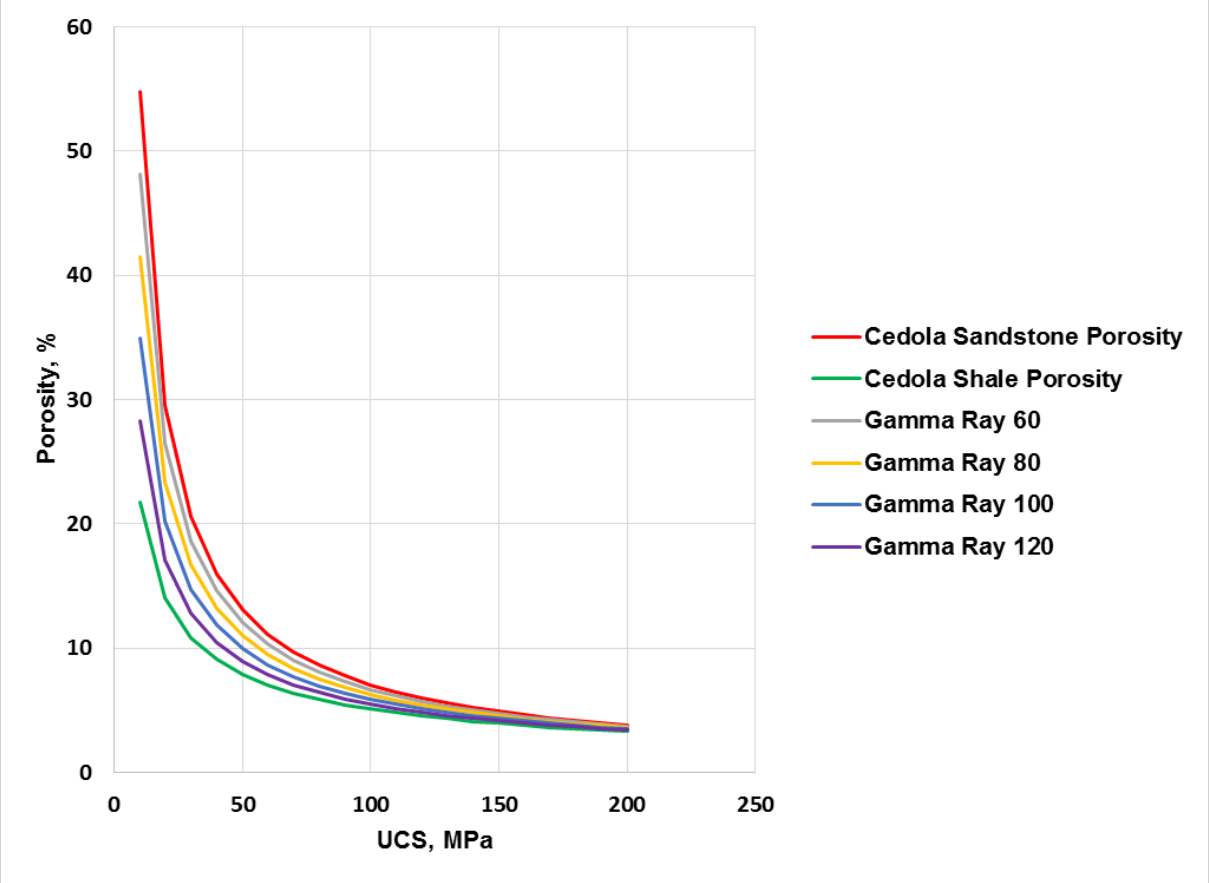

Figure 9. Linear Gamma Ray correlation plot.

The sandstone and shale API "cutoff" indicates that any gamma ray reading above a certain maximum point, which has been taken to be 140 API, and any gamma ray reading below a certain minimum API, in this case 40 API, are taken to be exclusively sandstone or shale lithologies, respectfully. This range has been verified by gamma ray measurements taken at the bit in that zones comprised completely of sandstone have shown gamma ray values slightly higher to very near 140 API while zones made up entirely of shale yield gamma ray measurements close to 40 API. The linear gamma ray correlation values are evenly spread out and don't appear to be highly indicative of lithologies containing various amounts of sand and shale. To better adjust for such lithology variation, UCS, neutron porosity, and gamma ray data from a previously drilled well is used to find sandstone and shale porosity values through the use of the Cedola correlations. The Cedola sandstone and shale porosity values were inserted into the power Gamma Ray porosity

correlation and the a1 constant from Eq. (15) was originally chosen, prior to optimization, to be 2.3. Using the same three Alberta well data sets, depth intervals that had varying sandstone and shale fractions were found and the neutron log, gamma ray log measurements, and drilling data were collected. Using the drilling data and inverted ROP model, UCS values were established and porosity have been determined using both the Cedola sandstone and Cedola shale correlations. The power Gamma Ray porosity correlation, which includes both the Cedola sandstone and Cedola shale porosity measurements as well as gamma ray API readings, appears to obtain porosity measurements that are better able to predict porosity in zones with varying sandstone and shale content. Using the power Gamma Ray correlation, a new model comparing porosity at different gamma ray log API measurements has been made (Fig. 10). Like the linear Gamma Ray plot, the lowest and highest API readings are considered to be the Cedola sandstone and the shale correlation.

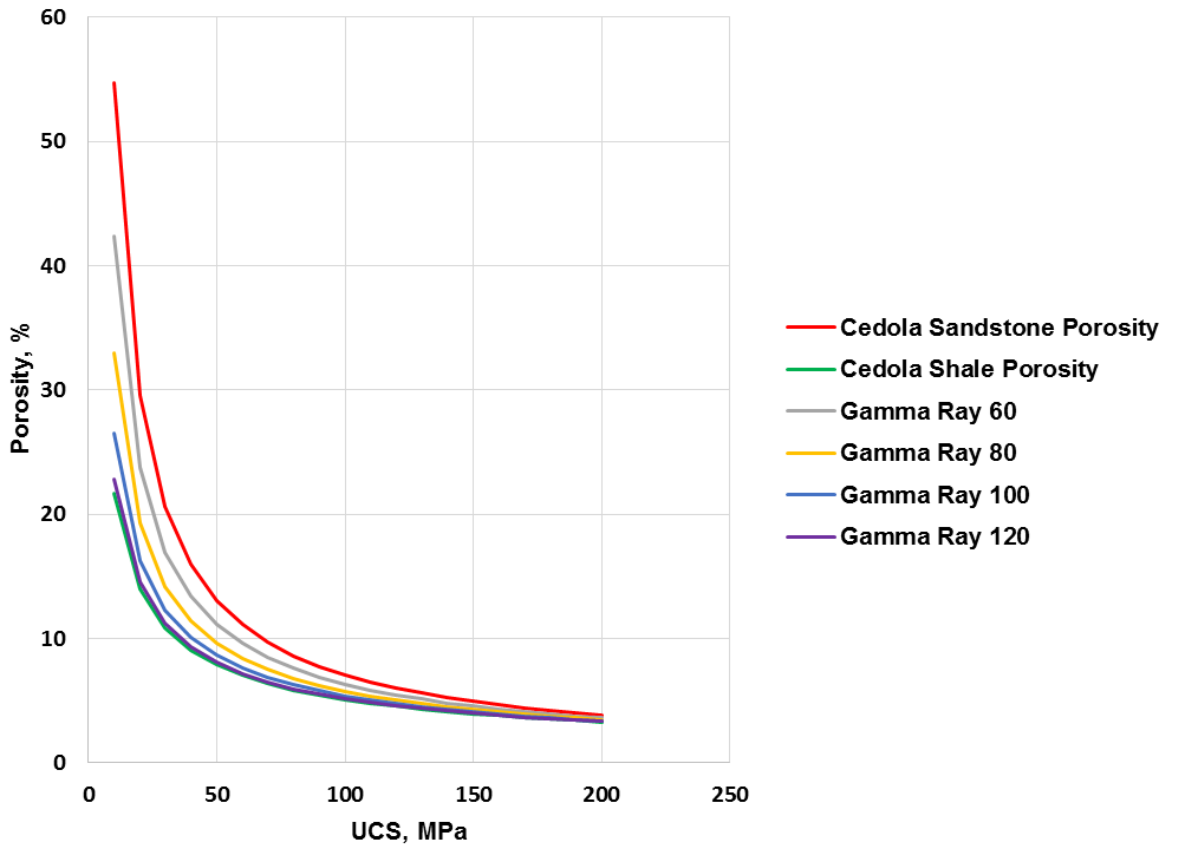

Figure 10. Power Gamma Ray correlation plot

While the original a1 constant provided reasonably accurate power Gamma Ray porosity values in mixed lithology zones, an optimization of the a1 constant is performed to ensure that the power Gamma Ray porosity is as accurate as possible. To achieve the optimal a1 constant, gamma ray and neutron porosity log data were collected for a mixed lithology interval from the previously drilled Alberta well. UCS values are found from drilling data and the inverted ROP model and are then used to find the Cedola sandstone and Cedola shale correlated porosities. The a1 constant in the power Gamma Ray porosity correlation, which will be referred to as a_ϕ, is varied and the absolute difference between the neutron log porosity and the power Gamma Ray porosity for a given constant is found for every measured point within the mixed lithology intervals. The absolute difference between the two porosities for the specified mixed lithology measurements were summed together for all a1 variations. The a_ϕ constants and the sum of the absolute difference in porosities are plotted and the optimal value is determined (Fig. 11).

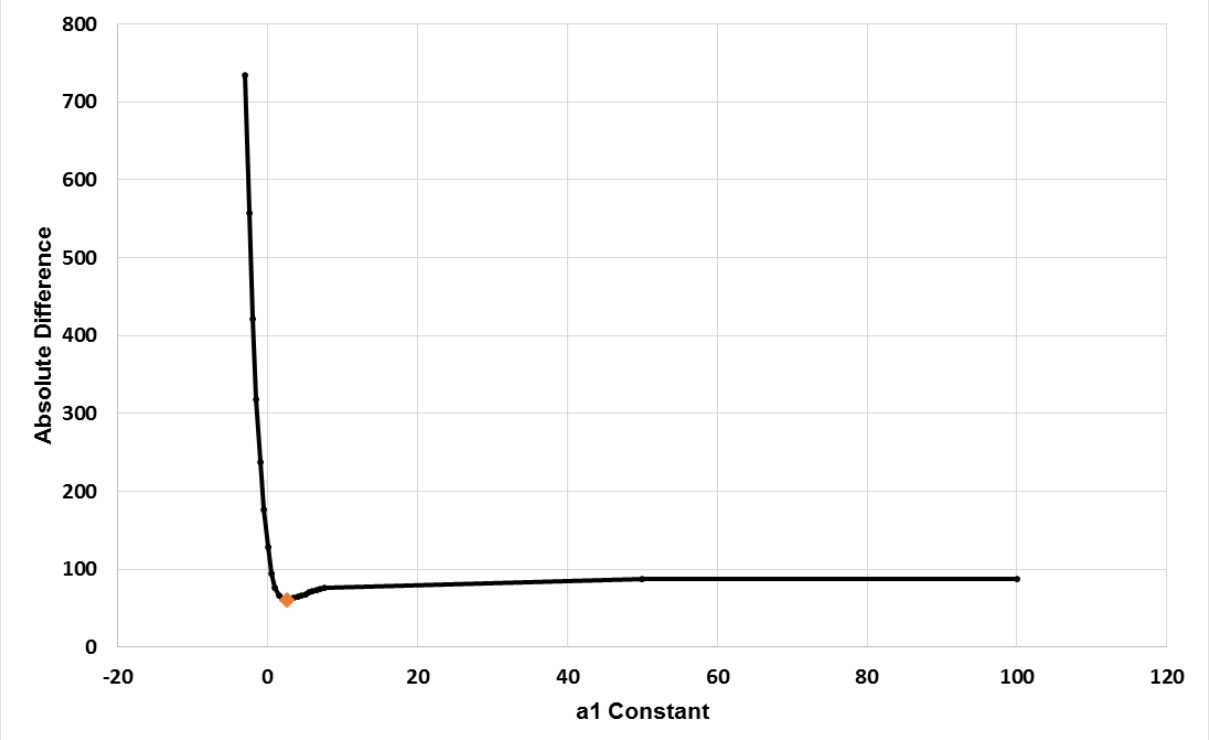

Figure 11. Power Gamma Ray porosity aϕ constant optimization.

Using the power Gamma Ray correlation with the optimal aϕ constant with a value of 2.53, a comparison between neutron porosity and the power Gamma Ray porosity are established for mixed lithology formations from UCS values obtained from the Alberta well drilling data. Porosity versus depth plots for the Dunvegan and Belly River formations are developed and include the gamma ray log readings and UCS data for the given interval (Fig. 12 & Fig. 13).

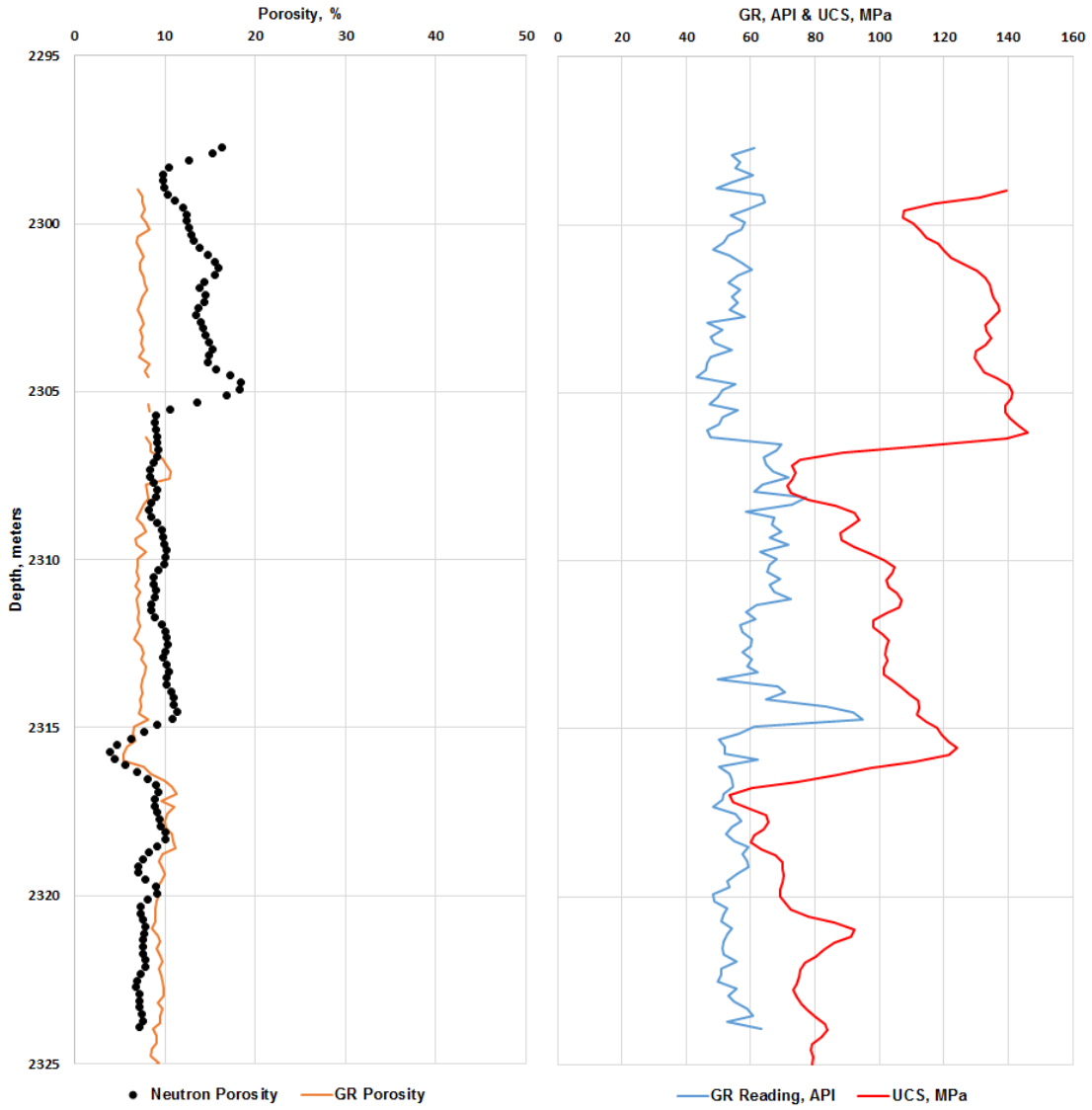

Figure 12. Dunvegan porosity, UCS, and gamma ray API data comparison.

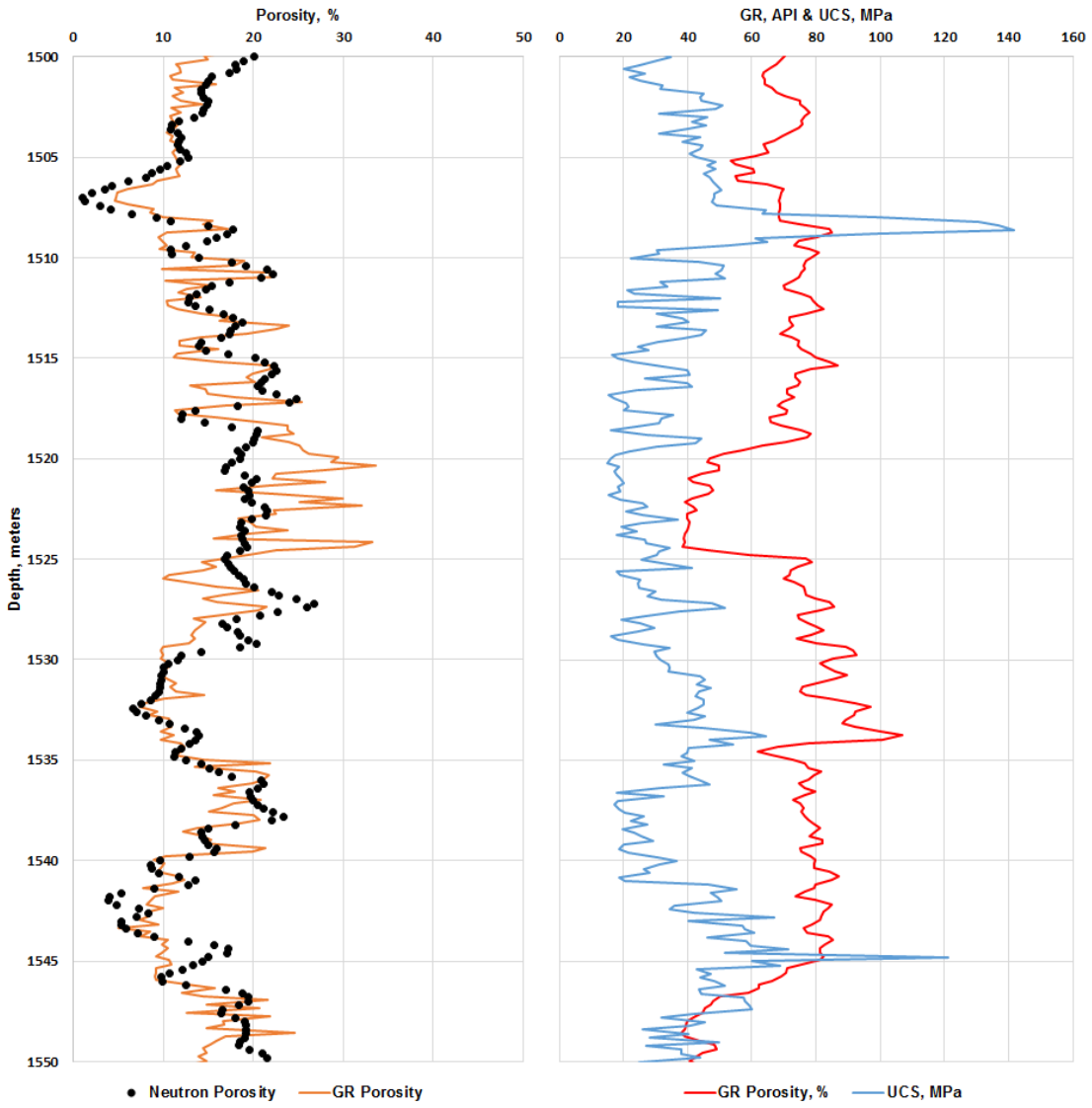

Figure 13. Belly River porosity, UCS, and gamma ray API data comparison.

The neutron porosity data for the mixed lithology Belly River interval are plotted with the power Gamma Ray correlation, Cedola sandstone correlation, and Cedola shale correlation to understand the areas where the power Gamma Ray correlation is most applicable (Fig. 14).

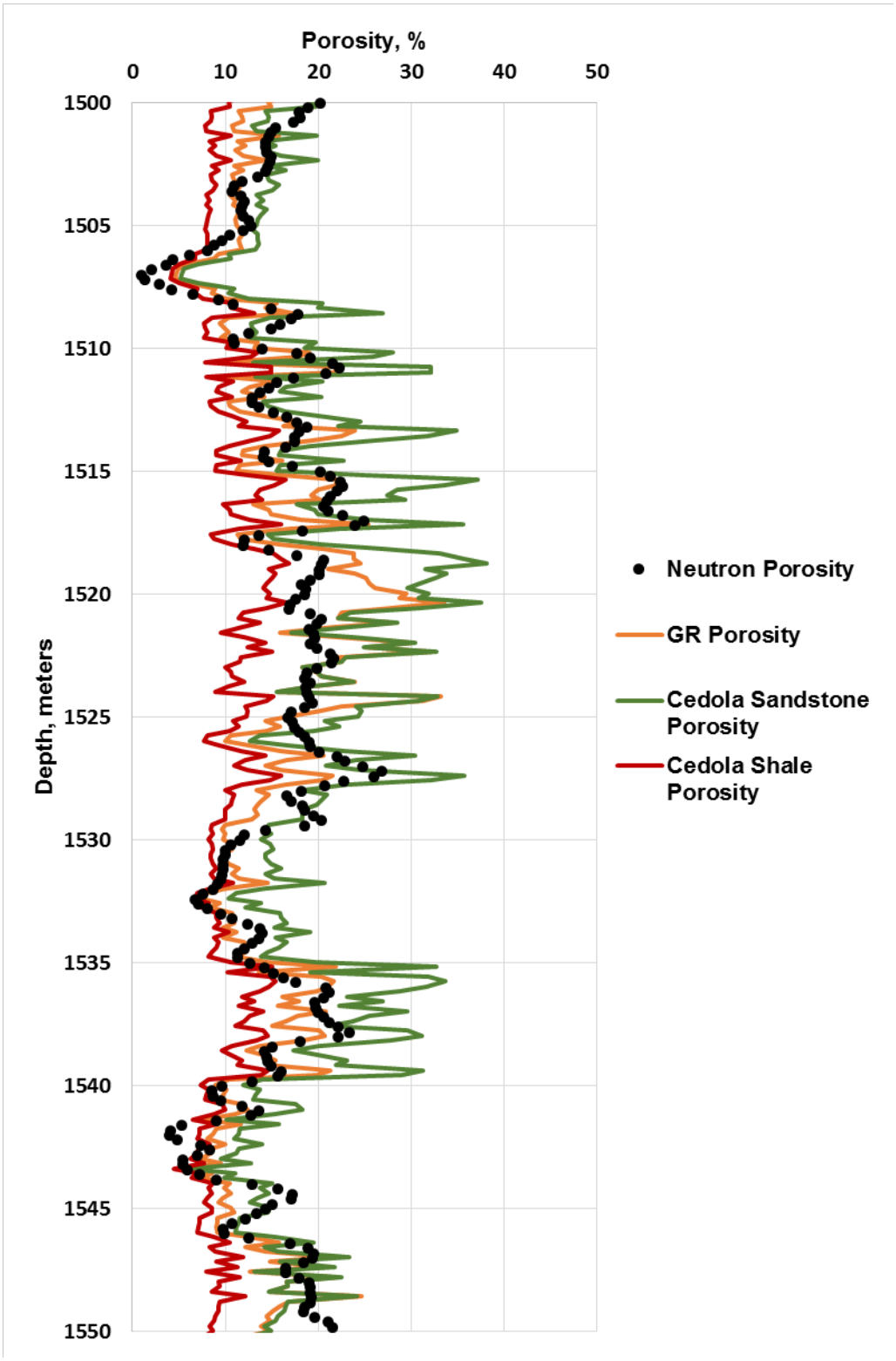

Figure 14. Comparison of neutron porosity, Cedola sandstone correlation, Cedola shale correlation, and power Gamma Ray correlation for the Belly River formation.

4.1.5 Gamma Ray Porosity Comparison Discussion

In zones containing various sand and shale content, the Cedola sandstone and shale correlations fail to provide accurate porosity values. In Fig. 15, a comparison between neutron log data for the Belly River formation and Cedola sandstone and Cedola shale correlation porosity. The Cedola sandstone correlation appears to overpredict the porosity while the Cedola shale correlation underpredicts porosity.

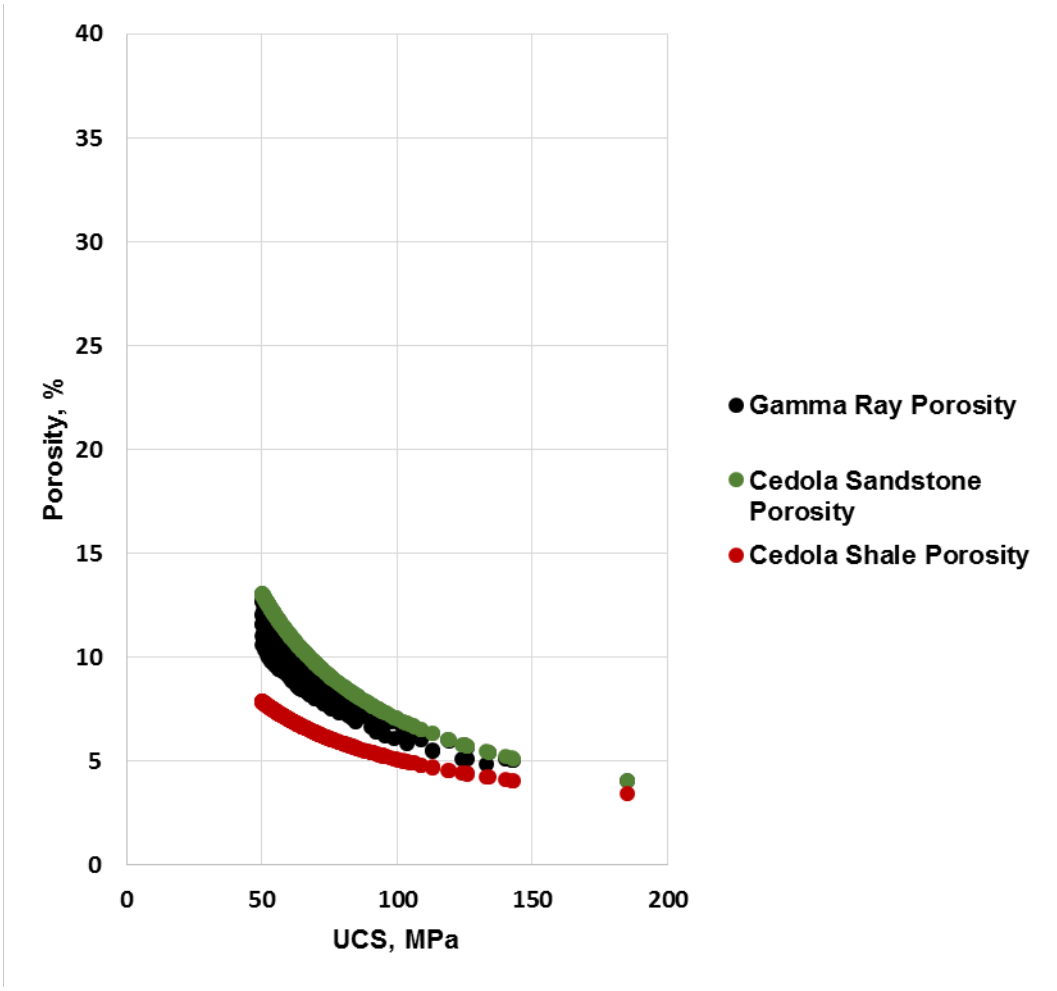

Figure 15. Belly River neutron log comparison to Cedola sandstone and Cedola shale correlation

The power Gamma Ray porosity correlation (Fig. 10) was chosen over the linear Gamma Ray correlation (Fig. 9) for mixed lithology porosity determination because this method provided

more accurate predictions. Gamma ray logs readings are highly influenced by sandstone and shale volume. This means that by using the power Gamma Ray correlation, porosity estimation is affected by the amount of sandstone or shale. For the mixed lithology Dunvegan formation, the power Gamma Ray correlation and neutron log porosity appear to be fairly similar in value and trend (Fig. 12). The power Gamma Ray correlation seems to better predict porosity when UCS is lower. A comparison between the power Gamma Ray correlation and neutron porosity for the Belly River formation shows that the power Gamma Ray porosity is in good agreement with neutron porosity values (Fig. 13). The correlated porosity exhibits the same trend between UCS and porosity as seen in Fig. 1 & Fig. 2. When UCS is higher, there is a decreased porosity. Examining the gamma ray log data and comparing it to both the power Gamma Ray porosity correlation and the neutron porosity a reverse response is seen. Plotting the Cedola sandstone, Cedola shale, power Gamma Ray porosity, and neutron porosity for the Belly River formation (Fig. 14) shows that in zones where the lithology is not solely sandstone or shale, the Cedola correlations are inaccurate. In these mixed lithology zones, the power Gamma Ray porosity is highly accurate. Depending on the sandstone and shale content, the Cedola sandstone or shale correlation is closer to the neutron porosity.

4.2 Permeability Determination

The goal of this section is to develop a correlation between permeability and UCS for numerous sandstone and shale reservoirs. Establishing a correlation between UCS found from conventional drilling data and permeability for individual lithologies requires knowledge and collection of porosity and permeability or permeability and UCS data for individual sandstone and shale reservoirs. UCS and permeability data are not commonly published for either sandstone or shale lithologies. Because the data is lacking, porosity and permeability data for numerous sandstone and shale reservoirs have been collected. The porosity and permeability measurements used in this section were performed on laboratory cores or cuttings analysis.

4.2.1 Sandstone Permeability Correlation

Sandstone porosity and permeability data have been collected and plotted for Cardium Type II, Cardium Type III, Nikanassin drill cuttings, and Nikanassin cores in Fig. 16 (Aguilera 2013).

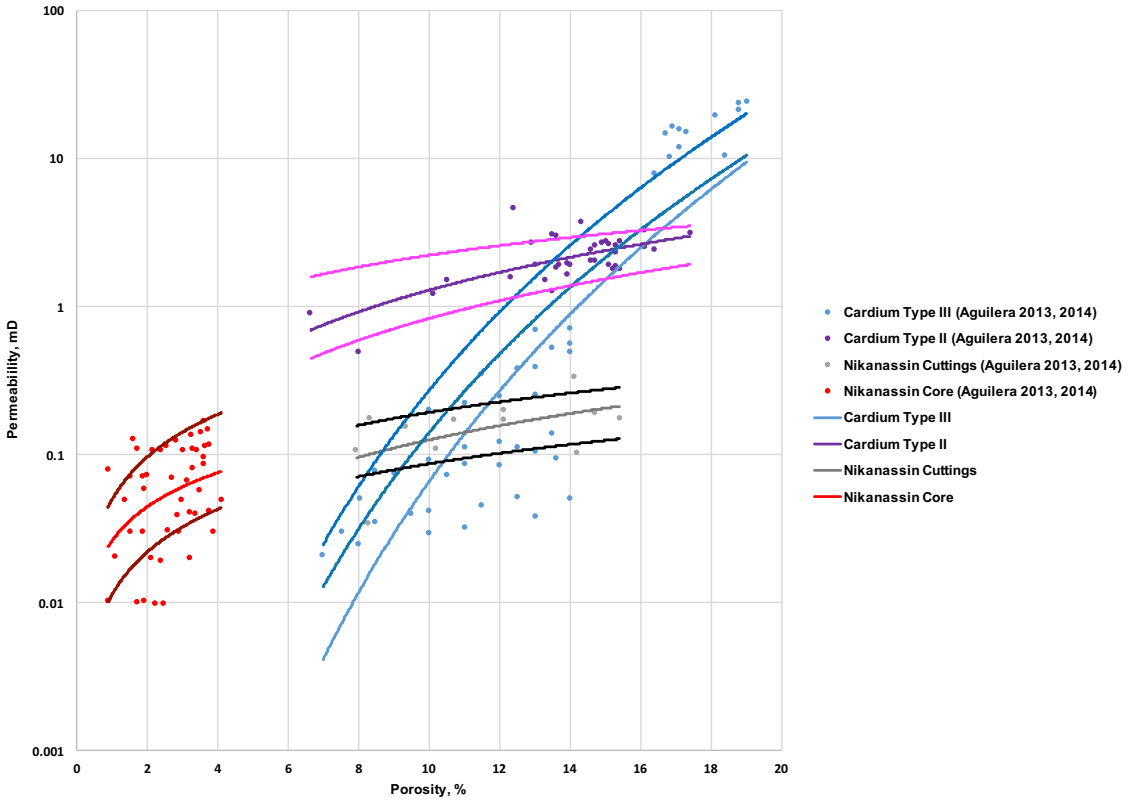

Figure 16. Collected sandstone porosity and permeability data.

Because of the difference in the amount of reservoir data, the standard deviation is used to show the possibility of the correlations being slightly higher or lower than the provided measurements. From the present data, a porosity-permeability correlation for each of the four reservoirs are found. The porosity-permeability correlations for all sandstone reservoirs are of the same form (Eq. 16).

$$k = a\emptyset^{b} \tag{16}$$

The a and b values, which are lithology constants, vary for different formations (Eq. 17, Eq. 18, Eq. 19, Eq. 20).

$$k_{Cardium\ Type\ III} = 1E(-08)\emptyset^{7.0876} \quad (17)$$

$$k_{Cardium\ Type\ II} = 0.0394\emptyset^{1.514} \quad (18)$$

$$k_{Nikanassin\ Cuttings} = 0.0179\emptyset^{0.8915} \quad (19)$$

$$k_{Nikanassin\ Cores} = 0.0306\emptyset^{0.9526} \quad (20)$$

The Cedola sandstone porosity correlation is rearranged so that UCS is a function of porosity (Eq. 21).

$$UCS_{Sandstone} = 419.99\emptyset^{-0.754} \quad (21)$$

Using the porosity data from the sandstone porosity-permeability plot, UCS data were found for each porosity measurement. Knowing that the porosity and permeability data have been taken simultaneously, the UCS and permeability measurements for a particular porosity value are plotted (Fig. 17).

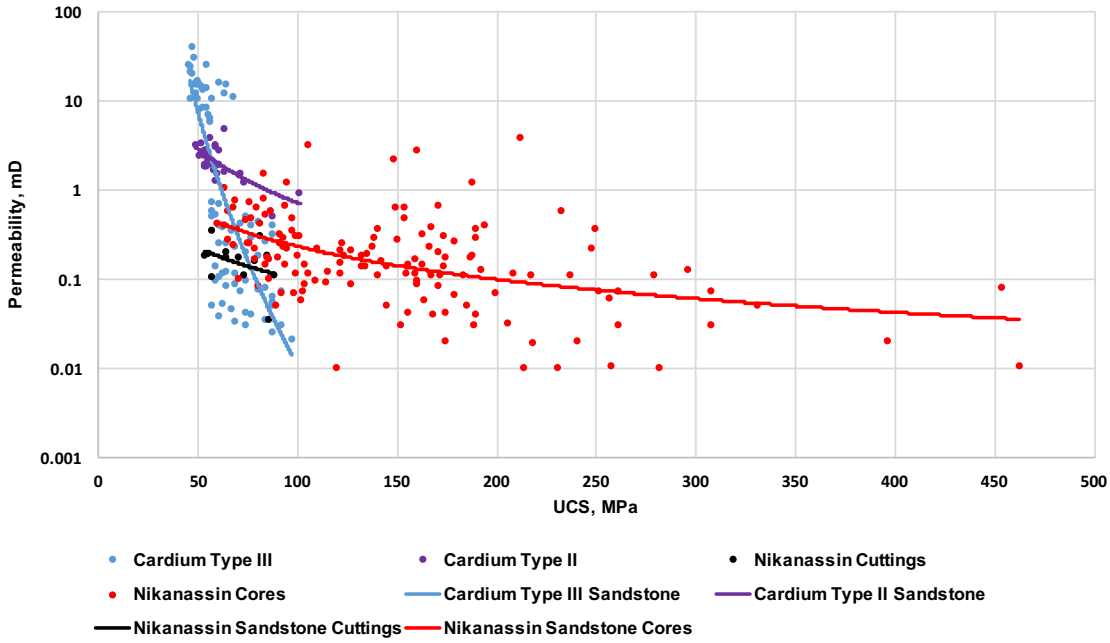

Figure 17. Sandstone permeability-UCS correlations.

4.2.2 Shale Permeability Determination

Porosity and permeability data for the Fayetteville shale, Bakken shale, Horn River/Barnett shale, and Montney shale have been collected and plotted in Fig. 18 (Aguilera 2013). Using standard deviation, an upper and lower margin of error has been plotted.

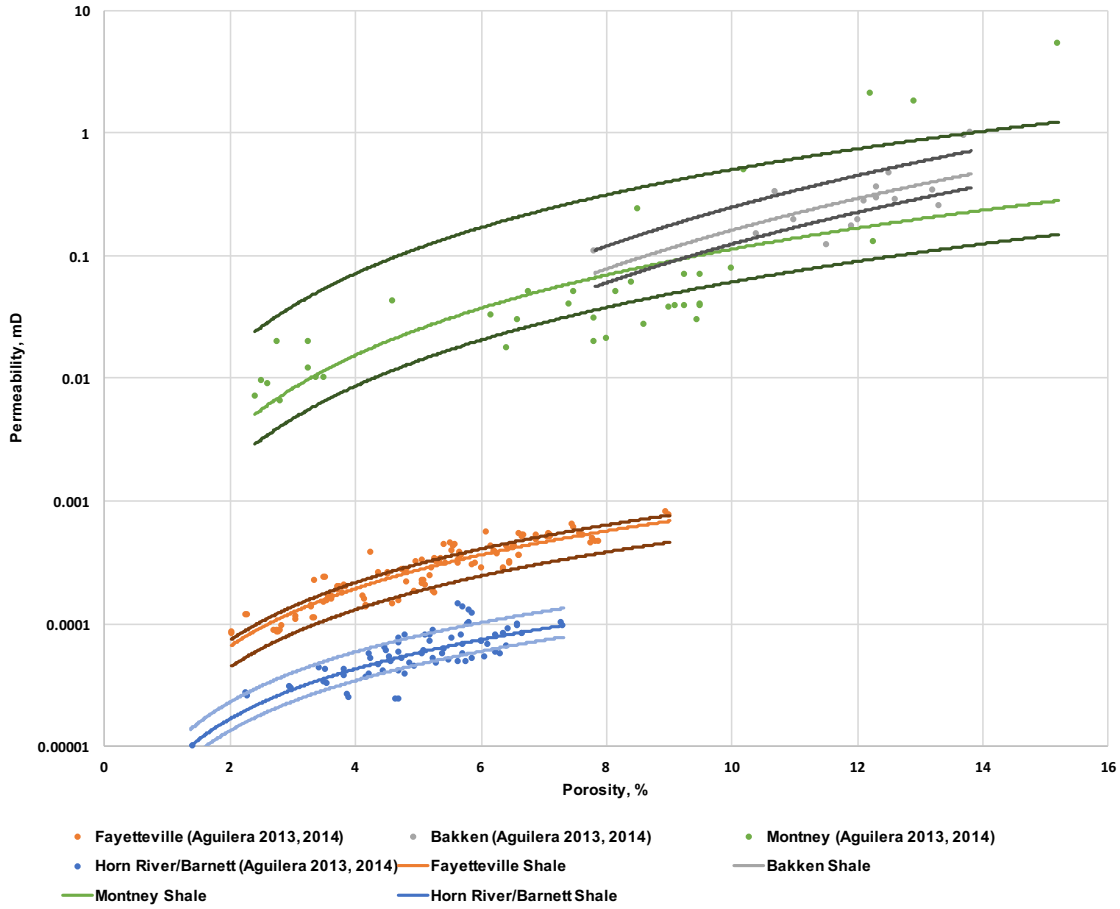

Figure 18. Collected shale porosity and permeability data.

Using the collected shale porosity data, UCS values can be found by rearranging the Cedola shale correlation (Eq. 22).

$$UCS_{Shale} = 525.52\emptyset^{-1.239} \tag{22}$$

Porosity and permeability measurements are taken concurrently and the collected permeability and UCS values are plotted for the individual reservoirs (Fig. 19). The porosity-permeability correlations for the shale reservoirs are all of the same form (Eq. 16) with different a and b values. The porosity-permeability correlations for the plotted shale reservoirs are expressed in Eq. (22), Eq. (23). Eq. (24), and Eq. (25).

$$k_{Fayetteville} = 2E(-05) * \emptyset^{1.5569} \tag{23}$$

$$k_{Bakken} = 9E(-05) * \emptyset^{3.2629} \quad (24)$$

$$k_{Horn\ River/Barnett} = 7E(-06) * \emptyset^{1.3539} \quad (25)$$

$$k_{Montney} = 0.0006 * \emptyset^{2.129} \quad (26)$$

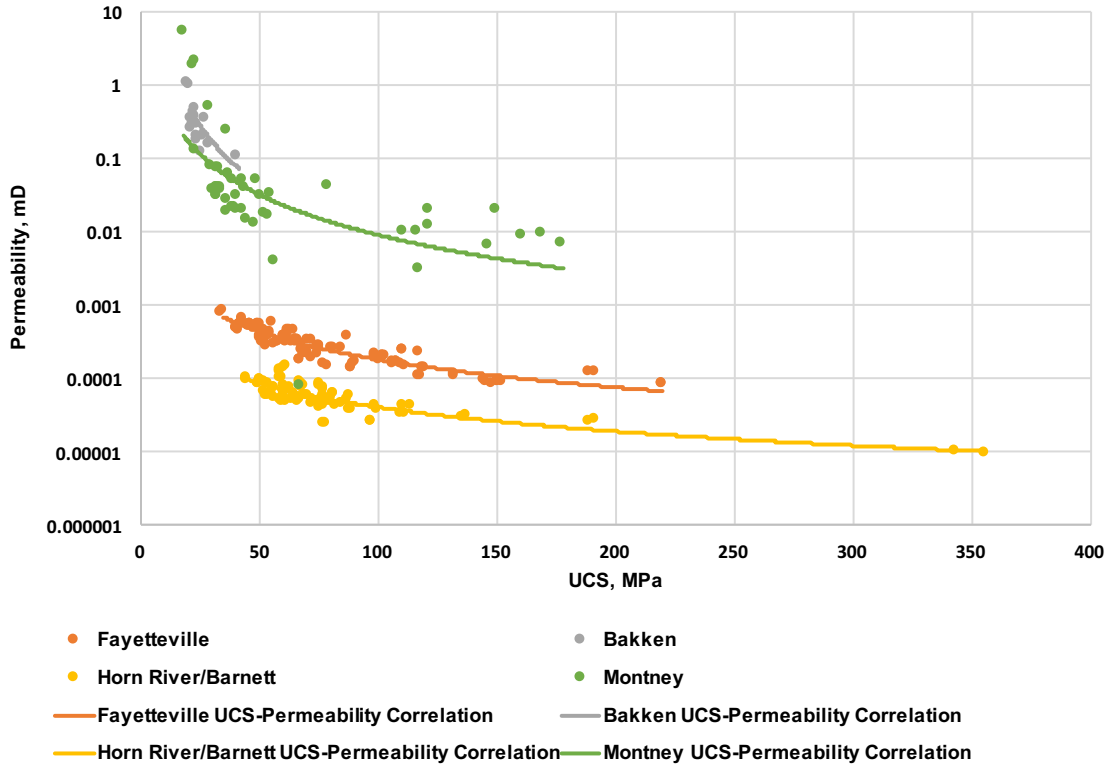

Figure 19. Shale permeability-UCS correlations.

4.2.3 Permeability Correlations Verification

UCS and permeability data for the Bakken shale, Montney shale, and Cardium sandstone reservoirs have been published by Ghanizadeh et al. (2014) and used to compare the permeability correlation to the reported permeability values. Taking a range of UCS values, porosity data specific for the Bakken shale, Montney shale, and Cardium sandstone reservoirs are found using the respective Cedola sandstone (Eq. 14) or Cedola shale correlation (Eq. 15). Using the porosity

values, the porosity-permeability correlations for the Bakken, Montney, and Cardium reservoirs are used to determine permeability from porosity. The permeability values are plotted for the corresponding UCS values.

$$k_{Bakken} = 234.43 \times UCS^{-2.056} \quad (27)$$

$$k_{Montney} = 9.2121 \times UCS^{-1.341} \quad (28)$$

$$k_{Cardium} = 375.46 \times UCS^{-1.347} \quad (29)$$

A plot with the original Bakken, Montney, and Cardium measurements as well as the correlated permeability values for these reservoirs at given UCS values (Fig. 20). Nikanassin sandstone correlated permeabilities have also been plotted in Fig. 19 to determine whether there is a similarity between trend and/or permeability values for different sandstone reservoirs.

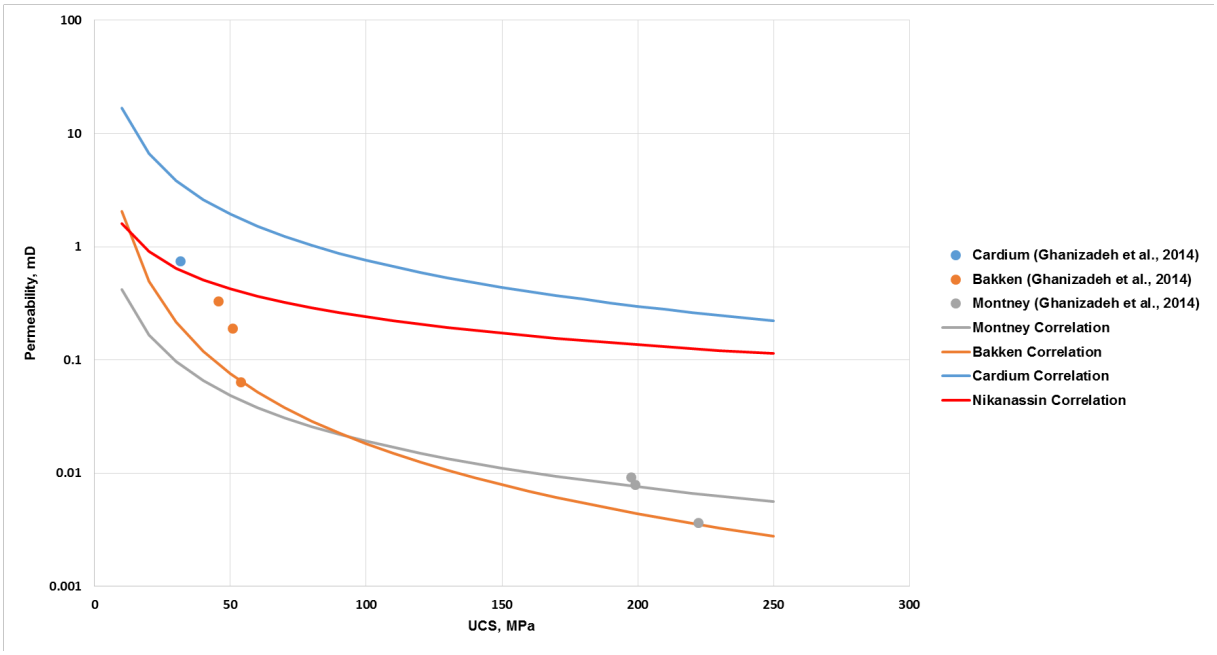

Figure 20. Ghanizadeh et al. Bakken shale, Montney shale, Cardium sandstone, and Nikanassin sandstone collected and correlated permeability comparison.

4.2.4 Nikanassin Sandstone and Montney Shale Permeability Comparison

The Nikanassin sandstone and Montney shale are two reservoirs that have been included in the permeability correlations mentioned in sections 4.2.1 and 4.2.2. Permeability, porosity, and collected depth values of Nikanassin sandstone drill cuttings established through laboratory testing have been collected and measured permeability data are plotted against depth. Drill cuttings have been collected for the Nikanassin sandstone and the depth at which the cuttings were "belong" has been noted; laboratory testing on the drill cuttings provided porosity and permeability measurements and these measurements can be found in Appendix B (Flores 2014). The permeability-porosity correlation for the Nikanassin cuttings is used for permeability determination because of the sample type (drill cuttings). The Cedola sandstone porosity correlation is utilized to determine UCS values corresponding to the laboratory measurements. A comparison between correlated permeability and collected permeability is seen in Fig. 21 as is the correlated sandstone UCS data. The average difference between the correlated sandstone permeability and permeability found through laboratory testing is 0.0195 mD.

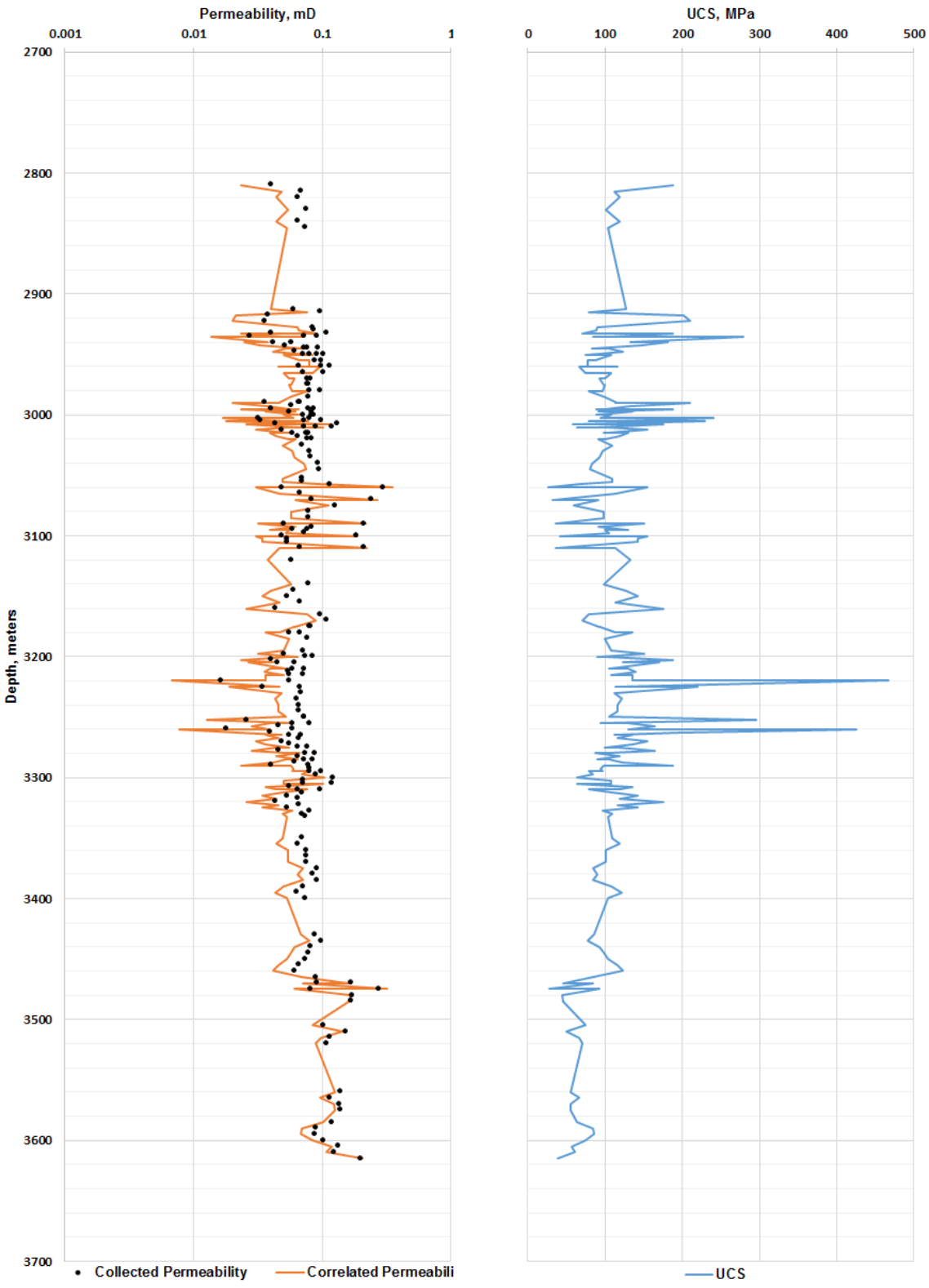

Figure 21. Comparison between collected permeability, correlated permeability, and UCS for the Nikanassin sandstone.

Montney shale cores were used for permeability and porosity determination via laboratory testing and the data can be found in Appendix C. Montney shale porosity data and the Montney shale porosity-permeability correlation were used to obtain permeability values. The Cedola shale porosity correlation was used to determine UCS values at the respective measurement. Montney shale correlated permeability and collected permeability have been plotted along with UCS in Fig. 22. The average difference between the correlated shale permeability and permeability found through laboratory testing is 0.012 mD.

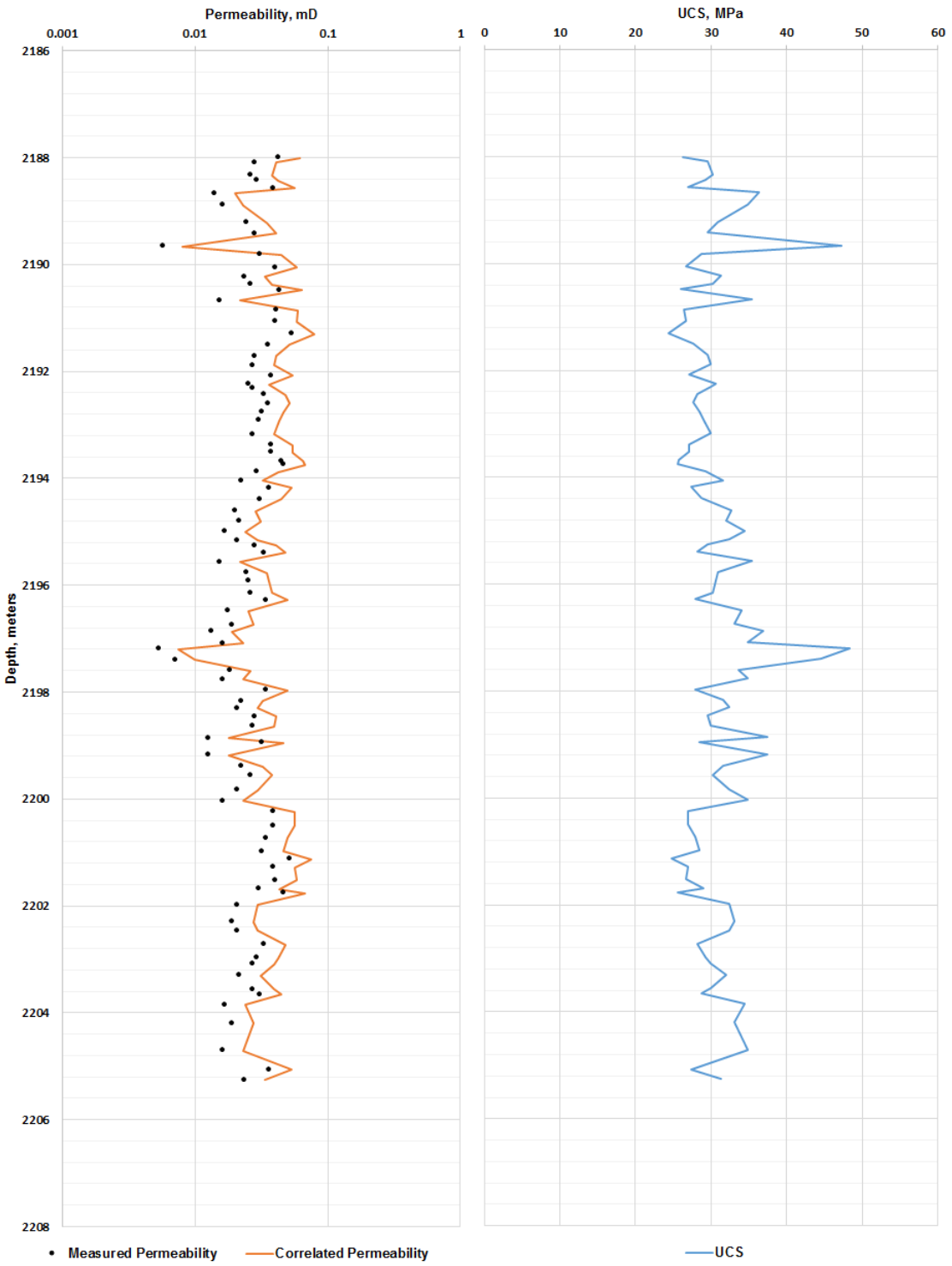

Fig. 22. Comparison between collected permeability, correlated permeability, and UCS for the Montney shale.

4.2.5 Collected and Correlated Permeability Comparison Discussion

Permeability comparison between collected and correlated permeability data for sandstone and shale lithologies is discussed within this section. The data collected from Ghanizadeh et al. (2014) were similar to the permeability correlation for the Montney formation but very different for the Cardium sandstone correlation (Fig. 20). This could be due to there only being a single Cardium datum and isn't a good indication of the actual reservoir. The Bakken permeability correlation has a similar value to one of the published data points but measured lower permeabilities than the two other points. The limited number of data points could provide a reason as to why the Cardium permeability and Bakken permeability correlations are less accurate. The Nikanassin sandstone permeability correlation appeared to be similar to the published Cardium data point and was lower than the correlated Cardium permeability. Both sandstone correlations predicted permeabilities that were significantly higher than the Bakken or Montney, which is in agreement with the trends in Fig. 17 & Fig. 19.

The Nikanassin sandstone permeability correlation was used to determine a correlated permeability to compare to the collected laboratory permeabilities. Because the measured samples were drill cuttings, the Nikanassin permeabilities for drill cuttings were used to compare collected and correlated permeabilities. The results show that the correlated permeability was fairly similar to the collected permeability (Fig. 21). Both permeability values were within the reported permeability range for the Nikanassin sandstone, which is between 0.01-0.25 mD (Solano et al., 2012). The UCS values mirrored both the collected and correlated permeability trends, which was the same trend seen in Fig. 17.

The Montney shale comparison between the Montney permeability correlation and the collected permeability from core lab analysis shows that the collected permeabilities were similar in trend but slightly less in value (Fig. 22). The range of Montney shale permeabilities is between 10 nD

to 0.1mD (Salimifard et al., 2015). Similar to the UCS-permeability trends seen in the Nikanassin, the correlated Montney shale UCS mirrors both collected and correlated permeability.

4.3 Benefits of Using Conventional Drilling Data for Porosity and Permeability Determination

The Cedola sandstone and shale porosity correlations appear to be consistent with neutron porosity and appear to be seemingly more accurate than the Onyia, Sarda, and Erfourth methods when utilizing drilling data and the inverted ROP model to determine UCS. Having the ability to predict porosity values that are highly similar to porosity found from logging could reduce the need for logging and/or laboratory testing. This could have an impact on drilling and completions cost reduction. In horizontal wells, the uncertainty associated with using drill cuttings or log tools to estimate the porosity and permeability could be alleviated. Depth measurements are measured simultaneously with UCS and other common drilling data. Using the Cedola sandstone correlation, Cedola shale correlation, and/or power Gamma Ray correlation to obtain porosity data allows for the porosity at any measured point can be found. In turn, this porosity can then be used to find permeability by means of the sandstone and shale permeability correlations established within this work.

Well stimulation design can be improved with the knowledge of porosity and permeability at any point within a well. In lateral sections, cores represent only a small portion of the well while cuttings can be misrepresentative if they are not from the area of question. Logging measurements can also prove incorrect if the tool is improperly calibrated or only running across the bottom of the well. The porosity and permeability can aid in determining where fractures should be placed, how they should be spaced, and the proper number of stages to accurately tap into the hydrocarbon bearing reservoir and achieve optimal hydrocarbon recovery. Correlating

these values from drilling data at any point could help in understanding reservoir characteristics and better formation evaluation at little to no additional cost.

CHAPTER V

SUMMARY & CONCLUSIONS

Porosity and permeability correlations are developed from drilling data in sandstone and shale lithologies. In mixed lithology zones, the integration of gamma ray log readings is done to improve porosity predictions. In comparison to previously published porosity correlations and neutron log porosity, the Cedola sandstone had similar porosity predictions while the Cedola shale correlation proved to be more accurate than the Onyia, Sarda, and Erfourth correlations. Permeability correlations specific to individual sandstone and shale reservoirs show similar results to permeability determined through lab analysis.

Previous techniques for porosity and permeability determination include logging, laboratory testing, and empirical correlations which can prove to be costly, inaccurate, or require knowledge of parameters that are extremely difficult to obtain. The benefits of the correlations presented within this work are that drilling data are available for all wells and can thus little to no additional logging costs, the correlations can be utilized for sandstone or shale lithologies, and the correlations can be used in horizontal wells.

Utilizing drilling data for porosity and permeability determination can help optimize stimulation design, lower the cost needed for well logging, and allow for better formation evaluation. Understanding these two parameters can also allow for a better understanding of hydrocarbons in

place as well as how to best “tap into” such reservoirs allowing for improved production. The Cedola sandstone, Cedola shale, and power Gamma Ray porosity correlations presented in this paper have been verified using drilling and log data from previously drilled wells, and there has been recent work done that uses drilling data to obtain multiple parameters, including porosity and permeability, in real-time or to determine a complete geomechanical log (Tahmeen et al. 2017). While the methods for determining these parameters vary from the methods presented in this work, it shows promise for future real-time and geomechanical mapping applications of the established correlations.

While the correlations presented within this paper show promise, they are only the first approach in developing a universal method for obtaining porosity and permeability.

5.1 Future Work

Future advances in establishing a universal method for porosity and permeability determination would begin by gathering more data to verify the porosity and permeability correlations. In addition to more data, an investigation as to whether an upper bound for the Cedola sandstone porosity and a lower bound for the Cedola shale porosity would improve the correlations accuracy. A data set with gamma ray log measurements, porosity, permeability, and UCS for sandstone and shale formations would also further improve the correlations. Much of the collected data have been obtained from North America, so applying the correlations to other areas of the world could prove advantageous.

REFERENCES

Aguilera, R. (2013, April 19). Flow Units: From Conventional to Tight Gas to Shale Gas to Tight Oil to Shale Oil Reservoirs, SPE-165360-MS, SPE Western Regional & AAPG Pacific Section Meeting 2013 Joint Technical Conference, Monterey, California, April 19-25, doi: 10.2118/165360-MS.

Allaby, M. (2017) "Unconfined compressive strength (uniaxial compressive strength)". A Dictionary of Geology and Earth Sciences 4th Edition. Oxford University Press, 2013. Web. 6 Mar. 2017.

Bachu, S. & Underschultz, J.R. (1992, April). Regional-Scale Porosity and Permeability Variations, Peace River Arch Area, Alberta, Canada. AAPG Bulletin, 76(04): 547-562.

Bazara, M. & Salman, S.M. (2009, March 15). Permeability Estimation Using Log Data, Abu Dhabi Offshore Field, U.A.E., SPE-118741-MS, SPE Middle East Oil and Gas Show and Conference, Manama, Bahrain, March 15-18, doi: 10.2118/118741-MS.

Borba, A.M., Ferreira, F.H., Santos, E.S.R., Menezes, V.M.D., & Strugale, M. (2014, September 9). UCS Estimation through Uniaxial Compressive Test, Scratch Test and Based Log Empirical Correlation, ISRM-SBMR-2014-042, ISRM Conference on Rock Mechanics for Natural Resources and Infrastructure-SBMR 2014, Goiania, Brazil, September 9-13.

Bowen. Y. (2015). Experimental Study and Numerical Modeling of Cryogenic Fracturing Process on Laboratory-Scale Rock and Concrete Samples. Master's Thesis, Colorado School of Mines, Golden, Colorado.

Bybee, K. (2011, July). Optimization of Completions in Unconventional Reservoirs. Journal of Petroleum Technology, SPE-0711-0102-JPT, 63(07): 102-104.

Calvert, S., Lovell, M., Harvey, P., Samworth, J.R., & Hook, J. (1998, May 26). Porosity Determination in Horizontal Wells, SPWLA-1998-BBB, SPWLA 39th Annual Logging Symposium, Keystone, Colorado, May 26-28.

Cedola, A.E., Atashnezhad, A., & Hareland, G. (2017A, March 27). Evaluating Multiple Methods to Determine Porosity from Drilling Data, SPE-185115-MS, SPE Oklahoma City Oil and Gas Symposium, Oklahoma City, Oklahoma, March 27-30.

Cedola, A.E., Atashnezhad, A., & Hareland, G. (2017B, April 11). Real-Time Porosity from Surface Drilling Data Prediction and Verification, AADE-17-NTCE-134, 2017 AADE National Technical Conference and Exhibition, Houston, Texas, April 11-12.

Cedola, A.E., Atashnezhad, A., & Hareland, G. (2017C, June 25). Method for Determining Permeability in Sandstone and Shale Reservoirs from Typical Drilling Parameters, ARMA-17-900, 51st US Rock Mechanics/Geomechanics Symposium, San Francisco, California, June 25-28.

Chang, C. (2004, August). Empirical Rock Strength Logging in Boreholes Penetrating Sedimentary Formations. Geophysics and Geophysical Exploration, 7(03):174-183.

Crawford, B.R., Gaillot, P.J., & Alramahi, B. (2010, June 27). Petrophysical Methodology for Predicting Compressive Strength in Siliclastic "sandstone-to-shale" Rocks, ARMA-10-196, 44th U.S. Rock Mechanics Symposium and 5th U.S.-Canada Rock Mechanics Symposium, Salt Lake City, Utah, June 27-30.

Cui, X., Bustin, R.M., Brezovski, R., Nassichuk, B., Glover, K., & Pathi, V. (2010, October 19). A New Method to Simultaneously Measure In-Situ Permeability and Porosity Under Reservoir Conditions: Implications for Characterization of Unconventional Gas Reservoirs, SPE-138148-MS, Canadian Unconventional Resources and International Petroleum Conference, Calgary, Alberta, October 19-21, doi: 10.2118/138148-MS.

Denney, D. (2008, August). Measuring Porosity and Permeability from Drill Cuttings, SPE-0808-0051-JPT, 60(08): 51-54, doi: 10.2118/0808-0051-JPT.

Derder, O.M. (2012, January). Characterizing Reservoir Properties for the Lower Triassic Montney Formation (Units C and D) Based on the Petrophysical Methods. Master's Thesis, University of Calgary, Calgary, Alberta.

Desport, O, Copping, K., & Johnson, B.L. (2011, November 15). Accurate Porosity Measurement in Gas Bearing Formations, SPE-147305-MS, Canadian Unconventional Resources Conference, Calgary, Alberta, November 15-17, doi: 10.2118/147305-MS.

Ellis, D.V., Case, C.R., & Chiaramonte, J.M. (2003, November). Tutorial-Porosity from Neutrom Logs I-Measurements. Petrophysics, 44(06): 383-395.

El-M Shokir E.M., Alsughayer, A.A., & Al-Ateeq, A. (2006, November). Permeability Estimation from Well Log Responses, PETSOC-06-11-05, 45(11): 41-46, doi: 10.2118/06-11-05.

Erfourth, B.S., Hudyma, N. and MacLaughlin, M.M. (2005, June 25). Comparison of Unconfined Compressive Strengths of Cast versus Cored Samples of Rock-like Materials with Large Voids, ARMA-05-876, Alaska Rocks 2005, the 40th Symposium on Rock Mechanics (USRMS), Anchorage, Alaska, June 25-29.

Farquhar, R.A., Smart, B.G.D., & Crawford, B.R. (1993, June 13). Porosity-Strength Correlation: Failure Criteria from Porosity Logs, SPWLA-1993-AA, SPWLA 34th Annual Logging Symposium, Calgary, Alberta, June 13-16.

Flores, L.J.Z. (2014, January). Reservoir Characterization of the Uppermost Monteith Formation-Tight Gas Sandstones in the Western Canada Sedimentary Basin in Alberta, Canada. Master's Thesis, University of Calgary, Calgary, Alberta.

Garcia-Hernandez, A., Miska, S.Z., Yu, M., Takach, N.E., & Zettner, C. (2007, November 11). Determination of Cuttings Lag in Horizontal and Deviated Wells, SPE-109630-MS, SPE Annual Technical Conference and Exhibition, Anaheim, California, November 11-14, doi: 10.2118/109630-MS.

Ghanizadeh, A., Aquino, S., Clarkson, C.R., Haeri-Ardakani, O., & Sanei, H. (2014, September 30). Petrophysical and Geomechanical Characteristics of Canadian Tight Oil and Liquid-Rich Gas Reservoirs, SPE-171633-MS, SPE/CSUR Unconventional Resources Conference-Canada, Calgary, Alberta, September 30-October 2, doi: 10.2118/171633-MS.

Goldberg, I. & Gurevich, B. (1998, May). A semi-empirical velocity-porosity-clay model for petrophysical interpretation of P- and S-velocities. Geophysical Prospecting, 46: 271-285.

Hareland, G. & Hoberock, L.L. (1993, February 23). Use of Drilling Parameters to Predict In-Situ Stress Bounds, SPE-25727-MS, SPE/IADC Drilling Conference, Amsterdam, The Netherlands, February 22-25, doi: 10.2118/25727-MS.

Hareland, G. & Rampersad, P.R. (1994, April 27). Drag-Bit Model Including Wear, SPE-26957-MS, SPE Latin America/Caribbean Petroleum Engineering Conference, Buenos Aires, Argentina, April 27-29, doi: 10.2118/26957-MS.

Hareland, G. & Nygaard, R. (2007, May 27). Calculating Unconfined Rock Strength From Drilling Data, ARMA-07-214, 1st Canada-U.S. Rock Mechanics Symposium, Vancouver, Canada, May 27-31.

Harris, N.B. (2014). Falher and Cadomin diagenesis and implications for reservoir quality, GeoConvention 2014: Focus, Calgary, Alberta, May 12-14.

Hashmy, K.H., Tonner, D., Abueita, S., and Jonkers, J. (2012, October 22). Shale Reservoirs: Improved Production from Stimulation of Sweet Spots, SPE-158881-MS, SPE Asia Pacific Oil and Gas Conference and Exhibition, Perth, Australia, October 22-24, doi: 10.2118/158881-MS.

Hawkins, A. & McConnell, B.J. (1991, September 16). Influence of Geology on Geomechanical Properties of Sandstones, ISRM-7CONGRESS-1991-051, 7th ISRM Congress, Aachen, Germany, September 16-20.

Holditch, S.A., Ayers, W.B., Bickley, J.A., Blasingame, T.A., Hoefner, M., Jochen, V.A., Lee, W.J., McVay, D.A., Perry, K.F., Sharma, M.M., Teodoriu, C. & Torres-Verdin, C. (2007). Topic Paper #29 Unconventional Gas. *Working Document of the NPC Global Oil & Gas Study.*

Horsrud, P. (2001, June). Estimating Mechanical Properties of Shale from Empirical Correlations, SPE-56017-PA, SPE Drilling and Completions, 16(02): 68-73.

Hursan, G.G., Deering, J.S., & Kelly, F.N. (2015, April 21). NMR Logs Help Formation Testing and Evaluation, SPE-177974-MS, SPE Saudi Arabia Section Annual Technical Symposium, Al-Khobar, Saudi Arabia, April 21-23, doi: 10.2118/177974-MS.

Katahara, K.W. (1995, July). Gamma Ray Log Response in Shaly Sands, SPWLA-1995-v36n4a4, The Log Analyst, 36(04): 50-71.

Kerkar, P.B., Hareland, G., Fonseca, E.R., & Hackbarth, C.J. (2014, January 20). Estimation of Rock Compressive Strength Using Downhole Weight-on-Bit and Drilling Models, IPTC-17447-MS, International Petroleum Technology Conference, Doha, Qatar, January 19-22, doi: 10.2523/IPTC-17447-MS.

Khaksar, A., Taylor, P.G., Fang, Z., Kayes, T., Salazar, A., & Rahman, K. (2009, June 8). Rock Strength from Core and Logs: Where We Stand and Ways to Go, SPE-121972-MS, EUROPEC/EAGE Conference and Exhibition, Amsterdam, The Netherlands, June 8-11, doi: 10.2118/121972-MS.

Kim, K-Y., Zhuang. L., Yang, H., Kim, H., &Min, K-B. (2016). Strength Anisotropy of Berea Sandstone: Results of X-Ray Computed Tomography, Compression Tests, and Discrete Modeling. Rock Mechanics Engineering, 49(04): 1201-1210.

Knackstedt, M., Carnerup, A., Golab, A., Sok, R., Young, B., & Riepe, L. (2013, June). Petrophysical Characterization of Unconventional Reservoir Core at Multiple Scales. Petrophysics, 54(03): 216-223.

Lacentre, P.E. & Carrica, P.M. (2003, 27). A Method to Estimate Permeability on Uncored Wells Based on Well Logs and Core Data, SPE-81058-MS, SPE Latin American and Caribbean Petroleum Engineering Conference, Port-of-Spain, Trinidad and Tobago, April 27-30, doi: 10.2118/81058-MS.

Lan, C., Chen, S., Mendez, F.E., & Sy, R. (2010, September 19). Sourceless Porosity Estimation in Gas Reservoirs Using Integrated Acoustic and NMR Logs, SPE-133487-MS, SPE Annual Technical Conference and Exhibition, Florence, Italy, September 19-22, doi: 10.2118/133487-MS.

Lashkaripour, G.R. (2002, February). Predicting mechanical properties of mudrock from index parameters. Bulletin of Engineering Geology and the Environment, 61(01): 73-77.

Lenormand, R. & Fonta, O. (2007, October 28). Advances in Measuring Porosity and Permeability from Drill Cuttings, SPE-111286-MS, SPE/EAGE Reservoir Characterization and Simulation Conference, Abu Dubai, UAE, October 28-31, doi: 10.2118/111286-MS.

Li, T., Han, S.Y., Liu, Y.M., Shi, H., Li, H., & Zhao, Y. (2015, October 13). Improved Permeability Estimation in Siliclastic Sands with Geochemical Logs and Formation Pressure Tests, SPWLA-JFES-2015-T, 21st Formation Evaluation Symposium of Japan, Chiba, Japan, October 13-14.

Liang, X., Chang-chun, Z., Zhi-qiang, S., Gao-ren, L., Hao-peng, G., & Xiu-hong, X. (2013, November 11). The Correlation Analysis Method and Its Application in Hydrocarbon-Bearing Formation Identification in Tight Sandstone Reservoirs, SPE-166988-MS, SPE Unconventional Resources Conference and Exhibition-Asia Pacific, Brisbane, Australia, November 11-13.

Logan, W.D. (2015, September 28). Engineered Shale Completions Based on Common Drilling Data, SPE-174839-MS, SPE Annual Technical Conference and Exhibition, Houston, Texas, September 28-30, doi: 10.2118/174839-MS.

Luffel, D.L. & Howard, W.E. (1987, May 18). Reliability of Laboratory Measurements of Porosity in Tight Gas Sands, SPE-16401-MS, Low Permeability Reservoirs Symposium, Denver, Colorado, May 18-19, doi: 10.2118/16401-MS.

Luffel, D.L., Hopkins, C.W., & Schettler Jr., P.D. (1993, October 3). Matrix Permeability Measurement of Gas Productive Shales, SPE-26633-MS, SPE Annual Technical Conference and Exhibition, Houston, Texas, October 3-6, doi: 10.2118/26633-MS.

Manseur, S., Djebbar, T., Berkat, A., & Zhu, T. (2002, May 20). Horizontal and Vertical Permeability Determination in Clean and Shaly Reservoirs Using In-Situ Measurements, SPE-76773-MS, SPE Western Regional/AAPG Pacific Section Joint Meeting, Anchorage, Alaska, May 20-22, doi: 10.2118/76773-MS.

Mohaghegh, S., Balan, B., & Ameri, S. (1997, September). Permeability Determination from Well Log Data, SPE-30978-PA, SPE Formation Evaluation, 12(03): 170-174, doi: 10.2118/30978-PA.

Nabaei, M. & Shahbazi, K. (2012, February 15). A New Approach for Predrilling the Unconfined Rock Compressive Strength Prediction, Petroleum Science and Technology, SPE-155746-PA, 30(04): 350-359, doi: 10.1080/10916461003752546.

Onyia, E.C. (1988, October 2). Relationships Between Formation Strength, Drilling Strength, and Electric Log Properties, SPE-18166-MS, SPE Annual Technical Conference and Exhibition, Houston, Texas, October 2-5, doi: 10.2118/18166-MS.

Ortega, C. & Aguilera, R. (2012, October 30). A Complete Petrophysical Evaluation Method for Tight Formations from Only Drill Cuttings in the Absence of Well Logs, SPE-161875-MS, SPE Canadian Unconventional Resources Conference, Calgary, Alberta, Canada, October 30-November 1, doi: 10.2118/161875-MS.

Ortega, C. & Aguilera, R. (2014, January). Quantitative Properties from Drill Cuttings to Improve the Design of Hydraulic-Fracturing Jobs in Horizontal Wells, SPE-155746-PA. Journal of Petroleum Technology, 53(01): 55-68, doi: 10.2118/155746-PA.

Saldungaray, P. & Palisch, T. (2013, March 20). Hydraulic Fracture Optimization in Unconventional Reservoirs, SPE-151128-MS, SPE Middle East Unconventional Gas Conference and Exhibition, Abu Dhabi, United Arab Emirates, January 23-25, doi: https://doi.org/10.2118/151128-MS.

Salimifard, B., Ruth, D.W., & Nassichuk, B. (2015, October 20). A Study of Mercury Intrusion on Montney Formation Rocks and How It Relates to Permeability, SPE-175968-MS, SPE/CSUR Unconventional Resources Conference, Calgary, Alberta, October 20-22, doi: 10.2118/175968-MS.

Sarda, J-P., Kessler, N., Wicquart, E., Hannaford, K., & Deflandre, J-P. (1993, October 3). Use of Porosity as a Strength Indicator for Sands Production Evaluation, SPE-26454-MS, SPE Annual Technical Conference and Exhibition, October 3-6, doi: 10.2118/26454-MS.

Smith, C.H. & Ziane, L. (2015, March 1). Mississippian Porosity and Permeability: Core Comparison to Nuclear Magnetic Resonance, SPE-173592-MS, SPE Production and Operations Symposium, Oklahoma City, Oklahoma, March 1-5, doi: 10.2118/173592-MS.

Snyder, D. & Seale, R.A. (2011, May 23). Optimization of Completions in Unconventional Reservoirs for Ultimate Recovery-Case Studies, SPE-143066-MS, SPE EUROPEC/EAGE Annual Conference and Exhibition, Vienna, Austria, May 23-26, doi: 10.2118/143066-MS.

Solano, N.A., Clarkson, C.R., Krause, F.F., Lenormand, R., Barclay, J.E., & Aguilera, R. (2012, October 30). Drill Cuttings and Characterization of Tight Gas Reservoirs-An Example from the Nikanassin Fm. In the Deep Basin of Alberta, SPE-162706-MS, SPE Canadian Unconventional Resources Conference, Calgary, Alberta, October 30-November 1, doi: 10.2118/162706-MS.

Tahmeen, M., Love, J., Rashidi, B., & Hareland, G. (2017, June 25). Complete Geomechanical Property Logs from Drilling Data in Unconventional Horizontal Wells, ARMA-17-591, 51st US Rock Mechanics/Geomechanics Symposium, San Francisco, California, June 25-28.

Valdes, C. & Raquel, C. (2013). Characterization of Geomechanical Poroelastic Parameters in Tight Rocks. Master's Thesis, Texas A&M University, College Station, Texas.

Yao, C.Y. & Holditch, S.A. (1993, November 2). Estimating Permeability Profiles Using Core and Log Data, SPE-26921-MS, SPE Eastern Regional Meeting, Pittsburgh, Pennsylvania, November 2-4, doi: 10.2118/26921-MS.

Zhang, H., Mendez, F., Frost Jr., E., McGlynn, I., Alarcon, N., Mezzatesta, A., Quinn, T., & Manning, M. (2016, June 25). Convergent Integrated Petrophyscial Analysis of TOC, Mineral Concentrations, and Porosity in Hydrocarbon-Bearing Unconventional Reservoirs, SPWLA-2016-EEE, SPWLA 57th Annual Logging Symposium, Reykjavik, Iceland, June 25-29.

Berg, R.R. (1970). Method for Determining Permeability from Reservoir Rock Properties, GCAGS Trans, v. 20: 303-317.

Coates, G.R. & Dumanoir, J.L. (1974, January). A New Approach to Improved Log Derived Permeability, The Log Analyst, 17-31.

Carman, P.C. (1937). Fundamental Principles of Industrial Filtration (A Critical Review of Present Knowledge), Transactions of the Institution of Chemical Engineers, 16: 168-188.

Coates, G.R. & Denoo, S. (1981). The Producibility Answer Product, Schlumberger Technical Review, 29(02): 55-63.

Timur, A. (1968, July). An Investigation of Permeability, Porosity, & Residual Water Saturation Relationships for Sandstone Reservoirs, The Log Analyst, 9(04): 8-17.

APPENDICES

APPENDIX A

SANDSTONE & SHALE POROSITY-UCS DATA

AUTHOR	LITHOLOGY	UCS, MPa	Porosity, %
Farquhar et al. 1993	Sandstone	262.5	5
Farquhar et al. 1993	Sandstone	170	5
Farquhar et al. 1993	Sandstone	157	6
Farquhar et al. 1993	Sandstone	103	7
Farquhar et al. 1993	Sandstone	98	7.2
Farquhar et al. 1993	Sandstone	60	10.5
Farquhar et al. 1993	Sandstone	73	12.5
Farquhar et al. 1993	Sandstone	56	19
Farquhar et al. 1993	Sandstone	52	22
Farquhar et al. 1993	Sandstone	37	28.5
Farquhar et al. 1993	Sandstone	92	9.5
Farquhar et al. 1993	Sandstone	100	11
Farquhar et al. 1993	Sandstone	101	11.5
Farquhar et al. 1993	Sandstone	99.5	12.5
Farquhar et al. 1993	Sandstone	75.5	11
Farquhar et al. 1993	Sandstone	80	11.25
Farquhar et al. 1993	Sandstone	70	15.5
Farquhar et al. 1993	Sandstone	35	18
Farquhar et al. 1993	Sandstone	40	19.95
Farquhar et al. 1993	Sandstone	60	19.5
Farquhar et al. 1993	Sandstone	63	20.5
Farquhar et al. 1993	Sandstone	45	22.5
Khaksar et al. 2009	Sandstone	352	0.5
Khaksar et al. 2009	Sandstone	330	0.75
Khaksar et al. 2009	Sandstone	320	0.5
Khaksar et al. 2009	Sandstone	321	2.5
Khaksar et al. 2009	Sandstone	303	3
Khaksar et al. 2009	Sandstone	300	2.5
Khaksar et al. 2009	Sandstone	297	3
Khaksar et al. 2009	Sandstone	295	1
Khaksar et al. 2009	Sandstone	285	1
Khaksar et al. 2009	Sandstone	280	2
Khaksar et al. 2009	Sandstone	275	2.5
Khaksar et al. 2009	Sandstone	271	3
Khaksar et al. 2009	Sandstone	270	2.5
Khaksar et al. 2009	Sandstone	270	4
Khaksar et al. 2009	Sandstone	267	0.5
Khaksar et al. 2009	Sandstone	260	2
Khaksar et al. 2009	Sandstone	255	2

Khaksar et al. 2009	Sandstone	260	2.5
Khaksar et al. 2009	Sandstone	255	2.5
Khaksar et al. 2009	Sandstone	260	4
Khaksar et al. 2009	Sandstone	260	3.25
Khaksar et al. 2009	Sandstone	255	3.5
Khaksar et al. 2009	Sandstone	252	4
Khaksar et al. 2009	Sandstone	250	4.5
Khaksar et al. 2009	Sandstone	215	4
Khaksar et al. 2009	Sandstone	210	2.5
Khaksar et al. 2009	Sandstone	225	4.8
Khaksar et al. 2009	Sandstone	220	4.8
Khaksar et al. 2009	Sandstone	202	2
Khaksar et al. 2009	Sandstone	198	2.5
Khaksar et al. 2009	Sandstone	190	4.5
Khaksar et al. 2009	Sandstone	170	4
Khaksar et al. 2009	Sandstone	151	4.75
Khaksar et al. 2009	Sandstone	145	6.5
Khaksar et al. 2009	Sandstone	140	3.5
Khaksar et al. 2009	Sandstone	125	5.25
Khaksar et al. 2009	Sandstone	125	6.5
Khaksar et al. 2009	Sandstone	130	6.5
Khaksar et al. 2009	Sandstone	105	10
Khaksar et al. 2009	Sandstone	110	10
Khaksar et al. 2009	Sandstone	115	4.25
Khaksar et al. 2009	Sandstone	110	4.5
Khaksar et al. 2009	Sandstone	107	6.2
Khaksar et al. 2009	Sandstone	105	6
Khaksar et al. 2009	Sandstone	103	6.2
Khaksar et al. 2009	Sandstone	105	8.5
Khaksar et al. 2009	Sandstone	97	9
Khaksar et al. 2009	Sandstone	95	5.5
Khaksar et al. 2009	Sandstone	55	5.5
Khaksar et al. 2009	Sandstone	75	5
Khaksar et al. 2009	Sandstone	77	5.5
Khaksar et al. 2009	Sandstone	40	12.5
Khaksar et al. 2009	Sandstone	50	13.5
Khaksar et al. 2009	Sandstone	60	10.25
Khaksar et al. 2009	Sandstone	60	11
Khaksar et al. 2009	Sandstone	55	11.5
Khaksar et al. 2009	Sandstone	80	6.5

Khaksar et al. 2009	Sandstone	80	7.5
Khaksar et al. 2009	Sandstone	75	6
Khaksar et al. 2009	Sandstone	70	6.1
Khaksar et al. 2009	Sandstone	60	7
Khaksar et al. 2009	Sandstone	65	7.5
Khaksar et al. 2009	Sandstone	85	11
Khaksar et al. 2009	Sandstone	85	12.5
Khaksar et al. 2009	Sandstone	87	12
Khaksar et al. 2009	Sandstone	65	14
Khaksar et al. 2009	Sandstone	55	14.5
Khaksar et al. 2009	Sandstone	55	19.5
Khaksar et al. 2009	Sandstone	70	15.5
Khaksar et al. 2009	Sandstone	70	16
Khaksar et al. 2009	Sandstone	70	18.5
Khaksar et al. 2009	Sandstone	70	21
Khaksar et al. 2009	Sandstone	60	16
Khaksar et al. 2009	Sandstone	52	16
Khaksar et al. 2009	Sandstone	47	18.5
Khaksar et al. 2009	Sandstone	50	20
Khaksar et al. 2009	Sandstone	60	22
Khaksar et al. 2009	Sandstone	35	19.5
Khaksar et al. 2009	Sandstone	20	17.5
Khaksar et al. 2009	Sandstone	22	18
Khaksar et al. 2009	Sandstone	7	24.5
Khaksar et al. 2009	Sandstone	5	24.25
Khaksar et al. 2009	Sandstone	10	33
Hawkins & McConnell 1991	Sandstone	141.3	6.2
Hawkins & McConnell 1991	Sandstone	237.9	2.5
Hawkins & McConnell 1991	Sandstone	247	1.1
Hawkins & McConnell 1991	Sandstone	227.29	1.6
Hawkins & McConnell 1991	Sandstone	161.37	5.2
Hawkins & McConnell 1991	Sandstone	59.33	13.2
Hawkins & McConnell 1991	Sandstone	49	12.6
Hawkins & McConnell 1991	Sandstone	123.4	11.9
Hawkins & McConnell 1991	Sandstone	119.1	12.6
Hawkins & McConnell 1991	Sandstone	108.1	12.9
Hawkins & McConnell 1991	Sandstone	198.4	1.9
Hawkins & McConnell 1991	Sandstone	59.9	13.7
Hawkins & McConnell 1991	Sandstone	89.9	12.9
Hawkins & McConnell 1991	Sandstone	91.8	12.1

Hawkins & McConnell 1991	Sandstone	37.1	20
Hawkins & McConnell 1991	Sandstone	298.2	1.4
Hawkins & McConnell 1991	Sandstone	114.2	8.6
Hawkins & McConnell 1991	Sandstone	106.2	11.1
Hawkins & McConnell 1991	Sandstone	103.4	10.4
Hawkins & McConnell 1991	Sandstone	66.3	19.3
Hawkins & McConnell 1991	Sandstone	65.9	10
Hawkins & McConnell 1991	Sandstone	34.6	16.3
Hawkins & McConnell 1991	Sandstone	82	8.8
Hawkins & McConnell 1991	Sandstone	101.2	6.1
Hawkins & McConnell 1991	Sandstone	59.7	16.5
Hawkins & McConnell 1991	Sandstone	36.1	18.2
Hawkins & McConnell 1991	Sandstone	23.2	24.9
Hawkins & McConnell 1991	Sandstone	42.2	26.8
Hawkins & McConnell 1991	Sandstone	53.4	25.9
Hawkins & McConnell 1991	Sandstone	30.6	29.4
Hawkins & McConnell 1991	Sandstone	74.5	22.5
Chang 2004	Sandstone	350	0.5
Chang 2004	Sandstone	342	2
Chang 2004	Sandstone	315	1
Chang 2004	Sandstone	315	3
Chang 2004	Sandstone	297	3
Chang 2004	Sandstone	295	1.5
Chang 2004	Sandstone	277	2
Chang 2004	Sandstone	275	2.5
Chang 2004	Sandstone	263	4
Chang 2004	Sandstone	260	0.5
Chang 2004	Sandstone	257	3.5
Chang 2004	Sandstone	257	4.5
Chang 2004	Sandstone	225	5
Chang 2004	Sandstone	223	5
Chang 2004	Sandstone	210	2
Chang 2004	Sandstone	200	3
Chang 2004	Sandstone	202	3
Chang 2004	Sandstone	180	4
Chang 2004	Sandstone	175	4.5
Chang 2004	Sandstone	174	4
Chang 2004	Sandstone	160	3.5
Chang 2004	Sandstone	155	5
Chang 2004	Sandstone	153	5.2

Chang 2004	Sandstone	150.5	4.5
Chang 2004	Sandstone	150	5
Chang 2004	Sandstone	150	7.5
Chang 2004	Sandstone	145	7
Chang 2004	Sandstone	145	3.5
Chang 2004	Sandstone	120	3.5
Chang 2004	Sandstone	115	4
Chang 2004	Sandstone	117	5
Chang 2004	Sandstone	75	5
Chang 2004	Sandstone	52	5.5
Chang 2004	Sandstone	63	6
Chang 2004	Sandstone	60	7.5
Chang 2004	Sandstone	62	7.75
Chang 2004	Sandstone	80	7.75
Chang 2004	Sandstone	70	6.5
Chang 2004	Sandstone	98	6.5
Chang 2004	Sandstone	80	6.75
Chang 2004	Sandstone	125	5
Chang 2004	Sandstone	75	5.5
Chang 2004	Sandstone	85	5.5
Chang 2004	Sandstone	105	6.5
Chang 2004	Sandstone	110	6.5
Chang 2004	Sandstone	107	6
Chang 2004	Sandstone	115	6
Chang 2004	Sandstone	115	7
Chang 2004	Sandstone	113	7
Chang 2004	Sandstone	107	7.5
Chang 2004	Sandstone	90	8.5
Chang 2004	Sandstone	80	9
Chang 2004	Sandstone	60	10
Chang 2004	Sandstone	100	10
Chang 2004	Sandstone	105	10
Chang 2004	Sandstone	100	15
Chang 2004	Sandstone	85	12.5
Chang 2004	Sandstone	85	12.5
Chang 2004	Sandstone	84	12
Chang 2004	Sandstone	70	12.5
Chang 2004	Sandstone	70	10.5
Chang 2004	Sandstone	65	11
Chang 2004	Sandstone	55	20

Chang 2004	Sandstone	75	11
Chang 2004	Sandstone	45	25
Chang 2004	Sandstone	47	13
Chang 2004	Sandstone	45	14.5
Chang 2004	Sandstone	53	14.5
Chang 2004	Sandstone	60	14
Chang 2004	Sandstone	104	12.5
Chang 2004	Sandstone	115	14
Chang 2004	Sandstone	75	15.5
Chang 2004	Sandstone	75	16
Chang 2004	Sandstone	75	18.5
Chang 2004	Sandstone	77	16.5
Chang 2004	Sandstone	78	16.5
Chang 2004	Sandstone	43	16.5
Chang 2004	Sandstone	40	16
Chang 2004	Sandstone	30	16
Chang 2004	Sandstone	27	19.5
Chang 2004	Sandstone	25	19.5
Chang 2004	Sandstone	60	19.5
Chang 2004	Sandstone	55	22
Chang 2004	Sandstone	45	18
Chang 2004	Sandstone	43	17.5
Chang 2004	Sandstone	25	17.5
Chang 2004	Sandstone	26	18
Chang 2004	Sandstone	52	19.75
Chang 2004	Sandstone	48	20
Chang 2004	Sandstone	50	21
Chang 2004	Sandstone	50	16
Chang 2004	Sandstone	50	16
Chang 2004	Sandstone	55	16.5
Chang 2004	Sandstone	65	21
Chang 2004	Sandstone	70	21
Chang 2004	Sandstone	65	22.5
Chang 2004	Sandstone	7	24.5
Chang 2004	Sandstone	2	24.5
Chang 2004	Sandstone	10	33.5
Chang 2004	Sandstone	12.5	35
Kim et al. 2015	Sandstone	63	5
Kim et al. 2015	Sandstone	45	10
Kim et al. 2015	Sandstone	41	14.5

Kim et al. 2015	Sandstone	22	22
Valdes 2013	Sandstone	43	18
Valdes 2013	Sandstone	55	20
Bowen 2015	Sandstone	41.41	11.52
Bowen 2015	Sandstone	53.569	11.41
Bowen 2015	Sandstone	29.391	11.58
Horsrud 2001	Shale	9	41
Horsrud 2001	Shale	12	31
Horsrud 2001	Shale	14	34
Horsrud 2001	Shale	9	31
Horsrud 2001	Shale	9	29
Horsrud 2001	Shale	9	30
Horsrud 2001	Shale	28	10
Horsrud 2001	Shale	22	17
Horsrud 2001	Shale	13	15
Horsrud 2001	Shale	2	45
Chang 2004	Shale	185	2.55
Chang 2004	Shale	111	4
Chang 2004	Shale	111	2.5
Chang 2004	Shale	113	2.5
Chang 2004	Shale	114	2.5
Chang 2004	Shale	101	2.5
Chang 2004	Shale	98	5.5
Chang 2004	Shale	78	6
Chang 2004	Shale	78	5.75
Chang 2004	Shale	76.5	4
Chang 2004	Shale	27	10
Chang 2004	Shale	25	12.5
Chang 2004	Shale	23	12.5
Chang 2004	Shale	15	14
Chang 2004	Shale	13	14.5
Chang 2004	Shale	24	16
Chang 2004	Shale	24	16.25
Chang 2004	Shale	18	23.5
Chang 2004	Shale	16	22
Chang 2004	Shale	15.5	22
Chang 2004	Shale	14	26
Chang 2004	Shale	12.5	27
Chang 2004	Shale	12.5	28.5
Chang 2004	Shale	12.5	30

Chang 2004	Shale	12.5	30.5
Chang 2004	Shale	12.5	34
Chang 2004	Shale	12.5	34.5
Chang 2004	Shale	12	27.5
Chang 2004	Shale	12	32
Chang 2004	Shale	12	33
Chang 2004	Shale	10	26.5
Chang 2004	Shale	10	29
Chang 2004	Shale	10	30
Chang 2004	Shale	10	31
Chang 2004	Shale	10	32
Chang 2004	Shale	10	33.5
Chang 2004	Shale	10	34
Chang 2004	Shale	10	34.5
Chang 2004	Shale	8	29
Chang 2004	Shale	8	29.7
Chang 2004	Shale	8	30.2
Chang 2004	Shale	8	31.5
Chang 2004	Shale	8	32.5
Chang 2004	Shale	1	29
Chang 2004	Shale	3	29
Chang 2004	Shale	6	34.7
Chang 2004	Shale	4	31.5
Chang 2004	Shale	3.5	32
Chang 2004	Shale	5	27.5
Chang 2004	Shale	1	28
Chang 2004	Shale	5	28
Chang 2004	Shale	8	28
Chang 2004	Shale	1	35
Chang 2004	Shale	1	37.5
Chang 2004	Shale	1.5	39.5
Chang 2004	Shale	1.5	40
Chang 2004	Shale	1.5	41
Chang 2004	Shale	10	42
Chang 2004	Shale	7	44
Chang 2004	Shale	2	44
Chang 2004	Shale	2	47.5
Chang 2004	Shale	1	49
Lashkarpour et al. 2002	Shale	240	1
Lashkarpour et al. 2002	Shale	230	0.9

Lashkarpour et al. 2002	Shale	215	1.5
Lashkarpour et al. 2002	Shale	183	2.25
Lashkarpour et al. 2002	Shale	200	2.5
Lashkarpour et al. 2002	Shale	100	2
Lashkarpour et al. 2002	Shale	110	1.75
Lashkarpour et al. 2002	Shale	111	2.25
Lashkarpour et al. 2002	Shale	120	4
Lashkarpour et al. 2002	Shale	95	4.5
Lashkarpour et al. 2002	Shale	82	4.5
Lashkarpour et al. 2002	Shale	97	3.5
Lashkarpour et al. 2002	Shale	90	4
Lashkarpour et al. 2002	Shale	100	4
Lashkarpour et al. 2002	Shale	110	3.75
Lashkarpour et al. 2002	Shale	30	17.5
Lashkarpour et al. 2002	Shale	35	18
Lashkarpour et al. 2002	Shale	35	17.25
Lashkarpour et al. 2002	Shale	37	16.5
Lashkarpour et al. 2002	Shale	37	16.75
Lashkarpour et al. 2002	Shale	20	21
Lashkarpour et al. 2002	Shale	20	23.5
Lashkarpour et al. 2002	Shale	22	24.25
Lashkarpour et al. 2002	Shale	5	34.5
Lashkarpour et al. 2002	Shale	5	32.5
Lashkarpour et al. 2002	Shale	20	26.5
Lashkarpour et al. 2002	Shale	3	31.5
Lashkarpour et al. 2002	Shale	30	20
Lashkarpour et al. 2002	Shale	25	21
Lashkarpour et al. 2002	Shale	25	21.5
Lashkarpour et al. 2002	Shale	3	29
Lashkarpour et al. 2002	Shale	4	27.5
Lashkarpour et al. 2002	Shale	4	29
Lashkarpour et al. 2002	Shale	7	28
Lashkarpour et al. 2002	Shale	10	27.5
Lashkarpour et al. 2002	Shale	7	29
Lashkarpour et al. 2002	Shale	65	9
Lashkarpour et al. 2002	Shale	60	10
Lashkarpour et al. 2002	Shale	20	12.5
Lashkarpour et al. 2002	Shale	25	12.5
Lashkarpour et al. 2002	Shale	20	12
Lashkarpour et al. 2002	Shale	20	11.75

Lashkarpour et al. 2002	Shale	45	8
Lashkarpour et al. 2002	Shale	30	12.25
Lashkarpour et al. 2002	Shale	50	12.25
Lashkarpour et al. 2002	Shale	25	11
Lashkarpour et al. 2002	Shale	30	11
Lashkarpour et al. 2002	Shale	35	11
Lashkarpour et al. 2002	Shale	45	11
Lashkarpour et al. 2002	Shale	45	10
Lashkarpour et al. 2002	Shale	25	10.25
Lashkarpour et al. 2002	Shale	25	10.5
Lashkarpour et al. 2002	Shale	30	9.5
Lashkarpour et al. 2002	Shale	50	9.5
Lashkarpour et al. 2002	Shale	55	9.5
Lashkarpour et al. 2002	Shale	32	8.5
Lashkarpour et al. 2002	Shale	50	8.5
Lashkarpour et al. 2002	Shale	60	8.5
Lashkarpour et al. 2002	Shale	65	6
Lashkarpour et al. 2002	Shale	75	6
Lashkarpour et al. 2002	Shale	50	6.5
Lashkarpour et al. 2002	Shale	50	7.5
Lashkarpour et al. 2002	Shale	60	7
Lashkarpour et al. 2002	Shale	65	7
Lashkarpour et al. 2002	Shale	75	7
Lashkarpour et al. 2002	Shale	80	7
Lashkarpour et al. 2002	Shale	50	7.5
Lashkarpour et al. 2002	Shale	55	8

APPENDIX B

NIKANASSIN CUTTINGS DATA

AUTHOR	DEPTH	Permeability, mD	Porosity, %
Flores 2014	2810	0.179	2.5
Flores 2014	2815	0.162	4.5
Flores 2014	2820	0.061	4.2
Flores 2014	2830	0.118	5
Flores 2014	2840	0.113	4.2
Flores 2014	2845	0.115	4.9
Flores 2014	2912.5	0.089	3.9
Flores 2014	2915	0.024	6.6
Flores 2014	2917.5	0.082	2.3
Flores 2014	2922.5	0.03	2.2
Flores 2014	2927.5	0.105	5.7
Flores 2014	2930	0.068	5.8
Flores 2014	2932.5	0.05	7.6
Flores 2014	2932.5	0.127	2.5
Flores 2014	2935	0.05	4.8
Flores 2014	2935	0.051	6.2
Flores 2014	2935	0.099	1.6
Flores 2014	2940	0.027	3.7
Flores 2014	2940	0.101	2.6
Flores 2014	2942.5	0.107	3.3
Flores 2014	2945	0.084	6.3
Flores 2014	2945	0.035	5.1
Flores 2014	2945	0.11	4.8
Flores 2014	2947.5	0.073	4
Flores 2014	2950	0.076	7.1
Flores 2014	2950	0.011	5.4
Flores 2014	2950	0.081	6.2
Flores 2014	2950	0.128	4.7
Flores 2014	2955	0.071	5.9
Flores 2014	2955	0.06	6.8
Flores 2014	2960	0.039	6.8
Flores 2014	2960	0.033	4.3
Flores 2014	2960	0.084	8
Flores 2014	2965	0.13	7.1
Flores 2014	2965	0.046	4.7
Flores 2014	2970	0.036	5.1
Flores 2014	2970	0.025	5.5
Flores 2014	2975	0.055	5.2
Flores 2014	2975	0.026	5.1

Flores 2014	2980	0.015	5.3
Flores 2014	2980	0.026	6.6
Flores 2014	2985	0.021	5.2
Flores 2014	2990	0.066	4.3
Flores 2014	2990	0.041	4.4
Flores 2014	2990	0.16	2.2
Flores 2014	2992.5	0.079	3.7
Flores 2014	2995	0.095	5.2
Flores 2014	2995	0.046	5.8
Flores 2014	2995	0.006	2.5
Flores 2014	2997.5	0.056	5.6
Flores 2014	2997.5	0.288	3.6
Flores 2014	3000	0.04	5.8
Flores 2014	3000	0.035	5.6
Flores 2014	3000	0.155	4.7
Flores 2014	3002.5	0.04	5.4
Flores 2014	3002.5	0.146	1.9
Flores 2014	3005	0.07	4.8
Flores 2014	3005	0.063	6.7
Flores 2014	3005	0.011	2
Flores 2014	3007.5	0.095	9.3
Flores 2014	3007.5	0.109	2.7
Flores 2014	3010	0.085	6.1
Flores 2014	3010	0.097	8.4
Flores 2014	3010	0.008	4.8
Flores 2014	3012.5	0.135	3.1
Flores 2014	3015	0.065	5
Flores 2014	3015	0.03	5.2
Flores 2014	3015	0.012	3.8
Flores 2014	3017.5	0.164	4.2
Flores 2014	3020	0.098	5.1
Flores 2014	3020	0.06	5.6
Flores 2014	3025	0.077	4.6
Flores 2014	3030	0.124	5.3
Flores 2014	3035	0.072	5.5
Flores 2014	3040	0.083	6.3
Flores 2014	3045	0.046	6.5
Flores 2014	3052.5	0.192	4.6
Flores 2014	3055	0.118	4.6
Flores 2014	3057.5	0.09	8

Flores 2014	3060	0.221	23.2
Flores 2014	3060	0.159	3.1
Flores 2014	3065	0.092	4.4
Flores 2014	3070	0.239	18.7
Flores 2014	3070	0.001	5.6
Flores 2014	3075	0.112	9
Flores 2014	3080	0.028	5.2
Flores 2014	3085	0.096	5.2
Flores 2014	3090	0.01	15.8
Flores 2014	3090	0.082	3.2
Flores 2014	3092.5	0.154	5.6
Flores 2014	3095	0.081	3.8
Flores 2014	3095	0.118	5.1
Flores 2014	3097.5	0.158	4.8
Flores 2014	3100	0.14	13.8
Flores 2014	3100	0.167	3.1
Flores 2014	3102.5	0.163	3.4
Flores 2014	3105	0.247	3.4
Flores 2014	3110	0.116	15.9
Flores 2014	3110	0.177	4.4
Flores 2014	3120	0.147	3.7
Flores 2014	3140	0.011	5.2
Flores 2014	3145	0.01	3.9
Flores 2014	3150	0.03	3.4
Flores 2014	3155	0.035	4.4
Flores 2014	3160	0.029	2.7
Flores 2014	3165	0.16	6.6
Flores 2014	3170	0.116	7.5
Flores 2014	3175	0.043	5.5
Flores 2014	3175	0.07	5.4
Flores 2014	3180	0.025	4.4
Flores 2014	3180	0.04	3.6
Flores 2014	3185	0.075	5.1
Flores 2014	3195	0.046	4.7
Flores 2014	3197.5	0.09	3.2
Flores 2014	3200	0.073	5.7
Flores 2014	3200	0.122	4.9
Flores 2014	3202.5	0.015	2.5
Flores 2014	3205	0.073	4
Flores 2014	3205	0.115	2.8

Flores 2014	3210	0.04	4.8
Flores 2014	3210	0.063	3.8
Flores 2014	3212.5	0.07	3.5
Flores 2014	3215	0.05	4.7
Flores 2014	3215	0.176	3.6
Flores 2014	3220	0.06	3.6
Flores 2014	3220	0.105	0.9
Flores 2014	3225	0.05	4.4
Flores 2014	3225	0.136	2.1
Flores 2014	3230	0.013	4.5
Flores 2014	3235	0.03	4.1
Flores 2014	3240	0.069	4.3
Flores 2014	3245	0.05	4.3
Flores 2014	3250	0.049	4.8
Flores 2014	3250	0.1	4.8
Flores 2014	3252.5	0.113	1.5
Flores 2014	3255	0.12	5.4
Flores 2014	3255	0.286	3.8
Flores 2014	3257.5	0.121	2.9
Flores 2014	3260	0.068	3.8
Flores 2014	3260	0.144	1
Flores 2014	3262.5	0.106	2.4
Flores 2014	3265	0.065	4.5
Flores 2014	3265	0.128	3.6
Flores 2014	3267.5	0.114	4.3
Flores 2014	3270	0.091	3.1
Flores 2014	3272.5	0.095	3.6
Flores 2014	3275	0.026	5.1
Flores 2014	3275	0.071	4.2
Flores 2014	3277.5	0.126	2.9
Flores 2014	3280	0.015	4.9
Flores 2014	3280	0.027	5.9
Flores 2014	3282.5	0.009	4.2
Flores 2014	3285	0.015	5.7
Flores 2014	3285	0.136	4.8
Flores 2014	3287.5	0.013	4
Flores 2014	3290	0.02	2.5
Flores 2014	3290	0.087	5.2
Flores 2014	3292.5	0.095	5.4
Flores 2014	3295	0.135	5.3

Flores 2014	3295	0.11	6.7
Flores 2014	3297.5	0.114	6.1
Flores 2014	3300	0.232	8.5
Flores 2014	3302.5	0.09	4.7
Flores 2014	3305	0.044	4.7
Flores 2014	3305	0.174	8.4
Flores 2014	3307.5	0.033	3.6
Flores 2014	3310	0.022	4.2
Flores 2014	3310	0.102	6.6
Flores 2014	3312.5	0.021	4.6
Flores 2014	3315	0.03	3.4
Flores 2014	3317.5	0.025	4.2
Flores 2014	3320	0.021	2.7
Flores 2014	3322.5	0.023	4.3
Flores 2014	3325	0.025	3.4
Flores 2014	3327.5	0.023	5.3
Flores 2014	3330	0.02	4.6
Flores 2014	3332.5	0.016	4.9
Flores 2014	3350	0.031	4.6
Flores 2014	3355	0.142	4.2
Flores 2014	3360	0.052	5
Flores 2014	3365	0.035	5
Flores 2014	3370	0.025	5
Flores 2014	3375	0.027	6.2
Flores 2014	3380	0.044	5.7
Flores 2014	3385	0.013	6.2
Flores 2014	3390	0.042	4.7
Flores 2014	3395	0.02	4.1
Flores 2014	3400	0.02	4.9
Flores 2014	3430	0.018	6
Flores 2014	3435	0.152	6.8
Flores 2014	3440	0.06	5.5
Flores 2014	3445	0.046	5.2
Flores 2014	3450	0.06	4.9
Flores 2014	3455	0.196	4.3
Flores 2014	3460	0.037	4
Flores 2014	3465	0.17	6.1
Flores 2014	3470	0.023	12.3
Flores 2014	3470	0.035	6.2
Flores 2014	3475	0.034	21.5

Flores 2014	3475	0.025	5.5
Flores 2014	3480	0.012	12.7
Flores 2014	3485	0.009	12.2
Flores 2014	3505	0.056	7.1
Flores 2014	3510	0.067	11.1
Flores 2014	3515	0.029	8.1
Flores 2014	3520	0.04	7.5
Flores 2014	3560	0.019	9.9
Flores 2014	3565	0.039	8
Flores 2014	3570	0.042	9.8
Flores 2014	3575	0.037	10
Flores 2014	3585	0.02	8.4
Flores 2014	3590	0.07	6.1
Flores 2014	3595	0.068	6
Flores 2014	3600	0.056	7.1
Flores 2014	3605	0.128	9.5
Flores 2014	3610	0.058	8.8
Flores 2014	3615	0.015	14.9

APPENDIX C

MONTNEY CORE DATA

AUTHOR	DEPTH	Permeability, mD	Porosity, %
Derder 2012	2188	7.4	0.08
Derder 2012	2188.09	6.1	0.04
Derder 2012	2188.33	5.9	0.09
Derder 2012	2188.43	6.2	0.05
Derder 2012	2188.57	7.1	0.06
Derder 2012	2188.67	4.4	0.02
Derder 2012	2188.89	4.7	0.03
Derder 2012	2189.22	5.7	0.06
Derder 2012	2189.42	6.1	0.05
Derder 2012	2189.66	2.9	0.02
Derder 2012	2189.82	6.4	0.06
Derder 2012	2190.06	7.2	0.07
Derder 2012	2190.23	5.6	0.07
Derder 2012	2190.37	5.9	0.08
Derder 2012	2190.48	7.5	0.11
Derder 2012	2190.67	4.6	0.04
Derder 2012	2190.86	7.3	0.08
Derder 2012	2191.07	7.2	0.08
Derder 2012	2191.3	8.3	0.1
Derder 2012	2191.5	6.8	0.08
Derder 2012	2191.71	6.1	0.04
Derder 2012	2191.89	6	0.03
Derder 2012	2192.08	7	0.07
Derder 2012	2192.24	5.8	0.06
Derder 2012	2192.31	6	0.05
Derder 2012	2192.44	6.6	0.06
Derder 2012	2192.6	6.8	0.06
Derder 2012	2192.76	6.5	0.11
Derder 2012	2192.92	6.3	0.05
Derder 2012	2193.18	6	0.38
Derder 2012	2193.38	7	0.05
Derder 2012	2193.52	7	0.05
Derder 2012	2193.68	7.6	0.1
Derder 2012	2193.75	7.7	0.1
Derder 2012	2193.88	6.2	0.06
Derder 2012	2194.05	5.5	0.07
Derder 2012	2194.18	6.9	0.05
Derder 2012	2194.39	6.4	0.05
Derder 2012	2194.61	5.2	0.06

Derder 2012	2194.81	5.4	0.09
Derder 2012	2195	4.8	0.05
Derder 2012	2195.16	5.3	0.06
Derder 2012	2195.26	6.1	0.05
Derder 2012	2195.39	6.6	0.05
Derder 2012	2195.57	4.6	0.03
Derder 2012	2195.77	5.7	0.05
Derder 2012	2195.92	5.8	0.04
Derder 2012	2196.15	5.9	0.06
Derder 2012	2196.28	6.7	0.05
Derder 2012	2196.48	4.9	0.02
Derder 2012	2196.74	5.1	0.06
Derder 2012	2196.87	4.3	0.02
Derder 2012	2197.09	4.7	0.02
Derder 2012	2197.2	2.8	0.03
Derder 2012	2197.4	3.2	0.01
Derder 2012	2197.6	5	0.03
Derder 2012	2197.76	4.7	0.02
Derder 2012	2197.97	6.7	0.04
Derder 2012	2198.17	5.5	0.05
Derder 2012	2198.3	5.3	0.04
Derder 2012	2198.46	6.1	0.04
Derder 2012	2198.64	6	0.03
Derder 2012	2198.86	4.2	0.08
Derder 2012	2198.95	6.5	0.05
Derder 2012	2199.18	4.2	0.08
Derder 2012	2199.39	5.5	0.26
Derder 2012	2199.56	5.9	0.05
Derder 2012	2199.84	5.3	0.04
Derder 2012	2200.04	4.7	0.02
Derder 2012	2200.24	7.1	0.08
Derder 2012	2200.5	7.1	0.07
Derder 2012	2200.73	6.7	0.04
Derder 2012	2200.98	6.5	0.06
Derder 2012	2201.13	8.1	0.07
Derder 2012	2201.28	7.1	0.06
Derder 2012	2201.52	7.2	0.05
Derder 2012	2201.69	6.3	0.1
Derder 2012	2201.76	7.7	0.09
Derder 2012	2201.98	5.3	0.04

Derder 2012	2202.3	5.1	0.04
Derder 2012	2202.47	5.3	0.03
Derder 2012	2202.73	6.6	0.05
Derder 2012	2202.98	6.2	0.04
Derder 2012	2203.09	6	0.03
Derder 2012	2203.3	5.4	0.02
Derder 2012	2203.56	6	0.06
Derder 2012	2203.66	6.4	0.06
Derder 2012	2203.85	4.8	4.43
Derder 2012	2204.2	5.1	0.07
Derder 2012	2204.71	4.7	0.02
Derder 2012	2205.07	6.9	0.04
Derder 2012	2205.26	5.6	0.06

APPENDIX D

RELATED PAPERS

SPE-185115-MS

Evaluating Multiple Methods to Determine Porosity from Drilling Data

A.E. Cedola, A. Atashnezhad, G. Hareland, Oklahoma State University

This paper was prepared for presentation at the SPE Oklahoma City Oil and Gas Symposium held in Oklahoma City, Oklahoma, USA, 27—30 March 2017.

Abstract

Porosity can be obtained from drilling data by using different correlations that relate the porosity to the unconfined compressive strength (UCS), which is obtained from drill bit inverted rate of penetration (ROP) models. Knowing the porosity at a given depth can benefit in helping to define the formations being penetrated and to characterize variations in a reservoir, thereby benefitting in selective stimulation. In this paper, previous studies that present methods for calculating porosity from UCS values will be compared and evaluated with sections of porosity that have been calculated from log data taken from three wells in Alberta, Canada. The correlations that will be compared include: Onyia, Sarda, Erfourth, and the UCS-gamma ray methods. The Onyia, Sarda, and Erfourth correlations are previously published while the UCS-gamma ray method correlates UCS in conjunction with the gamma ray at the bit. The porosity values that are found through these correlations are then plotted and their trends compared to each other as well as to the porosity obtained from log data in different sections from the well in Alberta, Canada. This process will help to determine what formation types are best correlated to the individual correlation. Typical drilling data is used in an inverted ROP model to obtain UCS. The UCS and gamma ray values are then taken and related to the porosity through the correlations presented in this paper and compared to the porosity determined from log data. Examining the different correlations that have been analyzed in various types of formations yield information indicating which correlation is best correlated to a specific formation type. The comparison's show that the predictability for some correlations are reasonable for limited datasets and sections of the well. To reasonably predict porosity

values for mixed lithologies or shale formations, the integration of gamma log data is necessary. The trends exhibited from the correlations show that the comparison between porosity in shale is better seen when using the integrated UCS-gamma ray correlation. Utilizing the new UCS-gamma ray model seemingly indicates that this useful new method can more accurately predict porosity variations in mixed lithologies and in shale reservoir sections. Bettering stimulation placement as well as minimizing logging in the reservoir can greatly reduce the overall cost of the operation. The improved selective stimulation process could also allow for higher production rates and/or potential reduced stimulation cost, thus increasing overall profit.

Background

Porosity determination can be a complex process. There have been many methods that utilize unconfined compressive strength (UCS) to find porosity. In these methods, UCS is found from laboratory testing and/or log data. While these techniques may yield fairly accurate UCS values, they can be extremely costly and potentially misrepresentative of large intervals. The accuracy of porosity found from drill cuttings can be greatly influenced by the size of the cuttings and desaturation time (Yu & Menouar 2015). Log analysis has also been used for porosity determination, however, certain logs may not accurately identify various lithologies within a formation. According to Heslop (1974), the gamma ray log is one of the only logs that are able to identify shale zones. To determine shale volume, a combination of gamma ray, density porosity, and neutron porosity must be known (Bhuyan and Passey 1994). Log analysis can also be affected by drilling fluids, which can over or underestimate porosity. The use of core analysis for determining porosity is considered the optimal approach, but this technique isn't commonly performed due to the high costs associated with coring (Smith and Ziane 2015).

Establishing empirical models has been useful in eliminating the need for excess logging tools and laboratory testing. In this paper, three methods that have been previously published will be analyzed and compared to determine their accuracy and applicability to field data. These methods are: the Onyia method (Onyia 1988), Sarda method (Sarda et al. 1993), Erfourth method (Erfourth et al. 2005) and a new Gamma Ray method presented within this paper.

Onyia Method

The Onyia method (Eq. 1) for determining a correlation between UCS and porosity uses Warren's roller cone penetration rate model to calculate UCS from drilling data. In this case, data from multiple logs were used to calculate the UCS and determine which log provided the most accurate results. Because the UCS is calculated directly from log and drilling data, there is potential for this method to be used in real time drilling (Onyia 1988). The Onyia method is applicable to a variety of lithologies, including both shale and sandstone.

$$\delta_{UCS} = 3.2205 + \frac{102.51}{\emptyset}, \quad (1)$$

Sarda Method

The Sarda method (Eq. 2) utilizes a combination of log and laboratory data to establish a correlation between porosity and UCS in sandstones (Sarda et al. 1993). A correlation that had been developed for ceramic materials was adapted to determine UCS values at different porosity ranges: 0-7% porosity, up to 30% porosity, and 30% porosity and higher. For the purpose of this paper, the Sarda equation for porosity ranging from 0-30% will be used.

$$\sigma_{UCS} = 258e^{-9\emptyset}, \quad (2)$$

Erfourth Method

The Erfourth method (Eq. 3) for relating UCS and porosity uses UCS data that has been collected from laboratory testing on core, cast, and tuff samples. Statistical analysis of the samples proved that both the cast and core samples are feasible for modeling rock UCS and porosity (Erfourth et al. 2005).

$$\sigma_{UCS} = 194.39e^{\left(-\frac{\emptyset}{12.55}\right)}, \quad (3)$$

To observe any differences between the three previously published correlations, normalized UCS and porosity values were plotted in **Fig. 1**. The plot shows that the Onyia method yields much higher porosity values for low UCS zones while the Erfourth method becomes inaccurate for high UCS areas. The Onyia correlation also becomes relatively constant at a UCS value of 100 MPa.

An alternate method for obtaining UCS is to take it from drilling data, which is less costly and time consuming than precious methods. Utilizing an inverted rate of penetration (ROP) model yields results similar to those obtained from log or laboratory data (Hareland & Nygaard 2007). The inverted ROP model takes conventionally recorded drilling data and calculates the corresponding UCS. This method is beneficial because there are no additional costs associated. It can be used to determine UCS for extended intervals or an entire well.

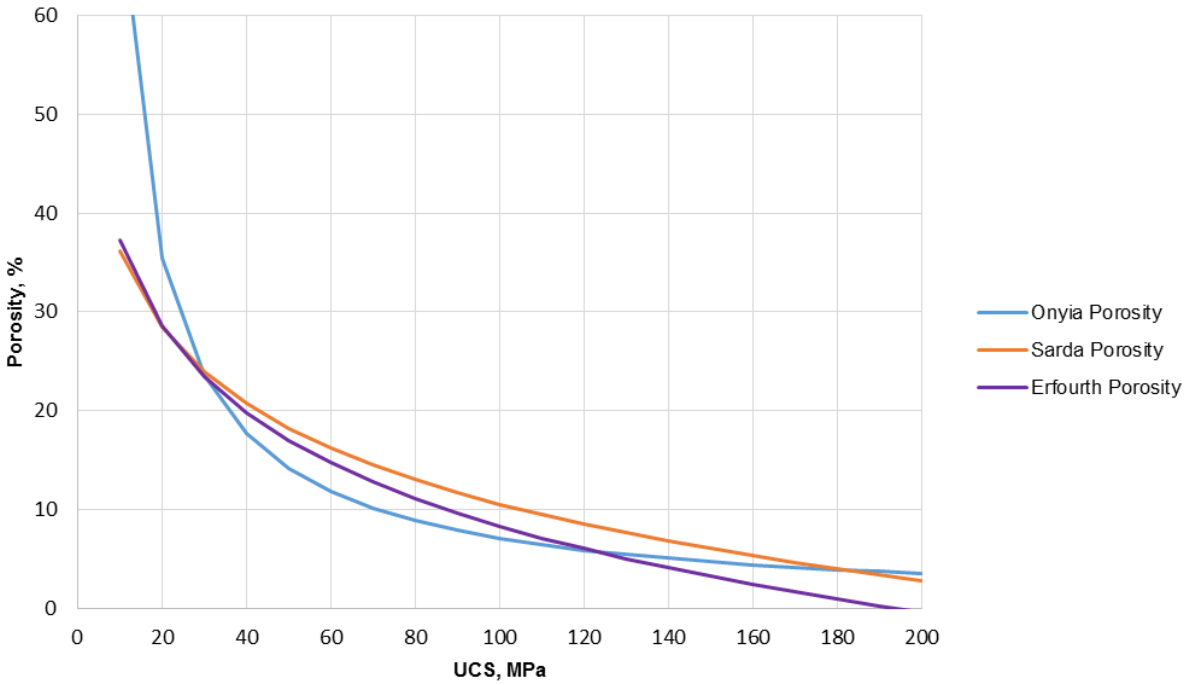

Fig. 1-Onyia, Sarda, and Erfourth porosity comparison for normalized UCS values

Gamma Ray Method

While the Onyia, Sarda, and Erfourth methods are good porosity indicators in sandstone, they lack the ability to accurately predict shale porosity. To establish accurate correlations for both sandstone and shale porosity versus UCS, data from multiple published sources was gathered and plotted (Horsund 2001, Chang 2004, Gutierrez et al. 2000, Lashkaripour 2002, Farquhar et al. 1993, Khaksaret al. 2009, Hawkins & Mcconnell 1991, Kim et al. 2015, Yao 2015). This data consisted of both core and cuttings analyses. A trendline was added and a correlation between the UCS and porosity was determined for sandstone and shale lithologies as seen in **Figs. 2 and 3**. These correlations will be referred to as the Cedola sandstone and Cedola shale correlations.

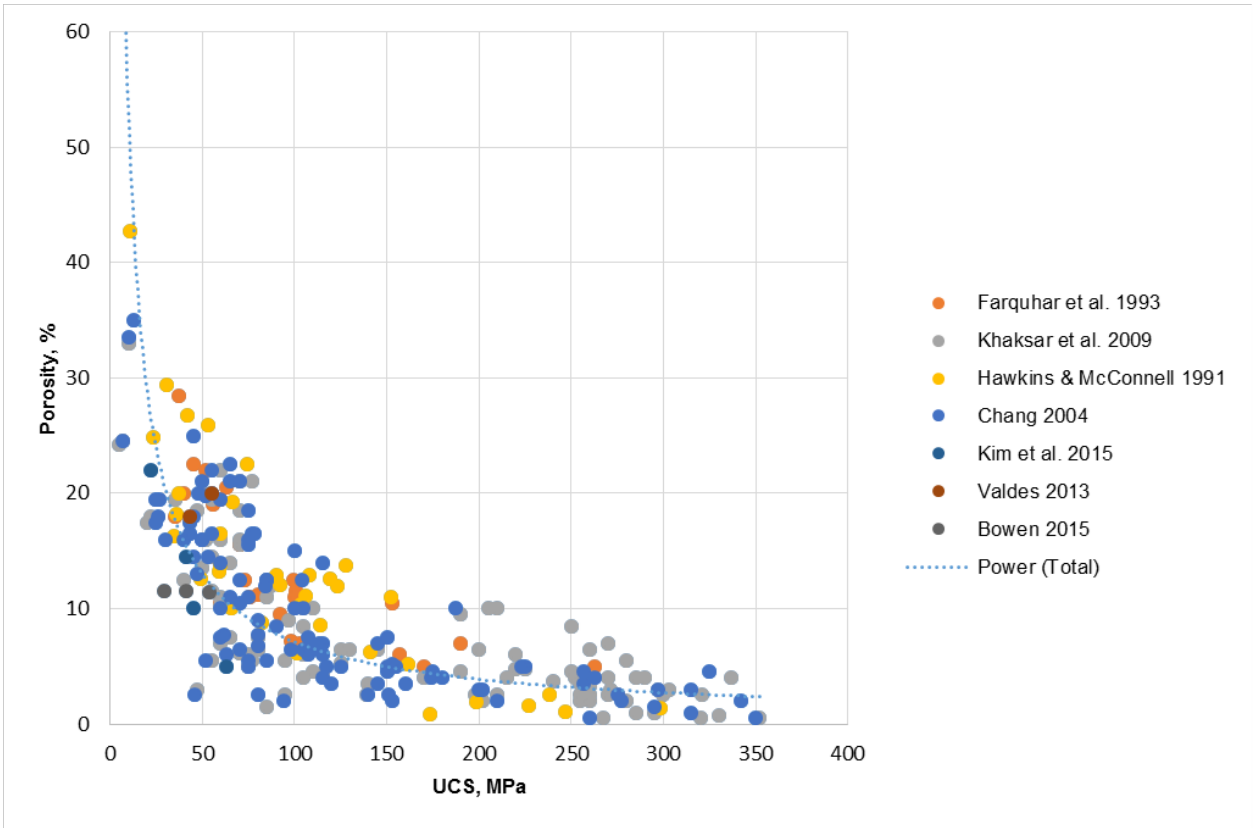

Fig. 2-Cedola sandstone correlation obtained from various sandstone formations core and cuttings analysis

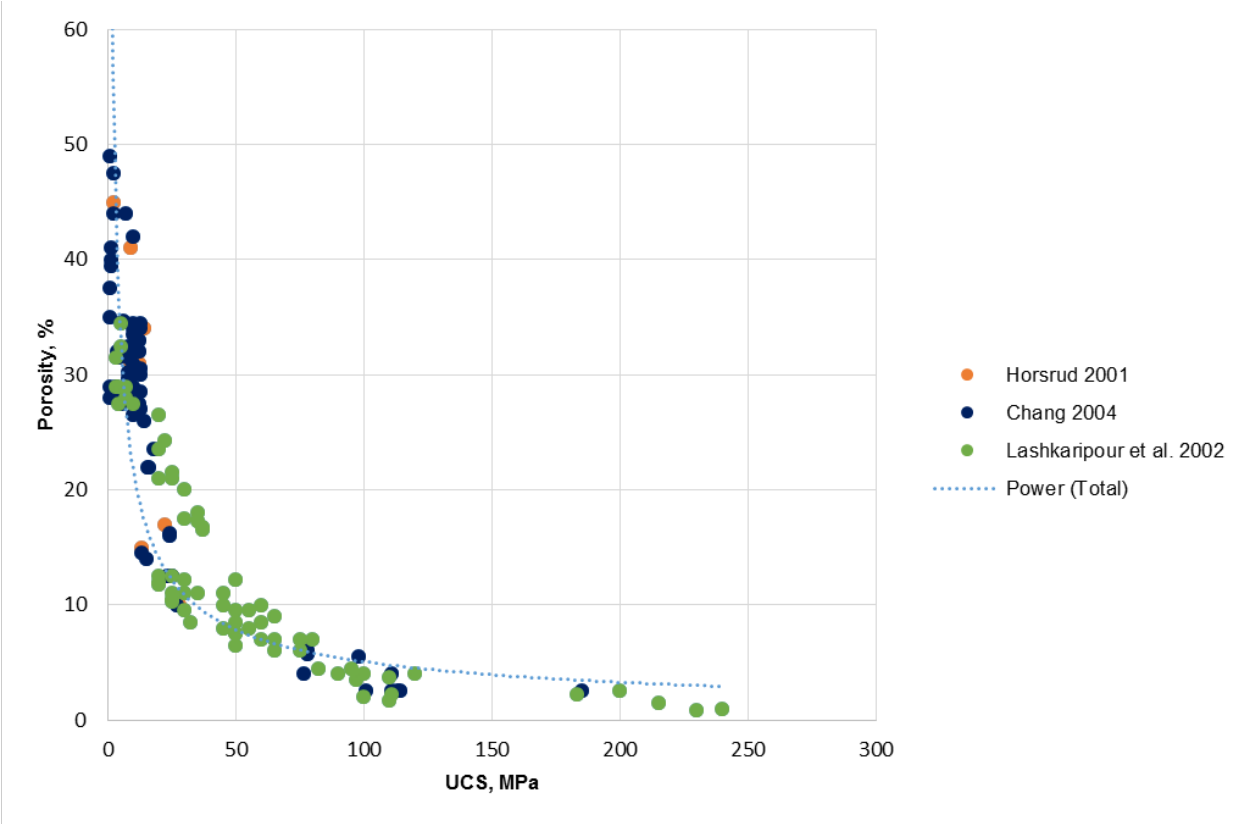

Fig. 3-Cedola shale correlation obtained from various shale formations core and cuttings analysis

The trendline equations for the sandstone and shale are given in Eqs. 4 & 5, respectively.

$$y = 424.8 \times UCS^{-0.825} \quad \text{.....} \quad (4)$$

$$y = 92.529 \times UCS^{-0.63} \quad \text{.....} \quad (5)$$

A comparison between normalized UCS versus porosity for the previously published methods and the Cedola sandstone and shale correlations is shown in **Fig. 4.** The plot shows that the Onyia and Cedola sandstone correlations are similar in both value and trend. The Cedola shale correlation has a similar trend to the Sarda and Erfourth correlations and it is seen that for all the correlations at high UCS values the porosities become much closer in values. Both the Cedola sandstone and shale correlations level out at UCS values of about 150 MPa.

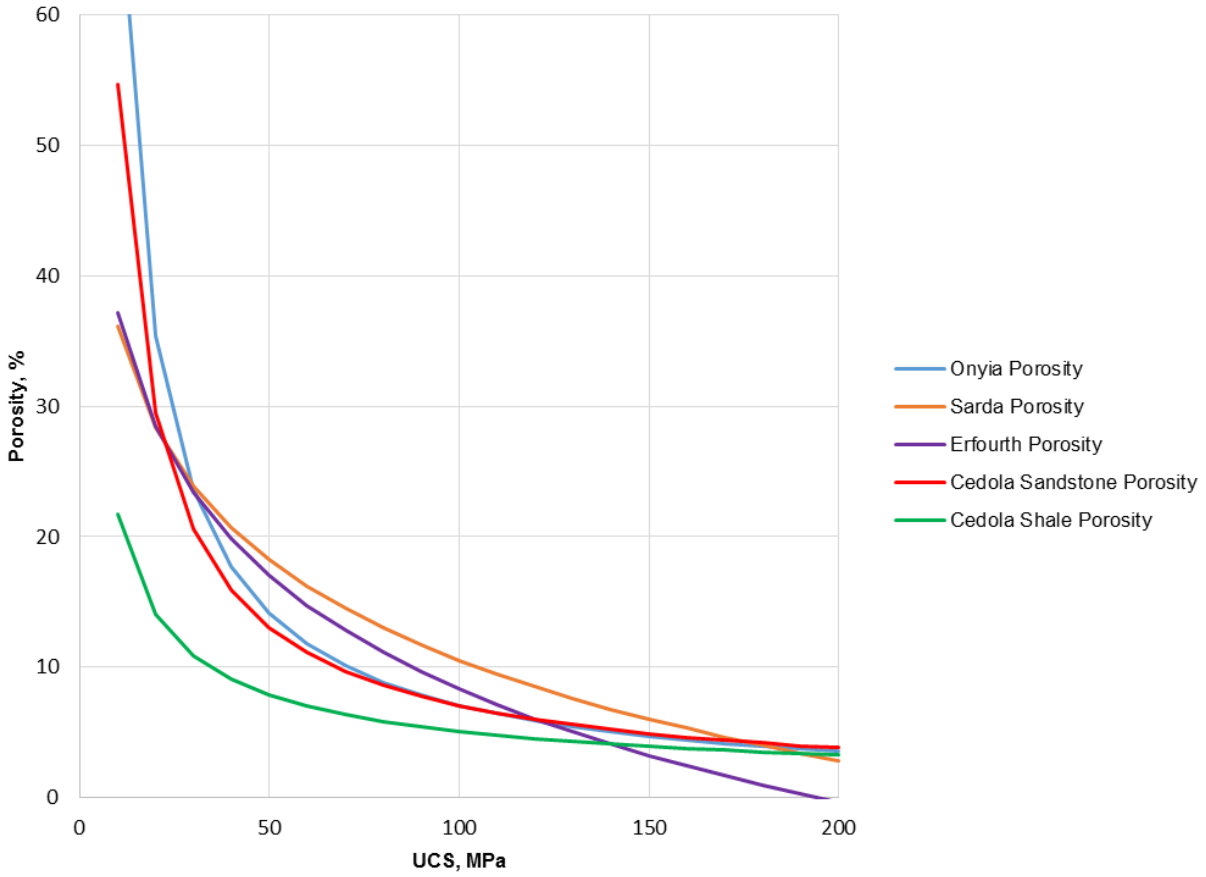

Fig. 4-Comparison between the Cedola sandstone and shale correlations to the Onyia, Sarda, and Erfourth methods

While it is believed that the Cedola sandstone and shale correlations are good porosity predictors in homogeneous formations, a new correlation must be used to evaluate the porosity in mixed lithologies. For these types of lithologies, the use of gamma ray log data

will be considered and used to establish a Gamma Ray Porosity. The Gamma Ray Porosity has been compared in two ways: linearly and as a power function (**Figs. 5 and 6**).

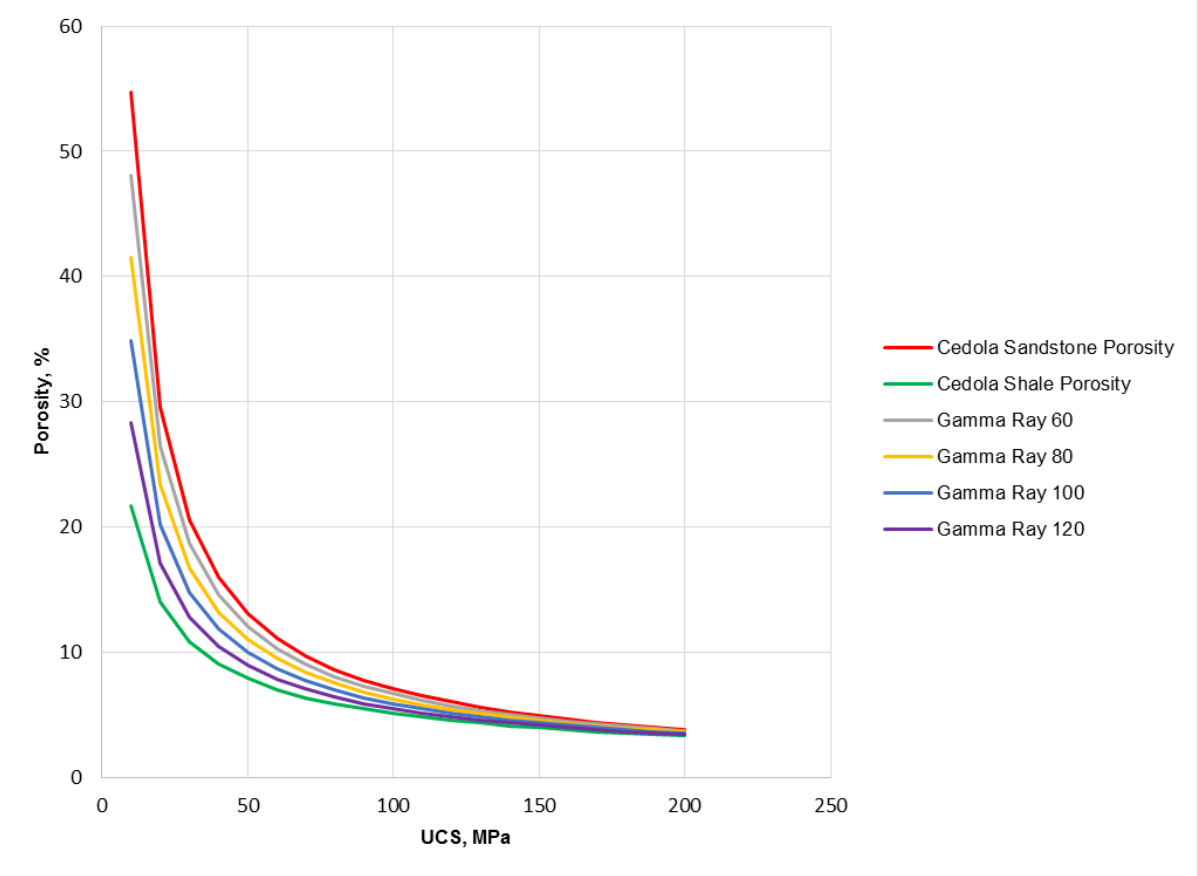

Fig. 5-Linear Gamma Ray Porosity plot

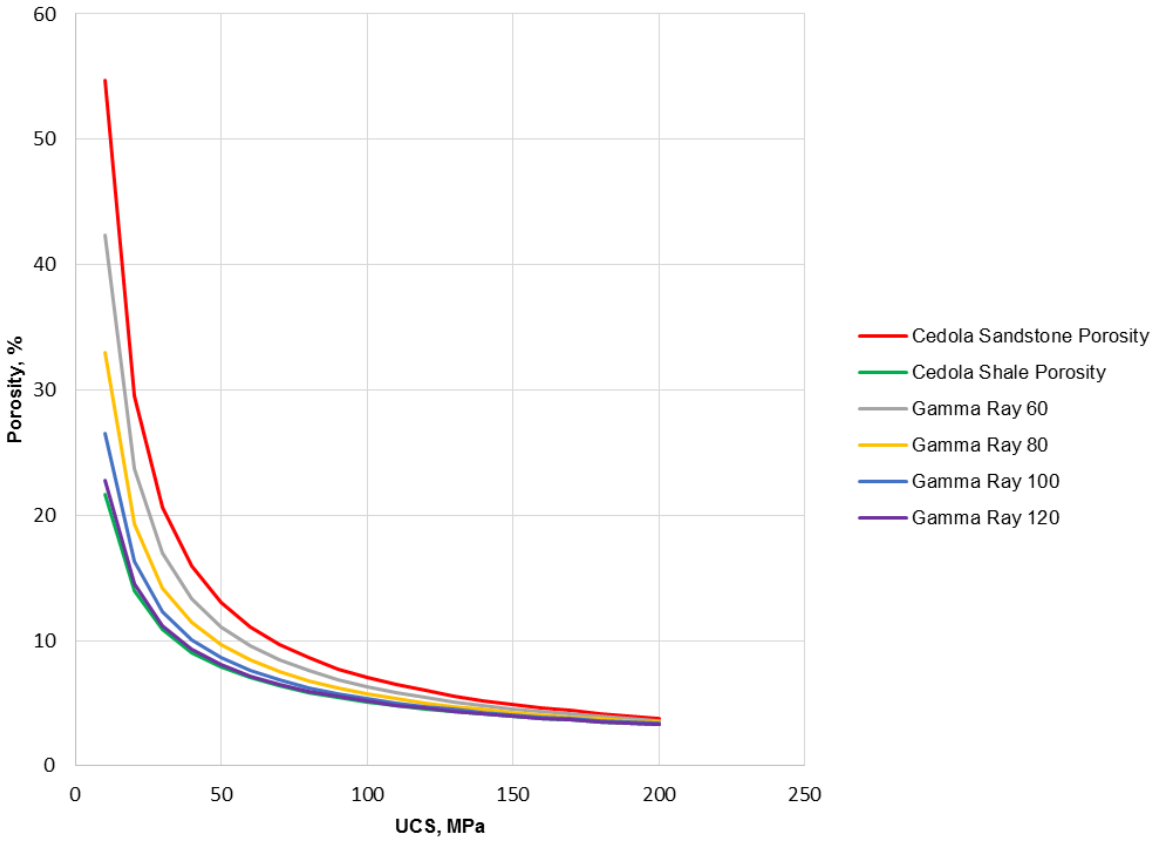

Fig. 6-Power Gamma Ray Porosity plot

Any gamma ray readings below 40 and above 140 are considered completely sandstone and shale, respectively. Because the Cedola sandstone and shale porosities are representative of entirely sandstone or entirely shale formations, they will be equivalent to the gamma ray readings 40 and 140 API. The Gamma Ray porosity equation is shown in **Eq. 7**.

$$\emptyset_{Gamma\ Ray} = \emptyset_{Cedola\ Shale} + (\emptyset_{Cedola\ Sandstone} - \emptyset_{Cedola\ Shale}) \times \left(\frac{140 - Gamma\ Ray\ Reading}{140 - 40}\right)^{a_1}, \quad (7)$$

To verify the accuracy of UCS obtained from drilling data, a previous study in which neutron porosity and gamma ray data has been taken for sandstone and shale formations in ten wells and correlated against their respective UCS obtained from an inverted ROP model was analyzed (Andrews et al. 2007). The inverted ROP model takes bit, operational drilling data, and lithological data into consideration. From the study, a linear gamma ray porosity interpolation was found and the best fit correlation is used to find the power Gamma Ray porosity method. For both the linear and power Gamma Ray methods, the upper and lower bounds are equivalent to the Cedola sandstone and shale correlations, respectively. The linear interpolation shown in Fig. 5 is obtained using a gamma ray coefficient, a_1 equal to 1.0 while the results shown in Fig. 6 are based on the analysis of the ten wells and the gamma ray coefficient, a_1 equal to 2.1 which was found

to be the best fit. The power Gamma Ray porosity values are more dependent on the formation composition and could be used to determine porosity in all lithologies.

Results and Discussion

A comparison between the correlations presented in this paper to the three previously published UCS-porosity correlations is done to see which method(s) is more accurate in both value and trend to log data porosity. Plotting the correlations for the three different lithological intervals gives insight as to which correlation works best in sandstone formations, shale formations, and mixed formations.

To analyze the Cedola sandstone and shale correlations potential for field application, drilling and log data from three previously drilled wells has been collected and separated by lithology. The Onyia, Sarda, and Erfourth correlations are plotted against neutron porosity to compare the correlation porosities to actual field data.

The shale plot comparison for the Onyia, Sarda, and Erfourth methods show that the neutron porosity is lower than any of the three methods (**Fig. 7**). The Onyia correlation result is unusual because this method has previously predicted accurate porosity values in sandstone, shale, and various other lithologies (Onyia 1988). The Cedola shale correlation shown in **Fig. 8** shows a similar match to the neutron porosity and is closer to the average porosity values reported for the Muskiki shale, 1.7-13.4% (Bachu & Underschultz 1992).

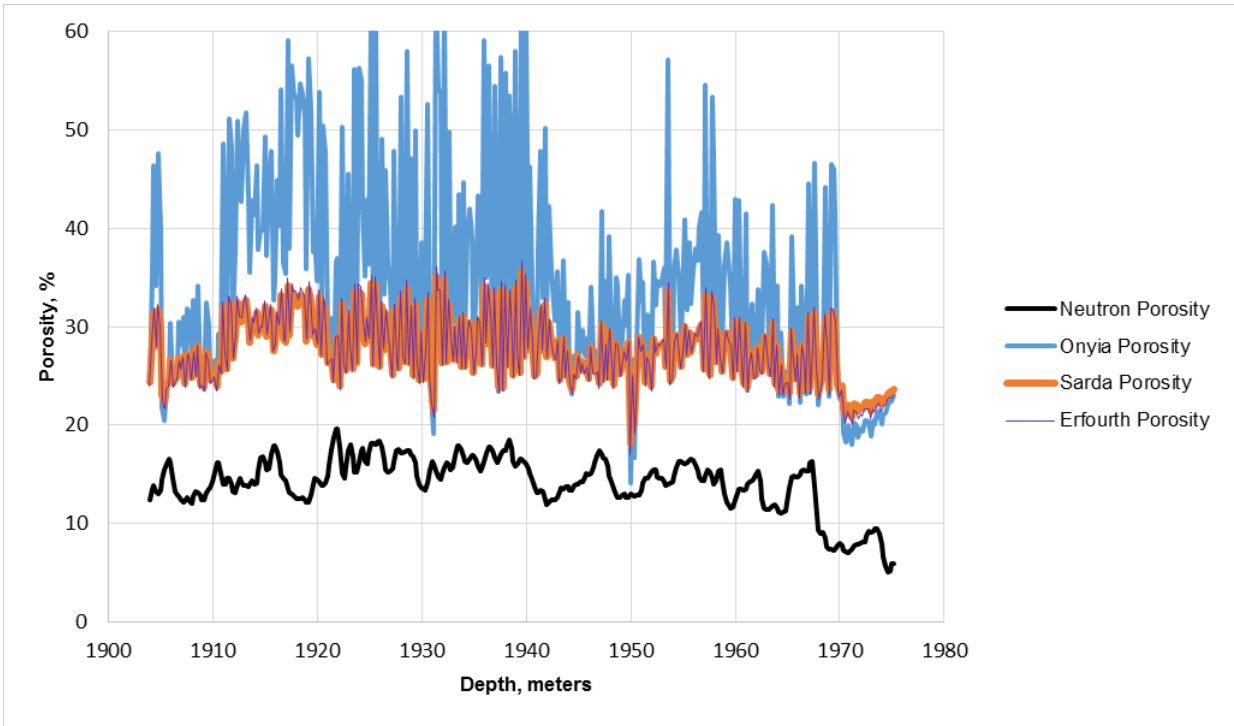

Fig. 7-Shale porosity comparison between the Onyia, Sarda, and Erfourth methods to the neutron porosity for the Muskiki shale

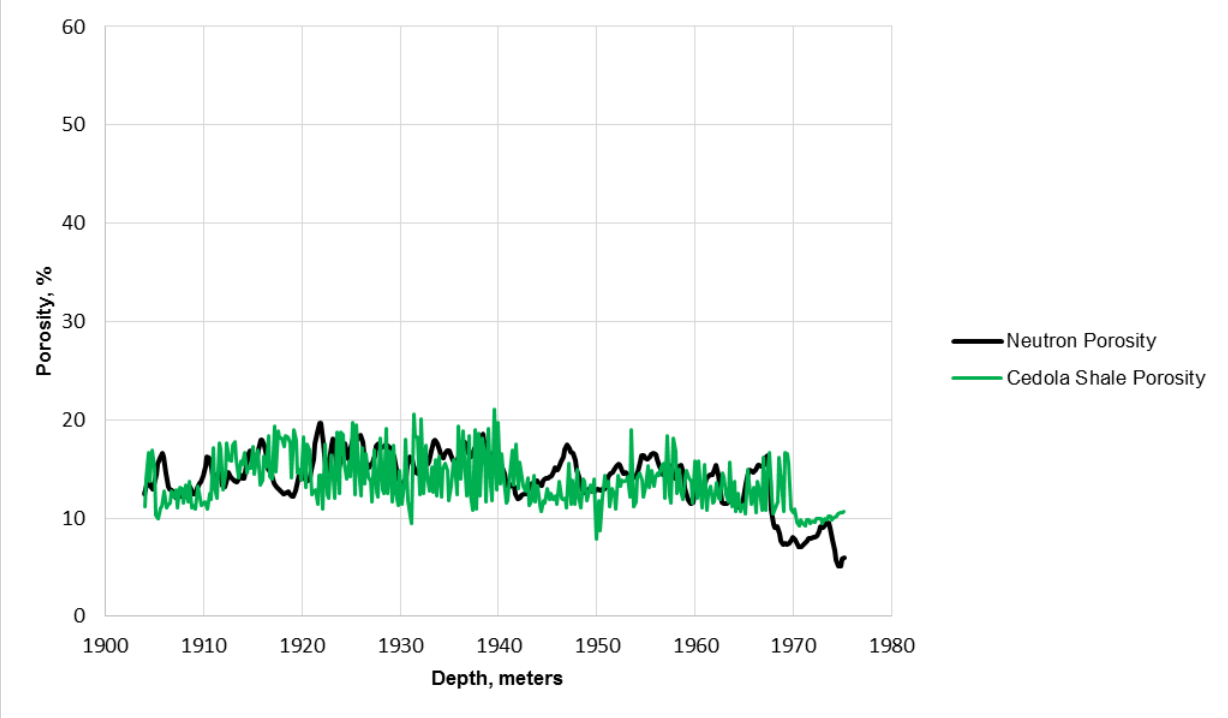

Fig. 8-Shale porosity comparison between the Cedola shale correlation and neutron porosity for the Muskiki shale

The sandstone porosity comparison shows great similarity between the Onyia, Sarda, and Erfourth plots to the neutron porosity (**Fig. 9**). The porosity values have a smaller range in variation and all three correlations match the neutron porosity data for a given depth interval. The Cedola sandstone correlation had similar porosity values to the three methods (**Fig. 10**). Such similarities indicate that UCS values obtained from drilling data predict sandstone porosity as accurate as correlations that require costly logging tools or laboratory tests. All correlations were within the average porosity range for the Falher sandstone, which does not exceed 15% (Harris 2014).

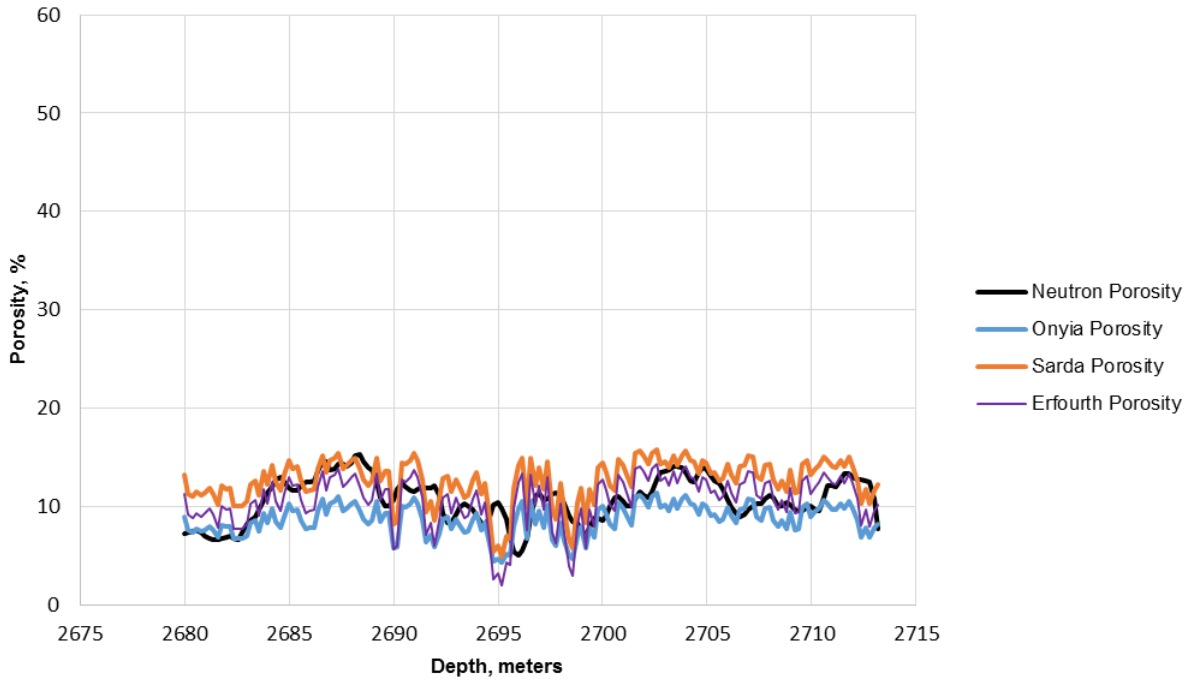

Fig. 9-Sandstone porosity comparison between the Onyia, Sarda, and Erfourth methods to the neutron porosity for the Falher sandstone

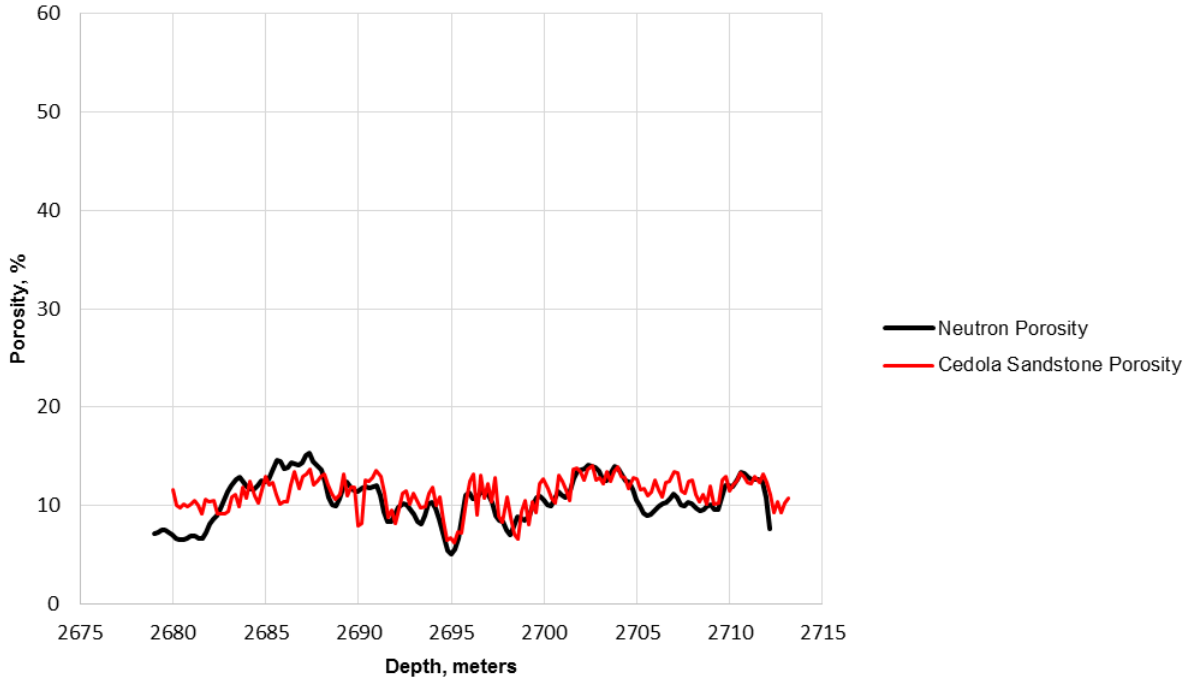

Fig. 10-Sandstone porosity comparison between the Cedola sandstone correlation and neutron porosity for the Falher sandstone

Previous methods for determining porosity in formations of complex lithology have required multiple types of log porosity combinations (Syngaevsky and Khafizov 2003). Analyzing a zone with mixed lithology indicates a large range in porosity values for the

Onyia, Sarda, and Erfourth methods (**Fig. 11**). The Onyia method has the greatest porosity variation with some porosity values exceeding 100%. The Sarda and Erfourth porosities have similar trends. The lower the neutron porosity, the less accurate the three methods become. Such variance implies that the Onyia, Sarda, and Erfourth methods may have the ability to predict porosity in zones where sandstone is the predominant lithology but could also give inaccurate values in regions of mainly shale or shaly sands.

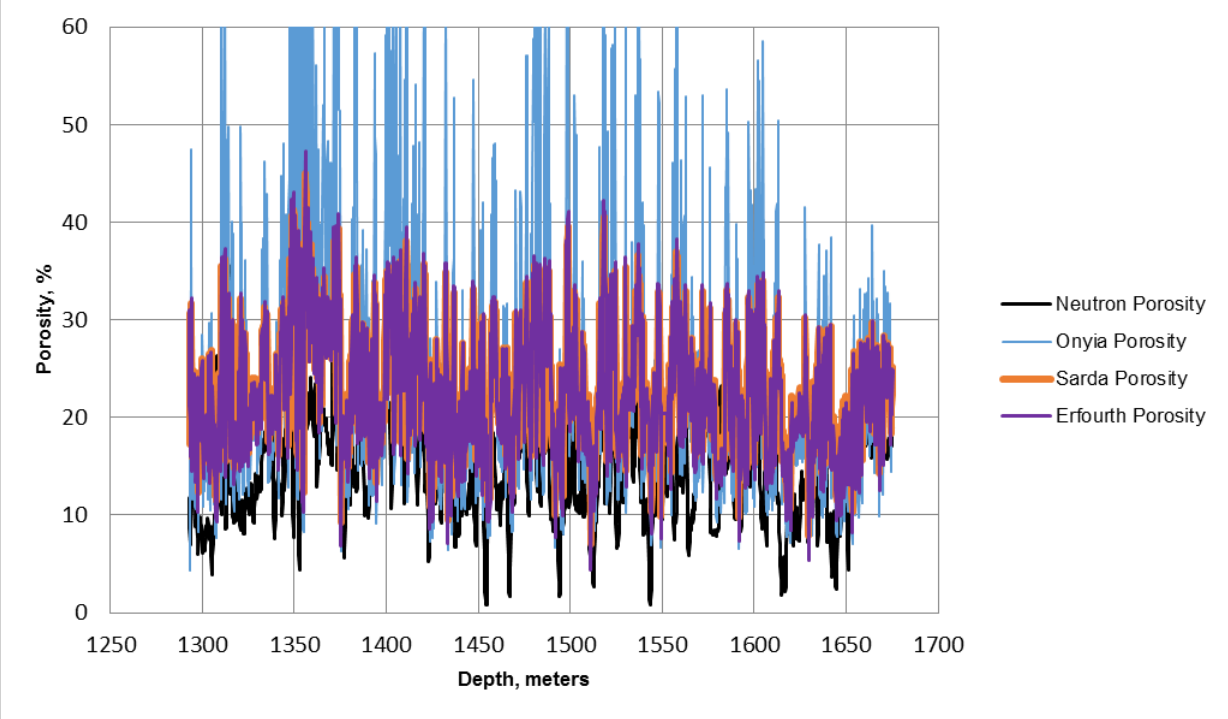

Fig. 11-Mixed lithology porosity comparison between the Onyia, Sarda, and Erfourth methods to the neutron porosity for the Belly River formation

A plot evaluating how the Gamma Ray correlation compares to neutron porosity is shown in **Fig. 12**. The plot shows that the Gamma Ray correlation doesn't match neutron porosity values that are significantly higher or lower than the average values. This is because the high neutron porosity values are in areas of high sandstone content while the low neutron porosity values are predominantly shale. For these areas, the Cedola sandstone and shale correlations prove more accurate in determining porosity. The Gamma Ray correlation has a better match to neutron porosity than the Onyia, Sarda, and Erfourth methods in a mixed lithology formation. This could be because both sandstone and shale porosities are included in the Gamma Ray method. The Onyia, Sarda, and Erfourth methods may be fairly accurate in sandy-shales, but the Gamma Ray correlation can better predict porosity in both sandy-shales, shaly-sands, and shale formations.

To visualize where the correlations presented within this paper are most accurate for a mixed lithology formation, a porosity versus depth plot has been created to determine how the Cedola sandstone, Cedola shale, and Gamma Ray correlations interact over various sand and shale contents (**Fig. 13**). The plot shows that while there are places where the Cedola sandstone or Cedola shale correlation matches with the neutron porosity, the Gamma Ray correlation does a much better job at predicting porosity in areas with a mixture of sandstone and shale.

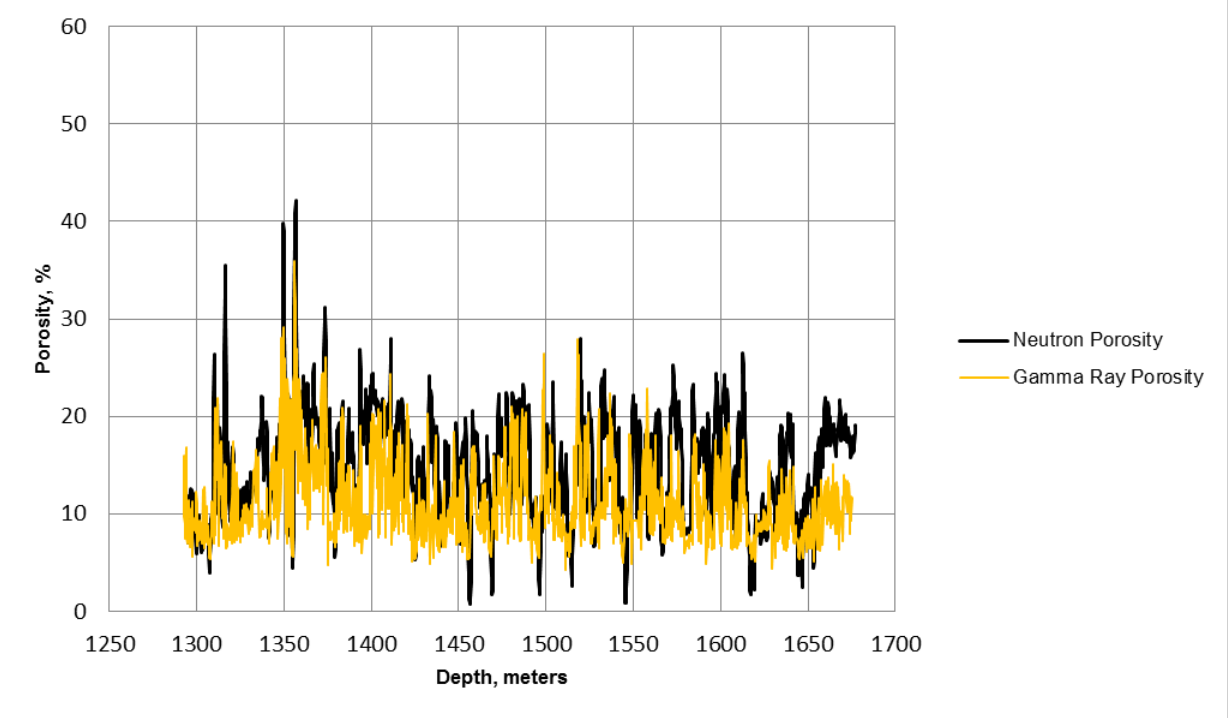

Fig. 12-Mixed lithology porosity comparison between the Gamma Ray correlation to neutron porosity for the Belly River formation

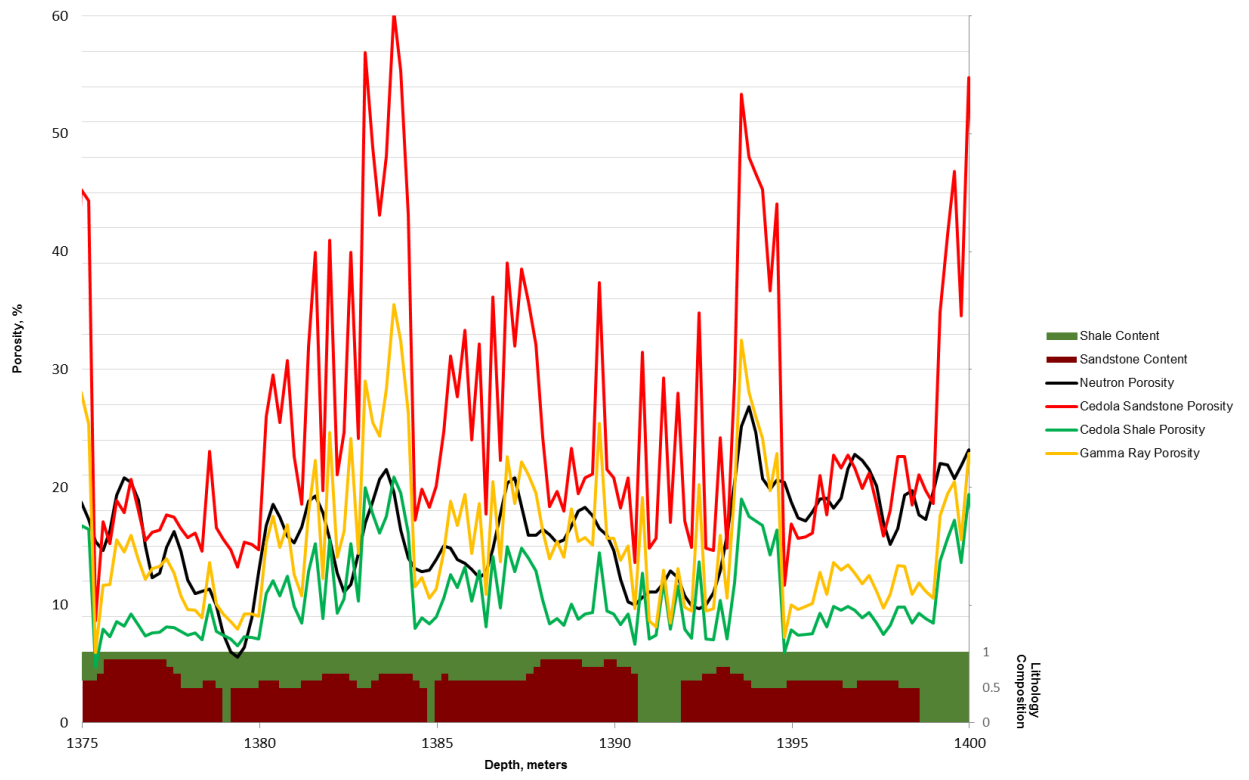

Fig. 13-Mixed lithology porosity comparison between the Cedola sandstone, shale, and Gamma Ray correlations to neutron porosity for a given depth interval within the Belly River formation

Application to Selective Stimulation

Understanding porosity variations within a well can affect stimulation placement and fracturing fluid design. Selectively stimulating a well can have a large impact on productivity and enhance fracture placement to better tap into hydrocarbon bearing zones. To determine optimal stimulation placement, geomechanical characterization near well bore must be known. This knowledge helps to identify areas where fractures are most likely to initiate and propagate as well as the required spacing to achieve maximum production (Glover et al. 2016).

The geomechanical data that is needed to establish selective stimulation schedules is found using well logs, cores, and/or cuttings analysis. Logs can show lithological composition and variation which can determine the areas that may be less successful at producing (Barree et al. 2014). Drill cuttings can help in reservoir characterization but aren't continuous for an entire well (Ortega & Aguilera 2014). While these methods can be indicative of areas in which selective stimulation could prove beneficial, the costs associated with such procedures could limit the amount of data collected.

Finding UCS and porosity from typical drilling data can reduce the cost associated with determining geomechanical properties as well as reduce the time needed to determine selective stimulation placement. Knowing the porosity for an extended interval can indicate where stimulation placement would optimize fracture initiation and propagation. UCS variations can be useful in determining zones where fracture propagation can best access the reservoir.

Conclusions

Utilizing drilling data to obtain correlations between porosity and UCS could prove beneficial in a variety of formations. The correlations are not only applicable to sandstone and shale formations, but the addition of gamma ray data allows such correlations to be feasible for predicting porosity in formations of mixed lithologies. While previously published methods for determining porosity from UCS yield relatively accurate porosity values for specific formations, the use of drilling data in conjunction with the gamma ray to determine porosity proves to be a potentially better indicator. Having a more accurate indication of porosity can benefit stimulation placement and in establishing a better sense of hydrocarbon bearing zones. The potential to reduce the need for logging tools could impact the overall operation cost while allowing for production maximization.

Nomenclature

UCS	Unconfined Compressive Strength, MPa
ROP	Rate of Penetration, meters per hour
ARSL	Apparent Rock Strength Log, MPa
Φ	Porosity, %
σ	Unconfined Compressive Strength, MPa
δ	Unconfined Compressive Strength, kPSI

References

Andrews, R., Hareland, G., Nygaard, R. et al. 2007. Methods of Using Logs to Quantify Drillability. Presented at the Rocky Mountain Oil & Gas Technology Symposium, Denver, Colorado, 16-18 April. SPE-106571-MS. http://dx.doi.org.argo.library.okstate.edu/10.2118/106571-MS.

Bachu, S. and Underschultz, J.R. 1992. Regional-Scale Porosity and Permeability Variations, Peace River Arch Area, Alberta, Canada. *AAPG Bulletin* **76** (4): 547-562.

Barree, R.D., Conway, M.W, and Miskimins, J.L. 2014. Use of Conventional Well Logs In Selective Completion Designs for Unconventional Reservoirs. Presented at the SPE Western North American and Rocky Mountain Joint Meeting, Denver, Colorado, 17-18 April. SPE-169565-MS. http://dx.doi.argo.library.okstate.edu/10.2118/169565-MS.

Bhuyan, K. and Passey, Q.R. 1994. Clay Estimation From GR abd Neutron-Density Porosity Logs. Presented at the SPWLA 20th Annual Logging Symposium,

Chang, C. 2004. Empirical Rock Strength Logging in Boreholes Penetrating Sedimentary Formations. *Geology and Environmenal Sciences, Chungnam National University, Daejeon* **7** (03): 174-183

Erfourth, B.S., MacLaughlin, M.M., and Hudyma, N. 2005. Comparison of Unconfined Compressive Strengths of Cast versus Cored Samples of Rock-like Materials with Large Voids. Presented at the Alaska Rocks 2005, The 40th U.S. Symposium on Rock Mechanics (USRMS), Anchorage, Alaska, 25-29 June. ARMA-05-876.

Farquhar, R.A., Smart, B.G.D., and Crawford, B.R. 1993. Porosity-Strength Correlation: Failure Criteria from Porosity Logs. Presented at the SPWLA 34th Annual Logging Symposium, Calgary, Alberta, 13-16 June. SPWLA-1993-AA.

Glover, K., Cui, A., Tucker, J. et al. 2016. Improved Geology-Based Geomechanical Models Using Drill Cuttings Data for Selective Fracture Stage Placement in the Montney, Duvernay, and Beyond. Presented at the AAPG 2016 Annual Convention and Exhibition, Calgary, Alberta, Canada, 19-22 June.

Hareland, G. and Nygaard, R. 2007. Calculating Unconfined Rock Strength from Drilling Data. Presented at the 1st Canada-U.S. Rock Mechanics Symposium, Vancouver, Canada, 27-31 May. ARMA-07-214.

Harris, N.B. 2014. Falher and Cadomin diagenesis and implications for reservoir quality. Presented at the GeoConvention 2014: Focus, Calgary, Canada, 12-14 May.

Hawkins, A. and Mcconnell, B.J. 1991. Influence of Geology on Geomechanical Properties of Sandstones. Presented at the 7th ISRM Congress, Aachen, Germany, 16-20 September. ISRM-7CONGRESS-1991-051.

Heslop, A. 1974. Gamma-Ray Log Response of Shaly Sandstones. Presented at the Fifteenth Annual Logging Symposium of SPWLA, McAllen, Texas, June 2-5 June. SPWLA-1974-vXVn5a2.

Horsrud, P. 2001. Estimating Mechanical Properties of Shale from Empirical Correlations. *SPE Drill & Compl* **16** (02): 68-73. SPE-56017-PA. http://dx.doi.org.argo.library.okstate.edu/10.2118/56017-PA.

Kerkar, P.B., Hareland, G., Fonseca, E.R. et al. 2014. Estimation of Rock Compressive Strength Using Downhole Weight-on-Bit and Drilling Models. Presented at the International Petroleum Technology Conference, Doha, Qatar, 19-22 January. IPTC-17447-MS. http://dx.doi.org.argo.library.okstate.edu/10.2523/IPTC-17447-MS.

Khaksar, A., Taylor, P.G., Fang, Z. et al. 2009. Rock Strength from Core and Logs, Where We Stand and Ways to Go. Presented at the EUROPE/EAGE Conference and Exhibition, Amsterdam, The Netherlands, 8-11 June. SPE-121972-MS. http://dx.doi.org.argo.library.okstate.edu/10.2118/121972-MS.

Kim, K-Y., Zhuang, L., Yang, H. et al. 2015. Strength Anisotropy of Berea Sandstone: Results of X-Ray Computed Tomography, Compression Tests, and Discrete Modeling. *Rock Mechanics and Rock Engineering* **49** (4).

Lashkaripour, G.R. 2002. Predicting mechanical properties of mudrock from index parameters. *Bulletin of Engineering Geology and the Environment* **61** (1): 73-77. 10.1007/s100640100116.

Onyia, E.C. 1988. Relationships Between Formation Strength, Drilling Strength, and Electric Log Properties. Presented at the SPE Annual Technical Conference and Exhibition, Houston, Texas, 2-5 October. SPE-18166-MS. http://dx.doi.or.argo.library.okstate.edu/10.2118/18166-MS.

Ortega, C. and Aguilera, R. 2014. Quantitative Properties from Drill Cuttings to Improve the Design of Hydraulic-Fracturing Jobs in Horizontal Wells. *J Can Pet Technol* **53** (01): 55-68. SPE-155746-PA. http://dx.doi.org.argo.library.okstate.edu/10.2118/155746-PA.

Sarda, J-P., Kessler, N., Wicquart, E. et al. 1993. Use of Porosity as a Strength Indicator for Sand Production Evaluation. Presented at the SPE Annual Technical Conference and Exhibition, Houston, Texas, 3-6 October. SPE-26454-MS. http://dx.doi.org.argo.library.okstate.edu/10.2118/26454-MS.

Smith, C.H. and L. Ziane. 2015. Mississippian Porosity and Permeability: Core Comparison to Nuclear Magnetic Resonance. Presented at the SPE Production and Operations Symposium, Oklahoma City, Oklahoma, 1-5 March. SPE-173592-MS.

Syngaevsky, P.E. and Khafizov, S.F. 2003. Application of Modern NMR Logging for Mixed-Lithology Carbonate Reservoirs (A Case Study). Presented at the Canadian International Petroleum Conference, Calgary, Alberta, 10-12 June. PETSOC-2003-016. http://dx.doi.org.argo.library.okstate.edu/10.2118/2003-016.

Valdes, C. and Raquel, C. 2013. *Characterization of Geomechanical Poroelastic Parameters in Tight Rocks.* Master's Thesis, Texas A&M University, College Station, Texas.

Yao, B. 2015. *Experimental Study and Numerical Modeling of Cryogenic Fracturing Process on Laboratory-Scale Rock and Concrete Samples.* Master's Thesis, Colorado School of Mines, Golden, Colorado.

Yu, Y. and Menouar, H. 2015. An Experimental Method to Measure the Porosity from Cuttings: Evaluation and Error Analysis. Presented at the SPE Production and Operations Symposium, Oklahoma City, Oklahoma, 1-5 March. SPE-173591-MS.

AADE-17-NTCE-134

Real-Time Porosity from Surface Drilling Data PredictionAnd Verification

A.E. Cedola, A. Atashnezhad, and G. Hareland, Oklahoma State University

Abstract

Porosity is a critical parameter during the drilling and completions process. Current methods to predict/determine porosity require expensive logging tools or time consuming laboratory tests. This paper outlines an empirical model developed to predict the formation porosity using surface drilling data and gamma ray (GR) at the bit without the need for log or lab data. An empirical model for porosity prediction through the use of drilling data has been developed using drilling strength or unconfined compressive strength (UCS) from drilling models. The UCS seen at the drill bit from an inverted rate of penetration (ROP) model and GR at the bit are used to estimate the formation porosity. Porosity calculated from log data from a well in Western Canada was used to validate the porosity model from drilling data with log calculated neutron density. The results from the model show good agreement between the model estimated porosity and porosity from the well log data. The comparison results show accurate quantitative matching as well as trends. The model presented can be applied to horizontal wells where the porosity can be mapped in addition to UCS values from the drilling data at no additional costs. Based on this formation porosity mapping log, better selective fracturing interval locations can be obtained taking the UCS and porosity of a formation into account.

Introduction

Porosity determination is crucial for identifying hydrocarbon bearing zones and optimal stimulation placement. Previous methods to estimate porosity include logging tools and laboratory testing. Core analysis techniques can be used to determine porosity, however, cores represent only a very small interval of the well and it can take time to obtain the results (Bodwadkar & Reis 1993). In zones with small scale heterogeneities, core samples can identify such differences but logging tools may not (Gyllensten et al. 2004). This implies that using one method to determine porosity measurements may be vastly different from the other. Wireline logging is subject to many errors. These errors can be due to a variety of factors including improper calibration, design, company, age, and alterations of data acquisition (Kane et al. 2005). Logging-while drilling (LWD) and wireline logging can give fairly accurate porosity estimations in limestone and sandstone lithologies, but these tools are less accurate in shales (Afonso de Andre et al. 2005). Wireline measurements may also be affected by excess mud and borehole factors (Bonnecaze et al. 2002). In previous literature it has been stated that the optimal approach to produce accurate porosity measurements in a well involves a combination of both log and core analysis (Patchett & Coalson 1982).

Aside from using laboratory testing and logging measurements to determine porosity, unconfined compressive strength (UCS) can also be used to obtain porosity measurements. UCS can be measured in a variety of ways including laboratory testing, log-based correlations, image logs, and from drilling data (Nabaei et al. 2010). While laboratory testing is an accurate UCS predictor when reliable cores are available, these tests are destructive and may give incorrect UCS values if identical core samples are not tested (Khaksar et al. 2014). One of the major issues associated with log-based UCS correlations is that log measurements may not be as accurate in heterogeneous formations and could ultimately yield inaccurate UCS estimations (Borba et al. 2014). A previous study to determine the accuracy of UCS values correlated to the rebound hardness numbers (RHN) found from an Equotip Hardness Tester (EHT) in shales concluded that this method yields similar UCS values found from laboratory UCS tests but core samples at various depths are necessary to build a UCS log (Lee et al. 2014).

Horizontal Well Application

Predicting formation parameters in horizontal wells can be harder than in vertical wells. Neutron and density logging may predict inaccurate porosity values due to invasion and direction of permeability (Cowan & Wright 1997). In horizontal wells, wireline tools tend to stay on the bottom of the wellbore where solid cuttings could remain. Rather than obtain information about the selected zone, the measurements taken are indicative of the cuttings properties (Bigelow & Cleneay 1992). The geometry of horizontal wells is also different from the geometry seen in vertical wells and most of the log measurements consider the formation characteristics below the wellbore. The

geometry in horizontal wells is important when the wellbore is not in a thick formation because log measurements would not pertain to the formation in question (Singer 1992).

Porosity determination in horizontal or deviated wells can be a challenging task. An understanding of formation characteristics can help benefit not only optimal perforating zones, but also perforation orientation within the horizontal wellbore (Benavides et al. 2003). While LWD tools can be used to measure water saturation, lithology, and porosity in both vertical and horizontal wells, these measurements may not be as affective in deep reservoirs and can yield inaccurate values for certain lithologies (Jackson & Fredericks 1996). Gamma ray measurements, which are the primary tool for monitoring depth and formation characteristics, can provide skewed porosity data when deviating from the vertical wellbore (King 1989). Calvert et al. (1998) proposed that the reason for such variations in porosity measurements when transitioning from vertical to horizontal wells could be due to changing the tool orientation and logging environment.

Using drilling data to determine porosity in horizontal wells can allow for a better understanding of stimulation placement. Unlike other tools used to measure porosity, this method is not susceptible to sudden lithology variations or tool orientation. Selective stimulation can allow perforation placement to be chosen in zones where the perforations are most likely to produce, which has been a problem in many horizontal wells.

Real-Time Application

Obtaining real-time drilling data can be advantageous in knowing lateral placement, optimizing drilling parameters, and understanding geomechanical factors in the well (Han et al. 2010). Real-time data can also allow for drilling, completions, and well testing decisions to be made much more quickly (Sadykov et al. 2016). Having the ability to collect UCS and GR data at any point throughout the drilling process would allow for porosity at depth to be determined. Determining porosity in real-time can also reduce the amount of lost time due to drilling hazards (Pritchard et al. 2016). To determine porosity real-time, drilling and GR data is collected at surface as the well is being drilled. UCS values can be calculated from an inverted ROP model for continously while drilling the well. The UCS, gamma ray data taken at the bit, and bit wear values (from the ROP models) can be used to determine porosity in real-time. The benefits of real-time drilling data and porosity prediction are a better understanding of sand control factors, stimulation design and optimization, and a better prediction of overall well performance (Brulè 2013).

Gamma Ray Method

Previous methods for estimating porosity in sandstone and shale formations are used to obtain an accurate correlation for porosity in a mixed lithology zone (Cedola et al. 2017). Knowing that gamma ray (GR) values can indicate the formation type over an interval, the measured GR can be used in conjunction with the Cedola Sandstone and Cedola Shale correlations to provide a porosity value in mixed lithologies.

To get UCS values, drilling data from a previously drilled well in Western Canada was collected. This data was inserted into an inverted rate of penetration (ROP) model and UCS values were calculated. The inverted ROP model works by taking certain drilling parameters and inserting the into ROP models dependent on bit type to determine accurate UCS values and is applicable to real-time application (Hareland et al. 2010 and Kerkar et al. 2014).

In order to develop a GR porosity correlation, the Cedola sandstone and Cedola shale correlations were used. These two correlations were developed by collecting porosity and UCS data from a variety of sandstone and shale reservoirs. The data collected has been found from both laboratory and log analysis. Figure 1 shows the UCS and porosity data that was collected for sandstone reservoirs as well as the Cedola sandstone correlation that was obtained. Figure 2 shows the plot used to determine the Cedola shale correlation from the collected shale data. The equations used to determine the linear GR correlation (Eqn. 1) and the power GR correlation (Eqn. 2) are shown below.

$$\emptyset_{Linear\ GR} = \emptyset_{Cedola\ Shale} + (\emptyset_{Cedola\ Sandstone} - \emptyset_{Cedola\ Shale}) * (\frac{140-GR\ Reading}{140-40}) \quad (1)$$

$$\emptyset_{Power\ GR} = \emptyset_{Cedola\ Shale} + (\emptyset_{Cedola\ Sandstone} - \emptyset_{Cedola\ Shale}) * (\frac{140-GR\ Reading}{140-40})^{a1} \quad (2)$$

To evaluate whether a linear GR porosity or a power GR porosity correlation would be the most accurate, a plot in which the Cedola correlation with normalized UCS values for both linear and power GR porosity has been made and can be seen in Figure 3 and Figure 4, respectively. For both GR plots, the Cedola sandstone porosity values are equivalent to GR measurements at 40 API or less while the Cedola shale porosity values are used in place of GR reading taken at 140 API or higher. While both the linear and power GR correlations take sandstone and shale porosity into consideration, the power GR correlation has been chosen because it is more accurate in determining the porosity in zones with varying sandstone and shale frequencies and fractions.

To obtain the most accurate power GR porosity an optimal value for the constant, a1, must be determined. This process is done using GR, UCS, neutron porosity and the Cedola sandstone and shale calculations. The a1 constant is varied and plotted for each value to observe which has the best fit with the log porosity.

Results & Analysis

The Cedola sandstone and shale correlations for determining porosity work well in solely sandstone and shale lithologies. In a reservoir with mixed lithology zones, the power

GR correlation should replace of the Cedola sandstone and Cedola shale correlation. To observe why GR porosity correlations are necessary in mixed lithology areas, a plot in which UCS versus log porosity data for mixed lithology sections of a previously drilled well in Alberta, British Columbia, Canada as well as the Cedola correlations has been made (Figure 5). It is apparent from the plot that because the data falls between the two Cedola trends, there are multiple intervals within the well that are not solely sandstone or shale, but a fraction of each. To solve this issue, gamma ray and neutron log data for mixed formations in the well were collected. These parameters were inserted into the power GR porosity correlation equation and the absolute difference between the neutron porosity and the GR porosity was determined. The a1 constant was varied over a range from -3 to 100 and the absolute difference for each of the porosity values has been plotted in Figure 6. The smaller the absolute difference between the neutron porosity and power GR porosity the more accurate the a1 coefficient. Figure 6 shows that the smallest absolute difference is achieved at an a1 value of 2.53, which is different from the constant of 1 for linear GR.

To verify the applicability of the GR correlation to mixed lithology intervals, porosity comparisons for two mixed lithology sections from a second Alberta well have been made and can be seen in Figures 7 and 8. The plots show that the GR porosity is a much better indicator in zones of mixed lithologies. It can be seen that the GR porosity in the Belly River formation (Figure 7) has similar trends to the neutron porosity taken from log data. The GR porosity calculations in the Dunvegan formation (Figure 8) are also very similar to the neutron porosity. The Dunvegan formation, which is known to be comprised of both sandstones and shales, can have porosities up to 20% (Hayes 2013). The Belly River formation can have average porosities ranging from 16-23% and is made up of sands, shales, and siltstones (Shouldice 1979). The GR porosity is primarily in average porosity ranges for both the Belly River and Dunvegan formation. Figure 9 shows a comparison between the Cedola sandstone, Cedola shale, and power GR porosities for the Belly River formation. In zones with higher sandstone content, the GR porosity values are much closer to the Cedola sandstone porosity values and in areas with high shale fractions the Cedola Shale correlation is similar. This is indicative of the fact that the GR correlation is influenced by the lithology mixture at any given depth.

Conclusions

Utilizing a combination of drilling and gamma ray log data has the ability to provide accurate porosity measurements. The power GR porosity correlation yields good results in sandstone, shale, and mixed lithology formations as compared to log derived porosity. Using the power GR method to determine porosity could greatly reduce the need for expensive logging tools and/or testing while providing similar results. This method allows for porosity measurements to be known at any point in a well and does not need to be adjusted for horizontal or deviated wells. Understanding porosity and lithology changes in horizontal sections can greatly impact hydrocarbon production and recovery through selective zone perforating and/or production. Real-time drilling and gamma ray data can be used to determine porosity at any point throughout the drilling process and could have a significant impact in identifying formations, understanding drilling fluid losses and drilling optimization.

Nomenclature

GR	*Gamma Ray*
UCS	*Unconfined Compressive Strength*
ROP	*Rate of Penetration*
LWD	*Logging-While-Drilling*
RHN	*Rebound Hardness Number*
EHT	*Equotip Hardness Tester*

References

1. Bodwakar, S.V. and Reis, J.C.: "Core Porosity Measurements Using Gamma Rays." SPE-26467-MS, SPE Annual Technical Conference and Exhibition, Houston, October 3-6, 1993.
2. Gyllensten, A., Tike, P., Al-Raisi, M. et al.: "Porosity Heterogeneity Analysis Using Geostatistics." SPE-88788-MS, Abu Dhabi International Conference and Exhibition, Abu Dhabi, October 10-13, 2005.
3. Kane, J.A. and Jennings Jr., J.W.: "A Method to Normalize Log Data by Calibration to Large-Scale Data Trends." SPE-96081-MS, SPE Annual Technical Conference, Dallas, October 9-12, 2005.
4. Afonso de Andre, C., Mainieri Vieira da Cunha, A., Boonen, P. et al.: "A Comparison of Logging-While-Drilling and Wireline Nuclear Porosity Logs in Shales from Wells in Brazil." Petrophysics v. 46, No. 04, 295-301.
5. Bonnecaze, R.T., Sharma, M.M., Butler, J.E. et al.: "High Resolution Downhole Measurements of Porosity and Fluid Saturation While Core Drilling." SPE-77561-MS, SPE Annual Technical Conference and Exhibition, San Antonio, September 29-October 2, 2002.
6. Patchett, J.G. and Coalson, E.B.: "The Determination of Porosity in Sandstone and Shaly Sandstone Part Two-Effects of Complex Mineralogy and Hydrocarbons." SPWLA-1982-T, SPWLA 23rd Annual Logging Symposium, Corpus Christi, July 6-9, 1982.
7. Nabaei, M., Shahbazi, K., Shadravan, A. et al.: "Uncertainty Analysis in Unconfined Compressive Strength Prediction." SPE-131719-MS, SPE Deep Gas Conference and Exhibition, Manama, January 24-26, 2010.
8. Khaksar, A., Gui, F., Geoffrey, P. et al.: "Enhanced Rock Strength Modelling, Combining Triaxial Compressive Tests, Non-Destructive Index Testing and Well Logs." SPE-171532-MS, SPE Asia Pacific Oil & Gas Conference and Exhibition, Adelaide, October 14-16, 2014.
9. Borba, A.M., Ferreira, F.H., Santos, E.S.R. et al.: "UCS Estimation through Uniaxial Compressive Test, Scratch Test and Based Log Empirical Correlation." ISRM-SBMR-2014-042, ISRM Conference on Rock Mechanics for Natural Resources and Infrastructure, Goiania, September 9-13, 2014.
10. Lee, J.S., Smallwood, L. and Morgan, E.: "New Application of Rebound Hardness Numbers to Generate Logging of Unconfined Compressive Strength in Laminated Shale Formations." ARMA-2014-6972, 48th U.S. Rock Mechanics/Geomechanics

Symposium, Minneapolis, June 1-4, 2014.
11. Cedola, A.E., Atashnezhad, A., and Hareland, G.: "Evaluating Multiple Methods to Determine Porosity from Drilling Data." SPE-185115-MS, SPE Oklahoma City Oil and Gas Symposium, Oklahoma City, March 27-30, 2017.
12. Bowman, H.R., Flexser, S., Hearst, J.R. et al.: "Low Radioactivity Spectral Gamma Calibration Facility." The Log Analyst v. 28, No. 05, (1987) 462-469.
13. Cowan, P. and Wright, G.A.: "Investigations Into Anomalous Responses of Gamma Density and Neutron Porosity Tools in Horizontal Gas Wells." SPWLA-1997-H, SPWLA 38th Annual Logging Symposium, Houston, June 15-18, 1997.
14. Bigelow, E.L. and Cleneay, C.A.: "A New Frontier: Log Interpretation in Horizontal Wells." SPWLA-1992-OO, SPWLA 33rd Annual Logging Symposium, Oklahoma City, June 14-17, 1992.
15. Singer, J.M.: "An Example of Log Interpretation in Horizontal Wells." The Log Analyst, v. 33, No. 02, (1992) 85-95.
16. Hareland, G., Wu, A. and Rashidi, B.: "A Drilling Rate Model for Roller Cone Bits and Its Application." SPE-129592-MS, CPS/SPE International Oil & Gas Conference and Exhibition, Beijing, June 8-10, 2010.
17. Kerkar, P.B., Hareland, G., Fonseca, E.R. et al.: "Estimation of Rock Compressive Strength Using Downhole Weight-on-Bit and Drilling Models." IPTC-17447-MS, International Petroleum Technology Conference, Doha, January 19-22, 2014.
18. Hayes, B.J.R.: "Subsurface Aquifer Study to Support Unconventional Gas and Oil Development, Liard Basin, Northeastern B.C." Petrel Robertson Consulting Ltd., Calgary, Alberta, Canada, 2013.
19. Shouldice, J.R.: "Nature and Potential of Belly River Gas Sand Traps and Reservoirs in Western Canada." Bulletin of Canadian Petroleum Geology v.27, No. 2, (June 1979) 229-241.
20. Han, S.Y., Kok, J.C.L., Tollefsen, E.M. et al.: "Shale Gas Reservoir Characterization Using LWD in Real Time." CSUG/SPE-137607-MS, Canadian Unconventional Resources & International Petroleum Conference, Calgary, October 19-21, 2010.
21. Sadykov, A., El-Batawi, A., Akbayev, B. et al.: "Real-Time Reservoir Characterization in Caspian Offshore Wells." SPE-182574-MS, SPE Annual Caspian Technical Conference & Exhibition, Astana, November 1-3, 2016.
22. Pritchard, D.M., York, P. and Roye, J.: "Achieving Savings Through Reliability Using Real Time Data." OTC-26935-MS, Offshore Technology Conference, Houston, May 2-5, 2016.
23. Brulè, M.R.: "Big Data in E&P: Real-Time Adaptive Analytics and Data-Flow Architecture." SPE-163721-MS, 2013 SPE Digital Energy Conference and Exhibition, The Woodlands, March 5-7, 2013.
24. Benavides, S.P., Myers, W.D., Van Sickle, E.W. et al.: "Advances in Horizontal Oriented Perforating." SPE-81051-MS, SPE Latin American and Caribbean Petroleum Engineering Conference, Port-of-Prince, April 27-30, 2003.
25. Jackson, C.E. and Fredericks, P.D.: "Proactive Use of Logging-While-Drilling (LWD) Measurements Improve Horizontal Well Drilling and Subsequent Evaluation." IADC/SPE-37157-MS, SPE/IADC Asia Pacific Drilling Technology Conference, Kuala Lumpur, September 9-11.
26. King, G.E.: "Perforating the Horizontal Well." Journal of Petroleum Technology, v. 41, No. 07, (1989) 671-672.
27. Calvert, S., Lovell, M., Harvey, P. et al.: "Porosity Determination in Horizontal Wells." SPWLA-1998-BBB, SPWLA 39th Annual Logging Symposium, Keystone, May 26-28, 1998.
28. Farquhar, R.A., Smart, B.G.D., and Crawford, B.R.: "Porosity-Strength Correlation: Failure Criteria from Porosity Logs." SPWLA-1993-AA, SPWLA 34th Annual Logging Symposium, Calgary, June 13-16, 1993.
29. Khaksar, A., Taylor, P.G., Fang, Z. et al.: "Rock Strength from Core and Logs, Where We Stand and Ways to Go." SPE-121972-MS, EUROPE/EAGE Conference and Exhibition, Amsterdam, June 8-11, 2009.
30. Hawkins, A. and McConnell, B.J.: "Influence of Geology on Geomechanical Properties of Sandstones." ISRM-7CONGRESS-1991-051, 7th ISRM Congress, Aachen, September 16-20, 1991.
31. Kim, K-Y., Zhuang, L., Yang, H. et al.: "Strength Anisotropy of Berea Sandstone: Results of X-Ray Computed Tomography, Compression Tests, and Discrete Modeling." Rock Mechanics and Rock Engineering v. 49, No. 4, (2015).
32. Valdes, C. and Raquel, C.: "Characterization of Geomechanical Poroelastic Parameters in Tight Rocks." Master's Thesis, Texas A&M University, College Station, Texas, (2013).
33. Yao, B.: "Experimental Study and Numerical Modeling of Cryogenic Fracturing Process on Laboratory-Scale Rock and Concrete Samples." Master's Thesis, Colorado School of Mines, Golden, Colorado, (2015).
34. Horsrud, P.: "Estimating Mechanical Properties of Shale from Empirical Correlations." SPE-56017-PA, SPE Drilling and Completions v. 16, No. 2, (2001) 68-73.
35. Chang, C.: "Empirical Rock Strength Logging in Boreholes Penetrating Sedimentary Formations." Geology and Environmental Sciences v. 7, No. 03, (2004) 174-183.
36. Lashkaripour, G.R.: "Predicting mechanical properties of mudrock from index parameters." Bulletin of Engineering Geology and the Environment v. 61, No. 1, (2002) 73-77.

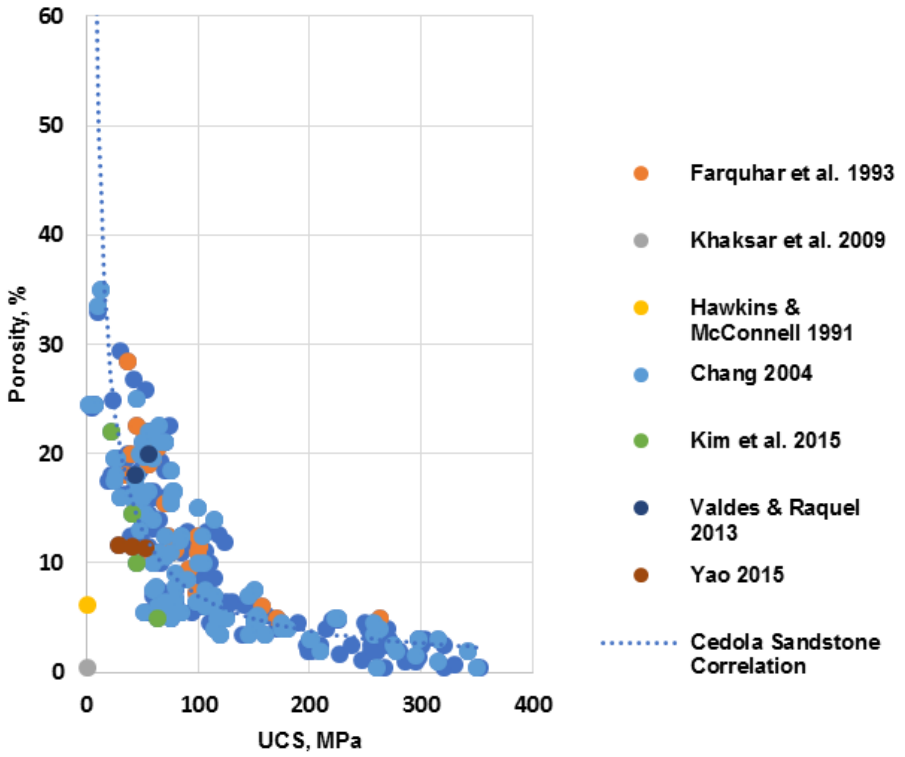

Figure 1. Cedola Sandstone Correlation (Cedola et al. 2017).

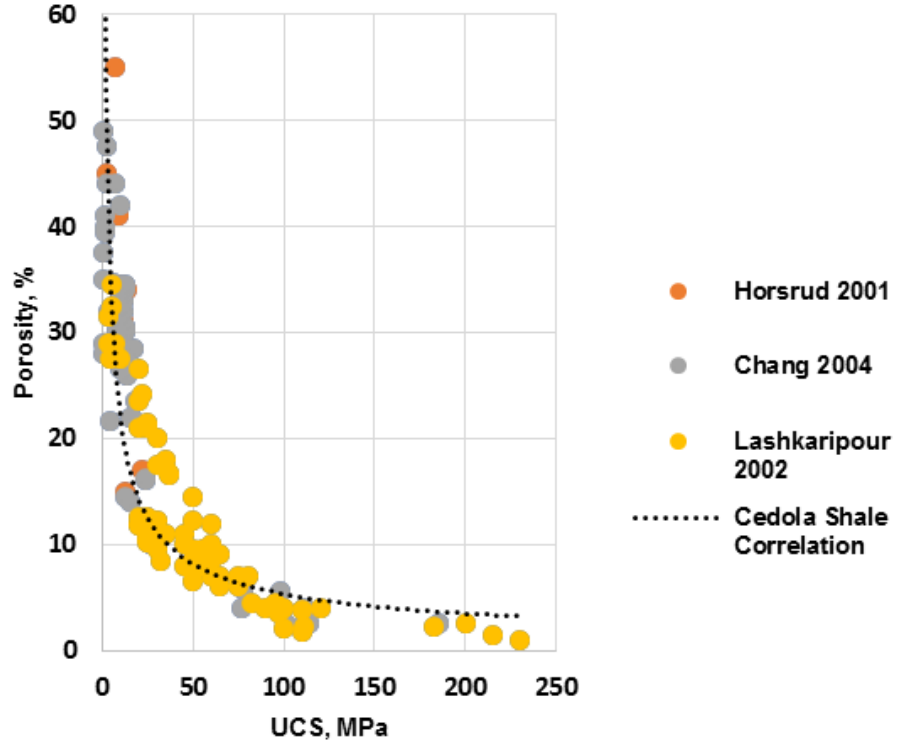

Figure 2. Cedola Shale Correlation (Cedola et al. 2017).

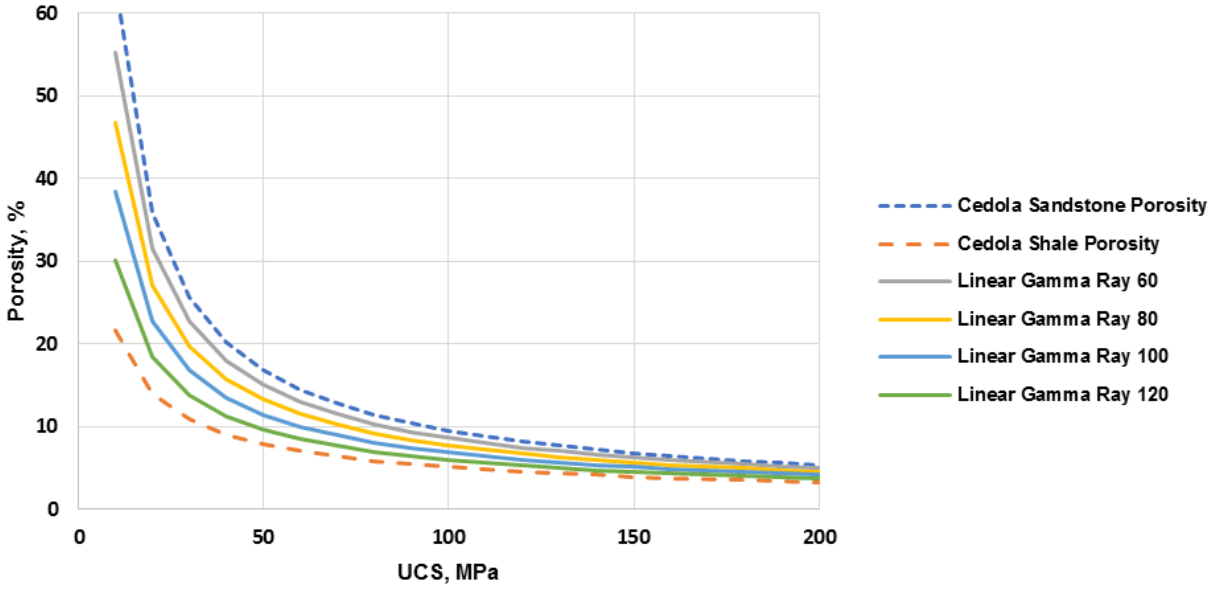

Figure 3. Linear GR Porosity Plot (Cedola et al. 2017).

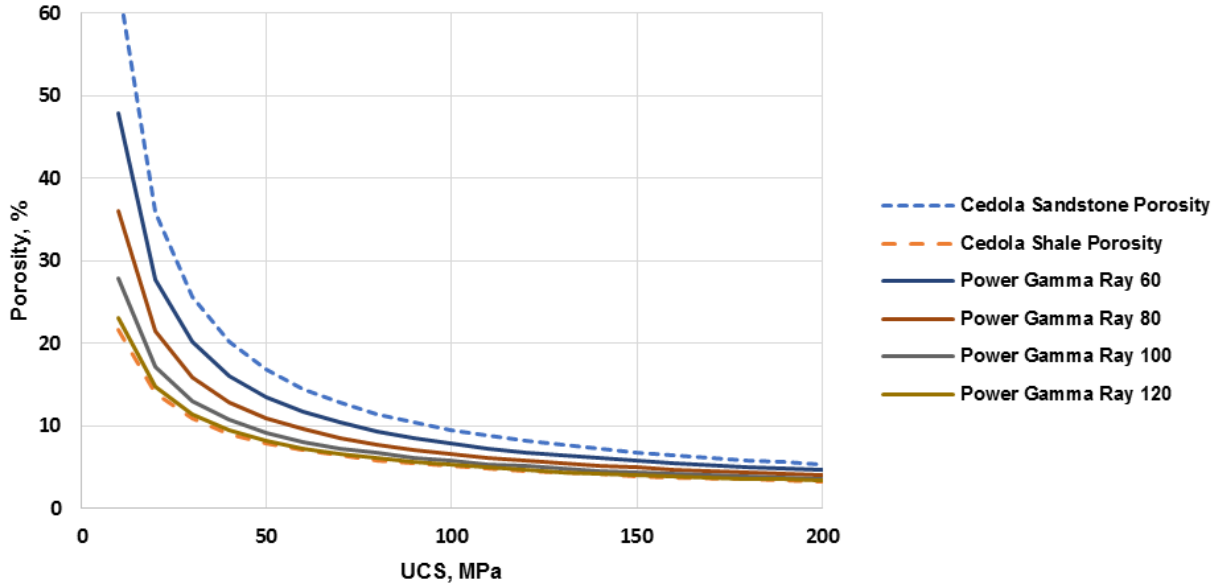

Figure 4. Power GR Porosity Plot (Cedola et al. 2017).

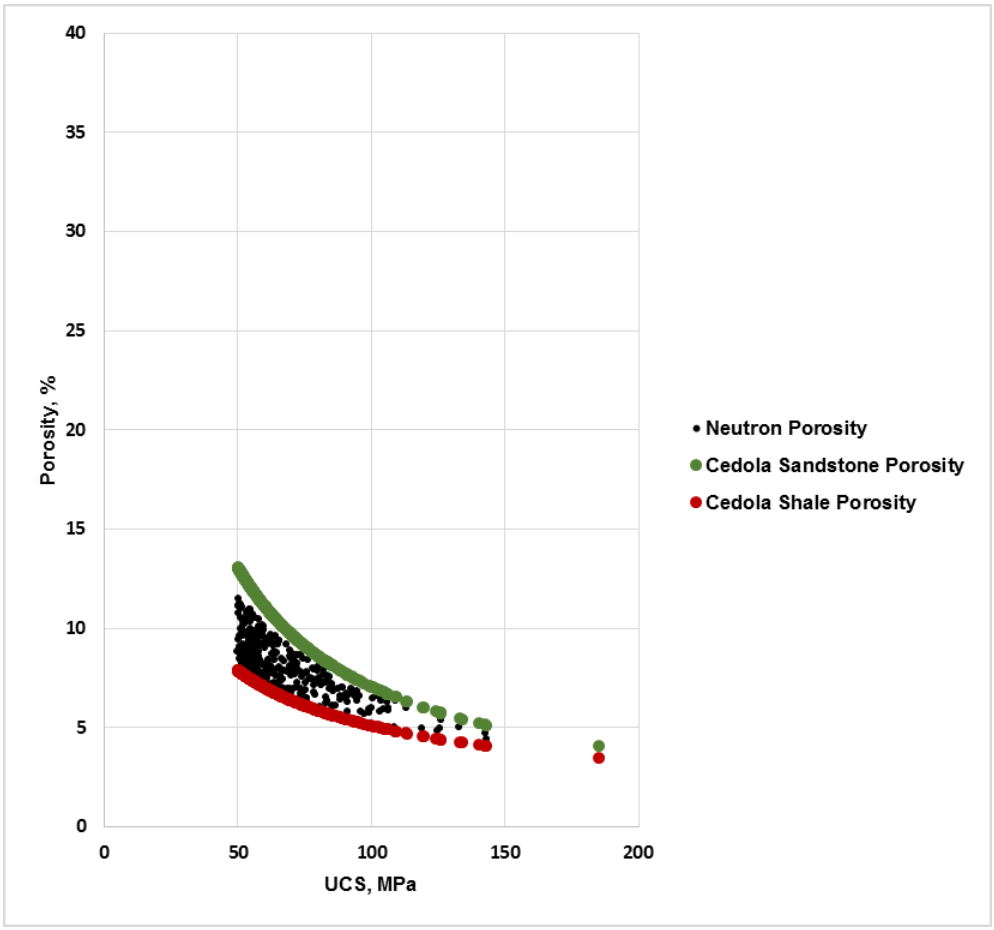

Figure 5. Cedola Sandstone and Cedola Shale Correlation Predictions in a Mixed Lithology Zone.

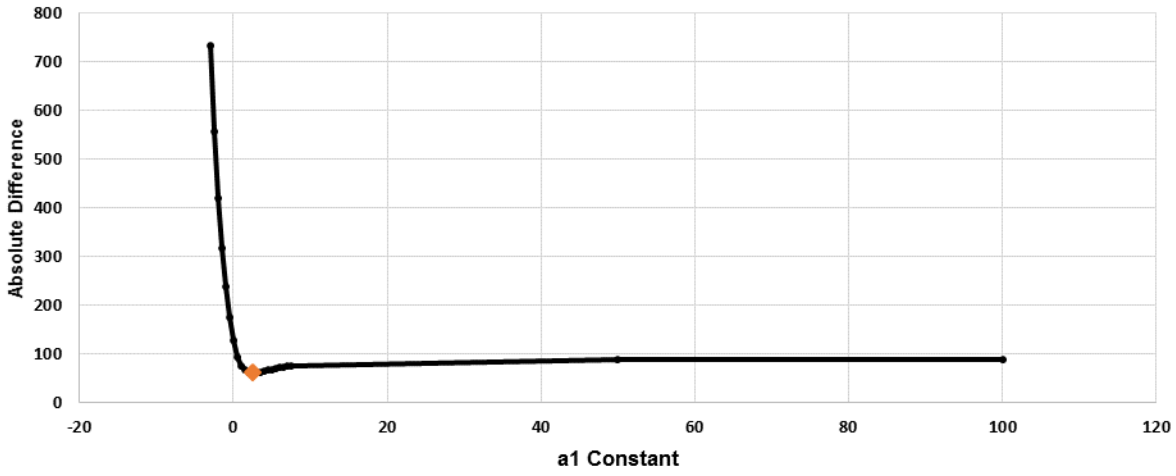

Figure 6. Optimal a_1 Constant Determination.

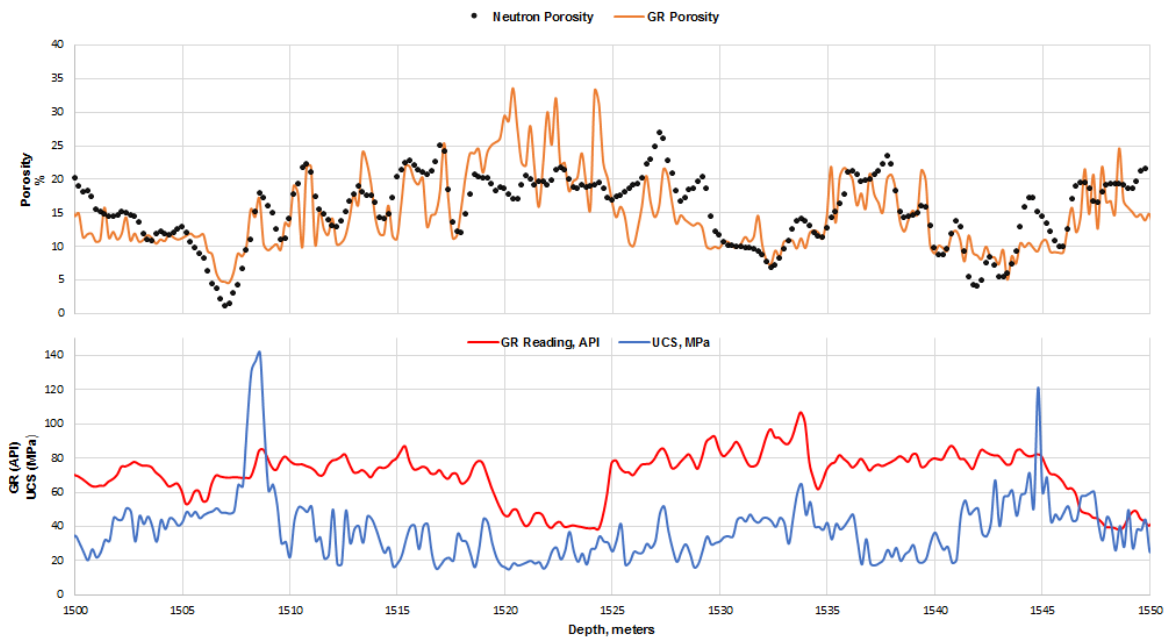

Figure 7. Mixed Lithology Neutron Porosity versus GR Porosity Comparison for the Belly River Formation.

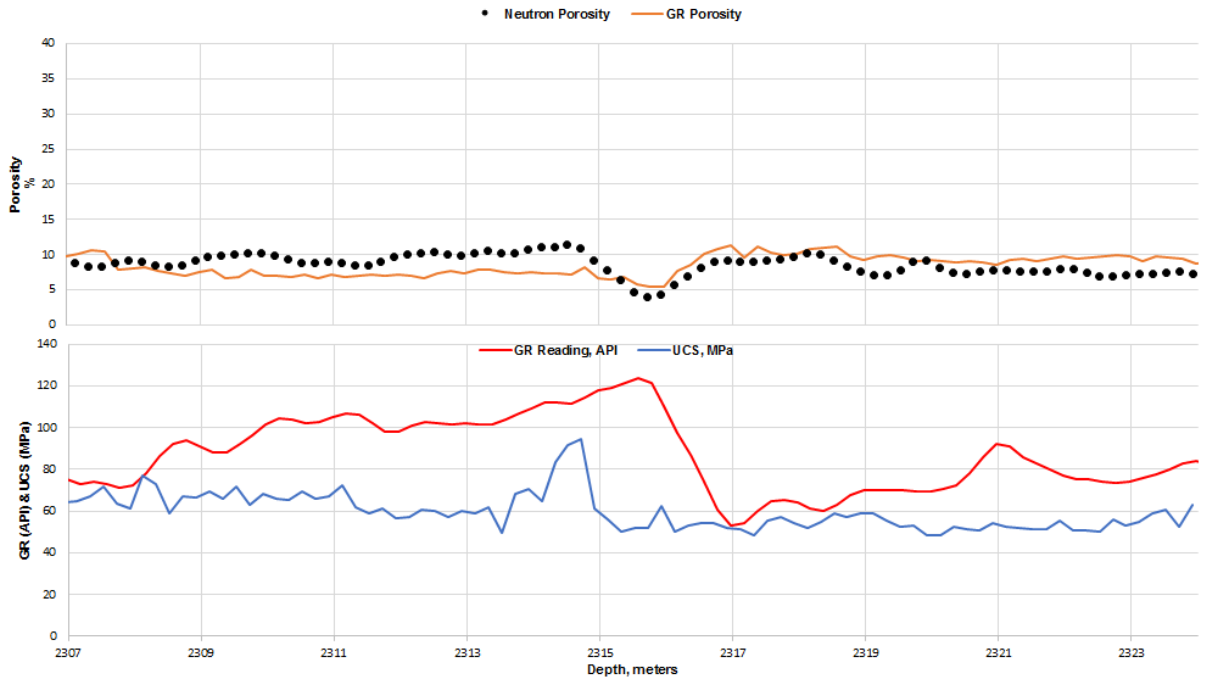

Figure 8. Mixed Lithology Neutron Porosity versus GR Porosity Comparison for the Dunvegan Formation.

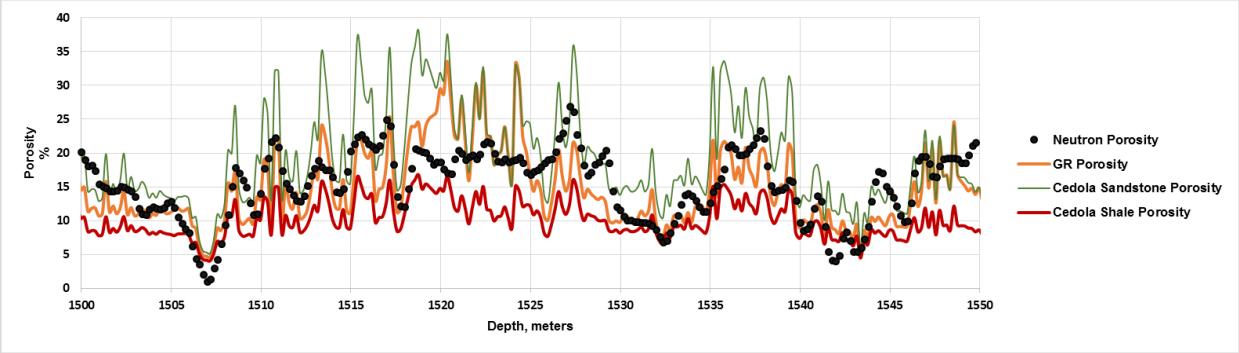

Figure 9. GR Porosity, Cedola Sandstone Correlation and Cedola Shale Correlation Comparison for the Belly River Formation.

ARMA 17-0900

Method for Determining Permeability in Sandstone Shale Reservoirs from Typical Drilling Parameters

Cedola, A.E., Atashnezhad, A. and Hareland, G.
Oklahoma State University, Stillwater, Oklahoma, U.S.A.

ABSTRACT: This paper describes a method for determining permeability variations for a continuous interval utilizing conventional drilling data for sandstone and shale reservoirs. The drilling data is used to find the unconfined compressive strength (UCS) within a well using an inverted rate of penetration (ROP) model. Previously published core and cuttings data for sandstone and shale reservoirs are used to create correlations for UCS and porosity as well as porosity and permeability. Porosity values can be calculated at any UCS values, and applied to the porosity and permeability correlation for the specific reservoir. This yields a permeability value for a specific reservoir at a given UCS. The verification of the correlation was done with permeability data from two wells penetrating the Montney shale and Nikanassin sandstone formations in British Columbia, Canada. The UCS calculation for the Montney and Nikanassin formations was compared to the permeability obtained from core and cuttings analysis data and a comparison between trend and accuracy can be done.

1. INTRODUCTION

Permeability determination can be a challenging task, but has proven advantageous to stimulation design and reservoir characterization. Determination of shale permeability has proven to be vastly different from the techniques employed for finding permeability in conventional reservoir rock (Moghadam and Chalaturnyk, 2015). The most common technique used to determine shale permeability is the GRI technique, but one of the downsides associated with this method is that the sample sizes used can alter the permeability results (Tinni et al., 2012). Civan et al., 2013, investigated the effect of Darcian flow on shale permeability and proposed that this method has the potential to predict shale permeability for a variety of conditions. One way that sandstone permeability can be determined is through the use of sonic and electrical logs, but these logs can be ineffective if shales are present (Jiang et al., 2013). Well logs can be used in conjunction with artificial neural networks or multiple regression analysis for permeability estimation (Pereira, 2004). There are also numerous correlations that utilize well logs to empirically determine permeability, including but not limited to the Timur, Tixier, and Coates-Dumanois methods. Many of these empirically calculated permeability methods require knowledge of the irreducible water saturation, and often times these correlations can be vastly different from core analysis results (Hunt and Pursell, 1997). One common issue with log methods is that depth correction between logs and core samples must be performed in order to obtain accurate results (Jiang-ming et al., 2013). Pressure transient data obtained from Wireline Formation Testers (WFT) can also be used for permeability determination, but it has been observed that this method may not be accurate in heterogeneous formations (Ramaswami et al., 2016). The cost of running WFT's can reduce the

number of measurements taken in a well and can sometimes misrepresent the permeability for the entire zone in question (Li et al., 2016).

There have been a variety of techniques suggested for determining permeability in horizontal wells. Drill cuttings analysis is one way to determine permeability in a horizontal well, but it is necessary to analyze cuttings from various points along the lateral to obtain relatively accurate values (Haghshensas et al., 2016). Using a CT-scan technique to measure rock properties from drill cuttings has also been described, but the cuttings must be at least 2.5 mm or larger to be considered for testing (Siddiqui et al., 2005, Lenormand and Fonta, 2007). Using drill cuttings to determine permeability may be limited to samples whose porosity and permeability are within the ranges detectible by the equipment (Olusola, 2013). Another way for permeability determination, according to Kristiansen et al., 1996, involves using horizontal log data to estimate permeability when multiple-linear-regression, principal-component-regression, or partial-least-squares-regression is applied.

Another method that has been used to determine permeability involves correlating the permeability to porosity that has been determined from laboratory core testing. Skalinski and Sullivan, 2001 described a method to estimate permeability throughout a field but requires multiple cores from all differentiating facies within a wellbore as well as cores from various wells within the field; this method is known as the Multivariate Facies Transform (MFT). Correlations between permeability and porosity is highly dependent on rock type as well as components like grain size, sorting, compaction, pore throat size, and cementation (Dahraj and Bhutto, 2014).

The above methods may provide relatively accurate permeability estimations, but they can prove costly and unreliable. Fleckenstein and Eustes, 2003, detail the issues that can arise from coring, including the cost for coring tools, rigtime costs, and core extraction locations. One limitation associated with logging techniques include issues in high-temperature wells (Briner et al., 2015). The use of measurement-while-drilling (MWD) or logging-while-drilling (LWD) and gamma ray (GR) tools are commonly run during the drilling process and are beneficial for formation evaluation in both vertical and horizontal wells (Gawankar et al., 2016).

2. PERMEABILITY DETERMINATION PROCESS

While there have been many correlations relating porosity to permeability, the techniques used to determine the parameters needed can be costly and often times, unreliable. In this paper, a technique that utilizes drilling data to determine unconfined compressive strength (UCS) and relates these values to porosity and permeability correlations. These previously published porosity correlations can then be further correlated to one another in order to obtain drilling data based porosity-permeability correlations that are specific to sandstone and shale lithologies. The correlations for determining porosity from UCS values, known as the Cedola sandstone and Cedola shale correlations, are presented in Eq.'s (1) and (2), respectively (Cedola et al., 2017).

$$\emptyset_{Cedola\ Sandstone} = 424.8 * UCS^{-0.89} \quad (1)$$

$$\emptyset_{Cedola\ Shale} = 92.529 * UCS^{-0.63} \quad (2)$$

In Eq.'s (1) & (2), the UCS was found by inserting the drilling data into an inverted rate of penetration (ROP) model, which was originally established by Warren, 1987, and revised by Nygaard et al., 2002, Hareland & Nygaard, 2007, and Kerkar et al., 2014 (Al Dushaishi et al., 2016). A UCS versus porosity plot for the Cedola sandstone and shale correlations is shown in Fig.'s 1 and 2 (Cedola et al. 2017).

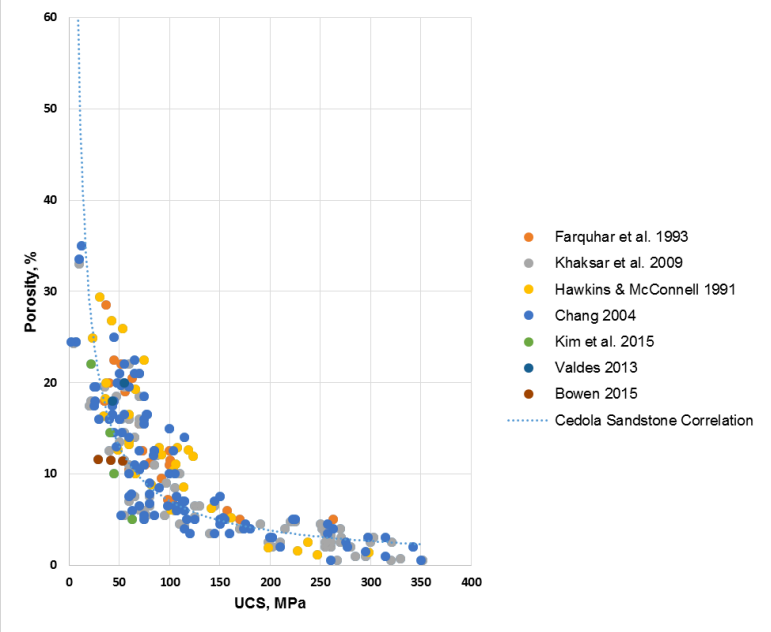

Fig. 1. Sandstone UCS and porosity data used to establish the Cedola sandstone correlation (Cedola et al. 2017).

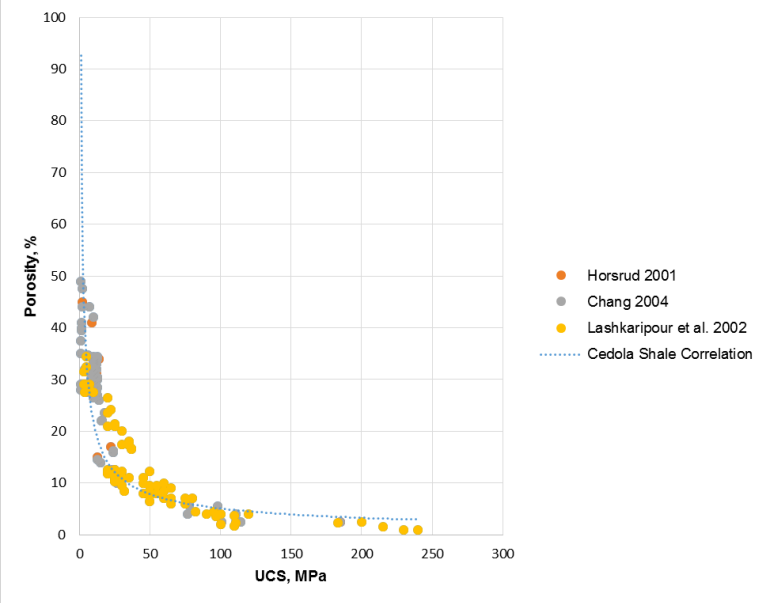

Fig. 2. Shale UCS and porosity data used to establish the Cedola shale correlation (Cedola et al. 2017).

Previously published porosity and permeability data, which has been obtained via laboratory testing, computer modeling, and well logs, has been collected for a variety of sandstone and shale reservoirs. Porosity versus permeability plots for various sandstone and shale formations have been created, and using the known porosity values for the various sandstone and shale reservoirs, the UCS and porosity plots can be utilized to determine a correlation between the permeability and UCS at a given porosity.

To observe the accuracy of the porosity-permeability correlations presented in this paper when applied to real-well applications, porosity and permeability data from the Nikanassin sandstone and Montney shale formations of British Columbia, Canada has been collected. The porosity-

permeability correlations for the Nikanassin sandstone and Montney shale have been used to obtain permeability values from previously published core and cuttings porosity data. These permeability trends are then compared to the collected permeability for both types of formations. The results are plotted and the trends between the correlated permeability, measured permeability, and UCS as determined from the Cedola sandstone and Cedola shale porosity correlations can be seen.

3. SANDSTONE AND SHALE PERMEABILITY METHOD

Obtaining a correlation between permeability and UCS begins by relating UCS data to porosity for sandstones and shales which has been described in detail by Cedola et al., 2017. Porosity and permeability data for numerous sandstone and shale formations has been collected and plotted, and a correlation between these two parameters can be made for individual sandstone and shale formations; these correlations will be referred to as the porosity-permeability correlations (Fig.'s 3 and 4). Because of the variation in amounts of collected data for different formations, a 15% upper and lower margin has been plotted for each formation. All sandstone and shale porosity-permeability correlations are of the form shown in Eq. (3) with varying a and b constants.

$$k = a * \emptyset^b \tag{3}$$

A plot in which collected permeability values and UCS values found from the Cedola sandstone and shale porosity correlations has been made to determine whether the obtaining these parameters from drilling data could provide accurate values and trends. To verify the accuracy of the Bakken shale, Montney shale, and Cardium sandstone porosity-permeability correlations, a UCS versus permeability plot containing data from these various formations has been obtained (Ghanizadeh et al., 2014). The Cedola sandstone porosity and Cedola shale porosity correlations were used to find porosity measurements at each UCS value. Utilizing the porosity-permeability correlations from Fig.'s 3 and 4, the porosity-permeability correlations for the respective formation was used to find permeability values that correspond to normalized UCS values. The UCS and permeability data for all three of the formations was plotted along with the published data from Ghanizadeh et al., 2014, to determine whether the porosity-permeability correlations matched the previously published trends for the respective formations.

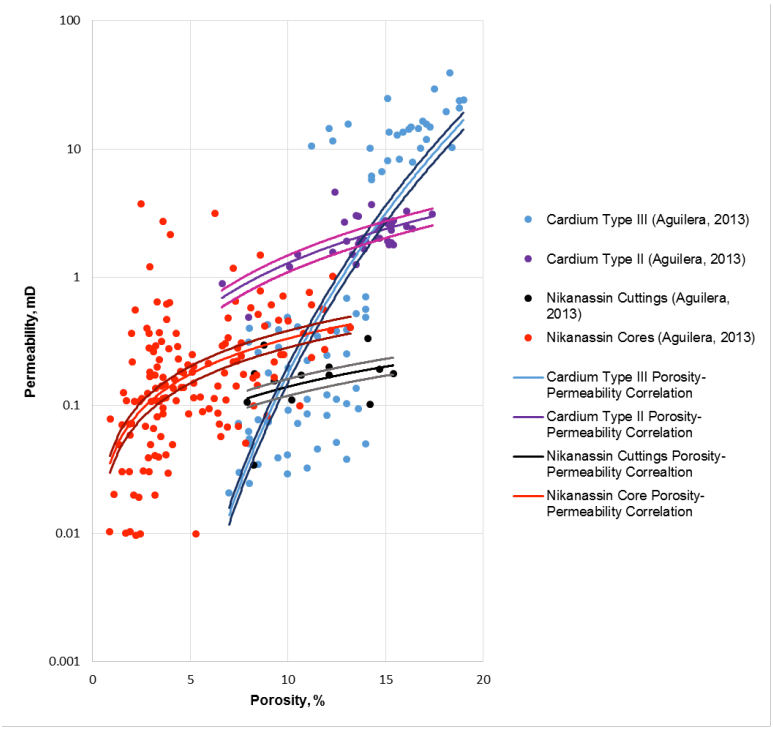

Fig. 3. Porosity versus permeability for collected sandstone data (Aguilera, 2013).

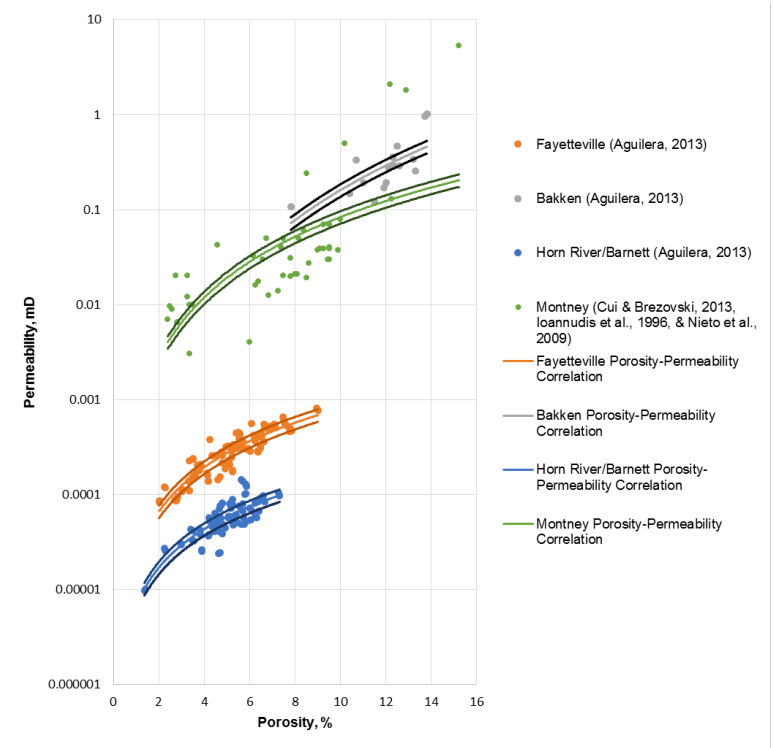

Fig. 4. Porosity versus permeability plot for collected shale data (Aguilera, 2013).

To understand the real-time/real-field application of the Cedola sandstone and Cedola shale permeability correlations, core and cuttings porosity and permeability data from the Nikanassin sandstone and Montney shale have been gathered. Using the collected porosity measurements and

the specific Nikanassin and Montney porosity-permeability correlations, permeability values can be determined for the Montney and Nikanassin formation. The Cedola porosity correlations can be utilized to determine UCS values for both formations.

4. DISCUSSION OF RESULTS

The porosity versus permeability plots shown in Fig.'s 3 and 4 for various sandstone and shale formations show that increasing the porosity will also increase permeability, however, some formations exhibit a much higher increase than others. For the sandstone plot, the Cardium Type III sandstones appear to have the largest range of permeability while the Nikanassin cuttings data doesn't experience much permeability increase over an approximate 7% porosity variance. The shale plot shown in Fig. 4 provides insight into how permeability can vary over different shale types and the 15% margins appear to include most of the published data.

The UCS-permeability plot for sandstone lithologies show that UCS decreases with increasing permeability (Fig. 5). In the Cardium Type III sandstone, the permeability decreases very rapidly over a short UCS range and the UCS-permeability correlation seems to fit the data fairly accurately. There is less collected data for the Cardium Type II and Nikanassin cuttings formations but the UCS-permeability correlation is still a valid UCS predictor given permeability. The collected Nikanassin core data was more spread out than the other data sets and appeared to have less of a trend than the other formations. Shale UCS-permeability for various reservoirs is shown in Fig. 6. The Fayetteville, Bakken, and Horn River/Barnett shales have similar trends and have less variation than the collected Montney shale data. The Montney shale appears more scattered and has less of a trend between the UCS and permeability.

The UCS versus permeability plot in Fig. 7 shows previously published data points for Montney shale, Bakken shale, and Cardium sandstone (Ghanizadeh et al., 2014). To determine whether the porosity-permeability correlations are in agreement with this previously published data, normalized UCS values were inserted into the Cedola shale porosity correlations for the Bakken and Montney formations and the Cedola sandstone porosity correlation for the Cardium. The porosity values were then used in each respective formation's porosity-permeability correlation to determine permeability values. The Bakken shale correlation appears to somewhat agree with the published data seeing as it matches one of the data points. For the other Bakken data, the correlation appears to be underpredicting permeability. The Montney shale correlation appears fairly accurate because it matches two of the three published data points. Because the published Cardium UCS versus permeability was limited and Nikanassin data was unavailable, the porosity-permeability correlations for these two sandstone formations were plotted to indicate the variation between the shale and sandstone trends.

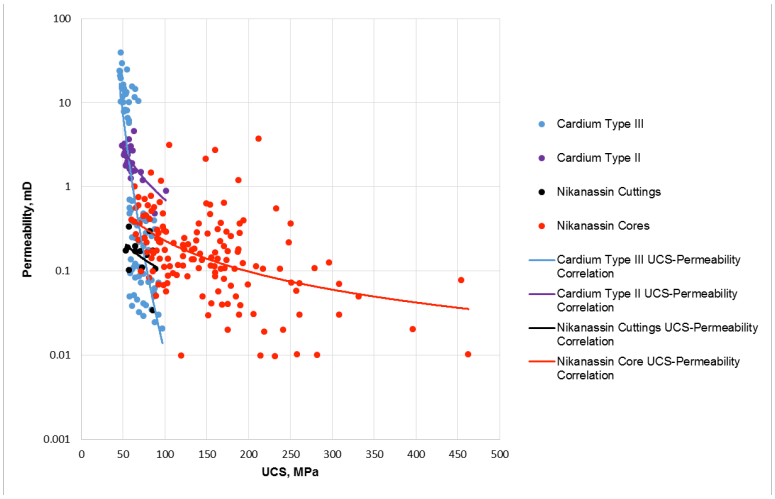

Fig. 5. Sandstone UCS versus permeability (Aguilera, 2013) plot.

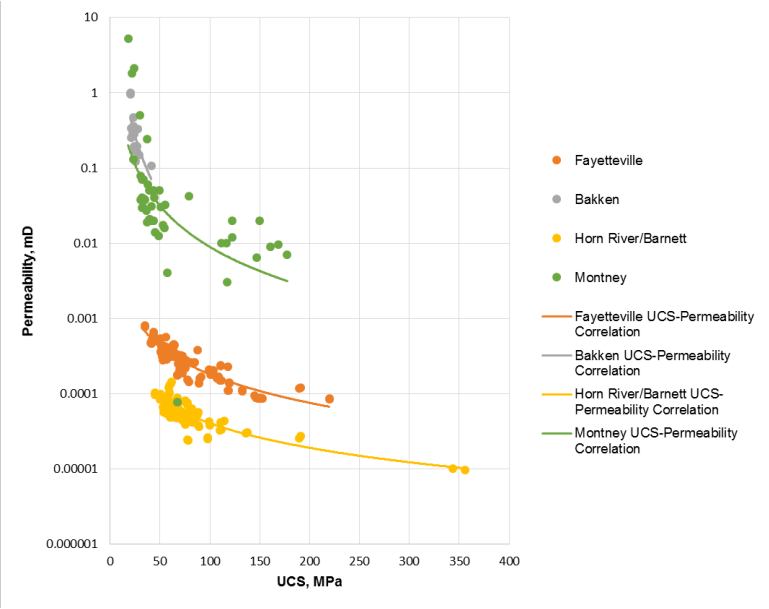

Fig. 6. Shale UCS versus permeability (Aguilera, 2013) plot.

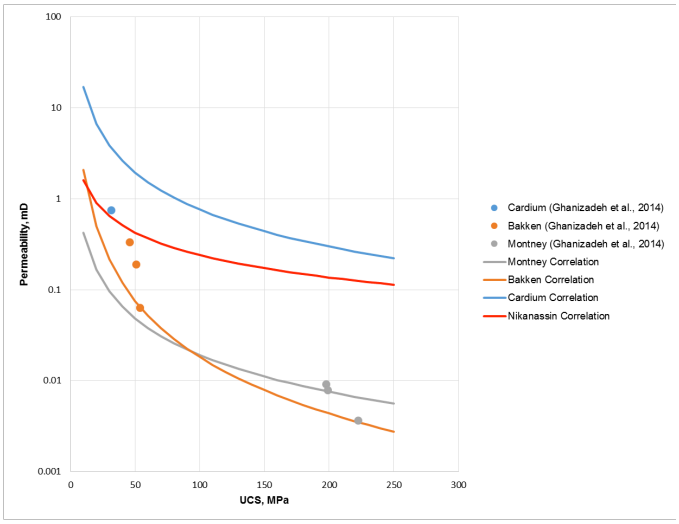

Fig. 7. Bakken, Montney, and Cardium UCS versus permeability data comparison (Ghanizadeh et al., 2014).

In Fig.'s 8 and 9, permeability and porosity data from the Nikanassin sandstone formation and Montney shale data have been collected and plotted alongside correlated permeability values and UCS. The Nikanassin correlated sandstone permeability appears to estimate fairly similar values in comparison to the collected permeability. While the collected Nikanassin permeability data appeared to have a larger range, the correlated permeability was primarily within the range of 0.1 to 0.5 mD. According to Gonzalez et al., 2012, Nikanassin sandstone has an average permeability of 0.05 mD which would be in considerable agreement with the correlated permeability. The Nikanassin UCS is lower with high permeability values, which is the trend seen in Fig. 5. The Montney shale correlated permeability is slightly lower than the measured permeability but is similar in trend. The correlated permeability appears to be primarily within the range of 0.006 to 0.04 mD, and according to Clarkson et al., 2011, average Montney permeability was found to be 0.01 mD which is much closer to the correlated permeability values. The Montney UCS is similar in trend to both collected and correlated permeability but exhibits an opposite response. When permeability is high the UCS is low, which is in agreement with the shale UCS-permeability plot in Fig. 6.

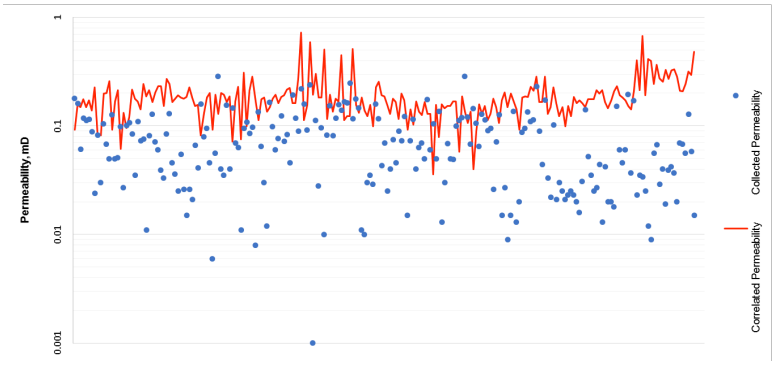

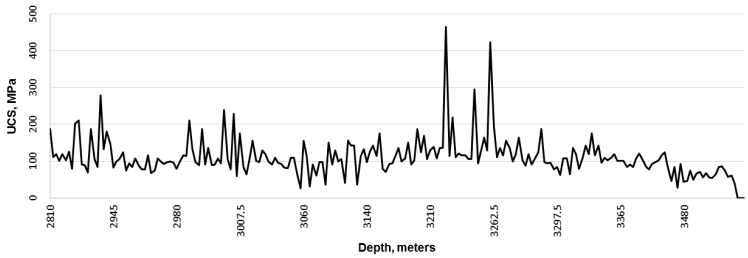

Fig. 8. Permeability comparison and UCS behavior for the Nikanassin sandstone (Flores, 2014).

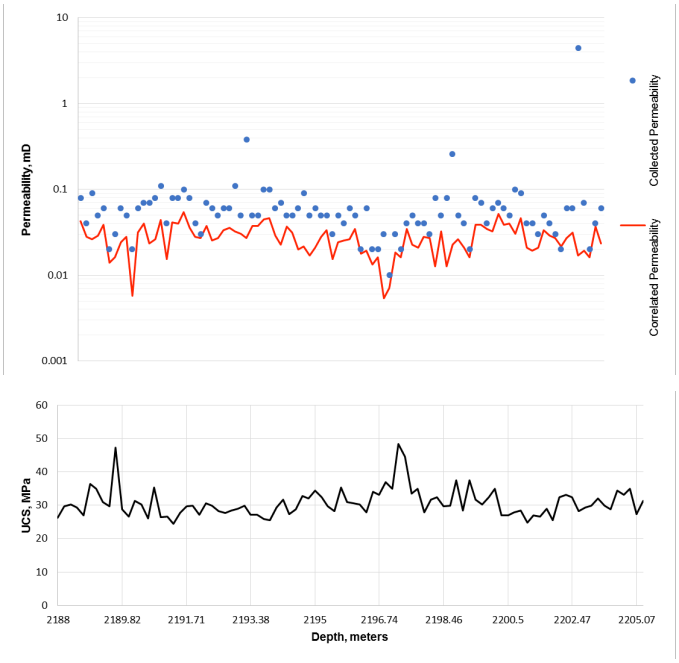

Fig. 9. Permeability comparison and UCS behavior for the Montney shale (Derder, 2012).

5. ADVANTAGES OF KNOWING PERMEABILITY

Permeability and other reservoir parameters are key components for stimulation design in horizontal wellbores. In horizontal tight shale gas wells, the use of wireline or LWD data has been used to estimate these parameters with the aim to identify "sweet spots", or areas with higher porosity and permeability, to hydraulically fracture (Hashmy et al., 2011). Knowing permeability and porosity values in lateral sections can allow for better, more successful fracture staging and hydrocarbon recovery (Han et al., 2010). Having a better understanding of permeability and other reservoir characteristics can also minimize the number of stage needed when fracturing and reduce cost and time (Ashton et al., 2013). While log interpretation can provide permeability estimations, but in high-angle and horizontal (HA/HZ) wells can be an intensive task involving necessary physics-based simulation techniques (Polyakov et al., 2013).

Using drilling data to determine permeability and other reservoir parameters has many benefits, including that excess tools don't need to be run because additional data doesn't need to be obtained (Lehman et al., 2016). Permeability measurements can also have an impact on the overall performance of a well (Britt et al., 2004). Permeability determination from the use of drilling data can also have real-time application potential. Because drilling data is available for any point in a well, UCS, porosity, and permeability measurements can be determined in a short amount of time. Knowing these parameters can allow for the reservoir to be selectively stimulated. Real-time

understanding of these variables can also allow for a reduction in stimulation costs, the ability to vary stimulation design based on parameter optimization, and determine the appropriate number of stages for successful hydrocarbon production (Acock et al., 1996).

6. CONCLUSIONS AND LEARNINGS

The UCS-permeability correlation presented in this paper can be applicable to pure sandstone and shale formations. Many of the current methods for used for permeability determination have a high price and/or extensive time to obtain results. Utilizing the correlation presented, permeability can be found in a much more economical and timely manner. Determining permeability from drilling data could allow for this method to be used in real-time applications. Optimizing the stimulation process is also highly possible when using such a method. This method could also greatly benefit horizontal well completions techniques in that permeability values can be found at any point in the lateral. Knowing permeability throughout an entire well could impact hydrocarbon recovery, recompletions, formation evaluation, and numerous other aspects of the petroleum industry.

NOMENCLATURE

UCS Unconfined Compressive Strength, MPa

ROP Rate of Penetration, meters per hour

WFT Wireline Formation Testers

MFT Multivariate Facies Transform

MWD Measuring While Drilling

LWD Logging While Drilling

GR Gamma Ray

HLD Mechanical Hardness

mD milliDarcy

a,b Formation Constant

REFERENCES

1. Acock, A.M., H. Sanders, and L.A. Fry. 1996. Real-Time Treatment Optimization. In *Proceedings of the SPE Gulf Coast Section/ICoTA North America Coiled Tubing Roundtable, Conroe, 26-28 February 1996.*
2. Aguilera, R. 2013. Flow Units: From Conventional to Tight Gas to Shale Gas to Tight Oil to Shale Oil Reservoirs. In *Proceedings of the SPE Western Regional & AAPG Pacific Section Meeting, 2013 Joint Technical Conference, Monterey, California, 19-25 April 2013.*
3. Flores, L.J.Z. 2014. Reservoir Characterization of the uppermost Monteith Formation-Tight Gas Sandstones in the Western Canada Sedimentary Basin in Alberta, Canada. M.S. Thesis, University of Calgary, Calgary, Alberta.
4. Davey, H. 2012. Geomechanical Characterization of the Montney Shale Northwest Alberta and Northeast British Columbia, Canada. MS Thesis, Colorado School of Mines, Golden, Colorado.
5. Gonzalez, L., Nasreldin, G., Rivero, J. et al. 2012. 3D Modeling of Multistage Hydraulic Fractures and Two-Way Coupling Geomechanics-Fluid Flow Simulation of a Horizontal Well in the Nikanassin

Tight Gas Formation, Western Canada Sedimentary Basin. Presented at the SPE Annual Technical Conference and Exhibition, San Antonio, Texas, 8-10 October. SPE-159765-MS.

6. Clarkson, C.R., Jensen, J.L., Pedersen, P.K. et al. 2012. Innovative methods for flow unit and pore structure analysis in a tight siltstone and shale gas reservoir. AAPG Bull. 96(02):355-374.

7. Ghanizadeh, A., Bhowmik, S., Haeri-Ardakani, O. et al. 2015. A comparison of shale permeability coefficients derived using multiple non-steady-state measurement techniques: Examples from the Duvernay Formation, Alberta (Canada). Fuel 140(2015): 371-387. http://dx.doi.org/10.1016/j.fuel.2014.09.073.

8. Britt, L.K., Jones, J.R., Heidt, J.H. et al. 2004. Application of After-Closure Analysis Techniques to Determine Permeability in Tight Formation Gas Reservoirs. Presented at the SPE Annual Technical Conference and Exhibition, Houston, Texas, 26-29 September. SPE-90865-MS.

9. Lehman, L.V., Jackson, K. and Noblett, B. 2016. Big Data Yields Completion Optimization: Using Drilling Data to Optimize Completion Efficiency in a Low Permeability Formation. Presented at the SPE Annual Technical Conference and Exhibition, Dubai, United Arab Emirates, 26-28 September. SPE-181273-MS.

10. Polyakov, V., Omeragic, D., Shetty, S. et al. 2013. 3D Reservoir Characterization Workflow Integrating High Angle and Horizontal Well Log Interpretation with Geological Models. Presented at the International Petroleum Technology Conference, Beijing, China, 26-28 March. IPTC-16828-MS.

11. Ashton, T., Ly, C.V., Spence, G. et al. 2013. Application of Real-Time Well-Site Tools for Enhanced Geosteering, Reservoir and Completions Characterization. Presented at the Unconventional Resources Technology Conference, Denver, Colorado, 12-14 August. SPE-168806-MS/URTeC-1581626-MS.

12. Derder, O.M. 2012. Characterizing Reservoir Properties for the Lower Triassic Montney Formation (Units C and D) Based on Petrophysical Methods. MS Thesis, University of Calgary, Calgary, Alberta.

13. Han, S.Y., Kok, J.C.L., Tollefsen, E.M. et al. 2010. Shale Gas Reservoir Characterization Using LWD in Real Time. Presented at the Canadian Unconventional Resources & International Petroleum Conference, Calgary, Alberta, Canada, 19-21 October. CSUG/SPE-137607-MS.

14. Hashmy, K., Abueita, S., Barnett, C. et al. 2011. Log-Based Identification of Sweet Spots for Effective Fracs in Shale Reservoirs. Presented at the Canadian Unconventional Resources Conference, Calgary, Alberta, Canada, 15-17 November. CSUG/SPE-149278-MS.

15. Olusola, B.K. 2013. Drill Cuttings, Petrophysical, and Geomechanical Models for Evaluation of Conventional and Unconventional Petroleum Reservoirs. M.S. Thesis, University of Calgary, Calgary, Alberta, Canada, September 2013.

16. Lenormand, R. and Fonta, O. 2007. Advances in Measuring Porosity and Permeability from Drill Cuttings. Presented at the 2007 SPE/EAGE Reservoir Characterization and Simulation Conference, Abu Dhabi, United Arab Emirates, 28-31 October. SPE-111286-MS.

17. Siddiqui, S., Grader, A.S., Touati, M. et al. 2005. Techniques for Extracting Reliable Density and Porosity Data from Cuttings. Presented at the SPE Annual Technical Conference and Exhibition, Dallas, Texas, 9-12 October. SPE-96918-MS. http://dx.doi.org/10.2118/96918-MS.

18. Cedola, A.E., Atashnezhad, A., and G. Hareland. 2017. Evaluating Multiple Methods to Determine Porosity from Drilling Data. Presented at the SPE Oklahoma City Oil and Gas Symposium, Oklahoma City, Oklahoma, 27-30 March. SPE-185115-MS.

19. Kerkar, P.., Hareland, G., Fonseca, E.R. et al. 2014. Estimation of Rock Compressive Strength Using Downhole Weight-on-Bit and Drilling Models. Presented at the International Petroleum Technology Conference, Doha, Qatar, 19-22 January. IPTC-17447-MS.

20. Hareland, G. and Nygaard, R. 2007. Calculating Unconfined Rock Strength from Drilling Data, 1st Canada-U.S. Rock Mechanics Symposium, Vancouver, British Columbia, Canada, 27-31 May. ARMA-07-214.

21. Nygaard, R., Hareland, G., Budiningsih, Y., et al. 2002. Eight Years Experience with a Drilling Optimization Simulator in the North Sea. Presented at the SPE/IADC Asian Conference, Jakarta, Indonesia, 9-11 September. SPE-77247-MS.

22. Warren, T.M. 1987. Penetration-rate performance of roller cone bits. SPE Drilling Engineering 2 (1): 9-18.

23. Al Dushaishi, M.F., Nygaard, R., Andersen, M. et al. 2016. Selecting Optimum Drilling Parameters by Incorporating Vibration and Drilling Efficiency Models. Presented at the IADC/SPE Drilling Conference and Exhibition, Fort Worth, Texas, 1-3 March. IADC/SPE-178834-MS.

24. Briner, A., Ketabchi, I. and Nadezhdin, S. 2015. Overcoming High-Temperature Logging Challenges While Staying Cost-Effective for a Tight Gas Project in the Sultanate of Oman. Presented at the SPE North Africa Technical Conference and Exhibition, Cairo, Egypt, 14-16 September. SPE-175729-MS.

25. Gawankar, K., Pate, C., Easow, I. et al. 2016. Cost-Effective Reservoir Characterization from Advanced Surface Logging Technologies in Unconventional Reservoirs. Presented at the Unconventional Resources Technology Conference, San Antonio, Texas, 1-3 August. URTEC-2460893-MS.

26. Dahraj, N.U.H. and Bhutto, A.A. 2014. Linear Mathematical Model Developed Using Statistical Methods to Predict Permeability from Porosity. Presented at the PAPG/SPE Pakistan Section Annual Technical Conference, Islamabad, Pakistan, 24-27 November. SPE-174716-MS.

27. Fleckenstein, W.W. and Eustes, A.W. 2003. Novel Wireline Coring System. Presented at the SPE Annual Technical Conference and Exhibition, Denver, Colorado, 5-8 October. SPE-84358-MS.

28. Kristiansen, J.I., Sognesand, S. and Bergum, R. 1996. Determination and Application of MWD/LWD and Core Based Permeability Profiles in Oseberg Horizontal Wells. Presented at the 1996 SPE European Petroleum Conference, Milan, Italy, 22-24 October. SPE-368 Haghshenas, B., Clarkson, C.R., Aquino, S.D. et al. 2016. Characterization of multi-fractured horizontal shale wells using drill cuttings: 2. Permeability/diffusivity estimation. Journal of Natural Gas Science and Engineering 32: 586-596. http://dx.doi.org/10.1016/j.jngse.2016.03.055. 57-MS.

29. Hunt, E.R. and Pursell, D.A. 1997. Fundamentals of log analysis. WorldOil 218 (11): 127-130.

30. Pereira, J.L.L. 2004. Permeability Prediction from Well Log Data Using Multiple Regression Analysis. Ms Thesis, West Virginia University, Morgantown, West Virginia.

31. Jiang, Z., Schrank, C., Mariethoz, G. et al. 2013. Permeability estimation conditioned to geophysical downhole log data in sandstones of the northern Galilee Basin, Queensland: Methods and application. Journal of Applied Geophysics 93 (2013):43-51. http://dx.doi.org/10.1016/j.jappgeo.2013.03.008.

32. Ghanizadeh, A., Aquino, S., Clarkson, C.R. et al. 2014. Petrophysical and Geomechanical Characteristics of Canadian Tight Oil and Liquid-Rich Gas Reservoirs. Presented at the SPE/CSUR Unconventional Resources Conference-Canada, Calgary, Alberta, Canada, 30 September-2 October. SPE-171633-MS. http://dx.doi.argo.library.okstate.edu/10.2118/171633-MS.

33. Civan, F., Devegowda, D. and Sigal, R. 2013. Improved Data Analysis and Interpretation Method for Laboratory Determination of Crushed-Sample Shale Gas Permeability. Presented at the Unconventional Resources Technology Conference, Denver, Colorado, 12-14 August. SPE-168840/URTeC 1582182.

34. Tinni, A., Fathi, E., Agarwal, R. et al. 2012. Shale Permeability Measurements on Plugs and Crushed Samples. Presented at the SPE Canadian Unconventional Resources Conference, Calgary, Alberta, Canada, 30 October-1 November. SPE-162235-MS.

35. Moghadam, A.A. and Chalaturnyk, R. 2015. Laboratory Investigation of Shale Permeability. Presented at the SPE/CSUR Unconventional Resources Conference, Calgary, Alberta, Canada, 20-22 October. SPE-175919-MS.

36. Jiang-ming, D., Xiao-peng, L., Xin-min, W. et al. 2013. Estimation of Porosity and Permeability from Conventional Logs in Tight Sandstone Reservoirs of North Ordos Basin. Presented at the SPE Middle

East Unconventional Gas Conference and Exhibition, Muscat, Oman, 28-30 January. SPE-163953-MS.

37. Li, X., Lu, Y., Zhu, J. et al. 2016. Calibrated Clay Parameter Improves Continuous Permeability Estimation with LWD Logs in Complex Siliclastic Reservoirs. Presented at the SPE Annual Technical Conference and Exhibition, Dubai, U.A.E., 26-28 September. SPE-181879-MS.

38. Skalinski, M.T. and Sullivan, M.J. 2001. Application of Improved Method for Permeability Estimation in Complex Lithology Reservoirs. Presented at the SPWLA 42nd Annual Logging Symposium, Houston, Texas, 17-20 June. .SPWLA-2001-C.

39. Ramaswami, S.R., Cornelisse, P.W., Elshahawi, H. et al. 2016. Extracting More from Wireline Formation Testing: Better Permeability Estimation. Presented at the International Petroleum Technology Conference, Bangkok, Thailand, 14-16 November. IPTC-18914-MS. http://dx.doi.org.argo.library.okstate.edu/10.2523/IPTC-18914-MS.

VITA

ALEXANDRA ELIZABETH CEDOLA

Candidate for the Degree of

Master of Science

Thesis: USING TYPICAL DRILLING DATA TO CALCULATE POROSITY & PERMEABILITY

Major Field: Petroleum Engineering

Biographical:

Education:

Completed the requirements for the Master of Science/Arts in your major at Oklahoma State University, Stillwater, Oklahoma in December, May, or July, Year.

Completed the requirements for the Bachelor of Science in Petroleum & Natural Gas Engineering at New Mexico Institute of Mining & Technology, Socorro, New Mexico in 2015.

Experience:
Engineering RA, Oklahoma State University, Fall 2015 – Spring 2017
• Developing correlations between porosity and permeability from drilling data

Professional Memberships:

Society of Petroleum Engineers

American Association of Drilling Engineers